UNIVERSITAT POLITÈCNICA DE VALÈNCIA

DEPARTAMENTO DE INGENIERÍA ELECTRÓNICA

STUDY OF DIFFERENT ANALOG MEASUREMENT SYSTEMS FOR MOS-TYPE GAS SENSORS

Javier Cervera Gómez

Tutor: José Pelegrí Sebastiá

Master's Thesis displayed in the Department of Electronics Engineering of the Universitat Politècnica de València, to obtain the Master's Degree in Electronic Systems Engineering

Academic course 2017-18

Valencia, 18th September 2018

Resumen

Este proyecto tiene como objetivo principal el desarrollo e implementación de las diferentes etapas involucradas en un sistema de sensado, en particular para sensores de gas. Se trabajarán nuevas técnicas para alimentar sensores resistivos, así como la aplicación de diferentes métodos para el acondicionamiento de la señal que actualmente no se utilizan en estos sensores. Se realizará un estudio de la influencia de la alimentación del sensor con la deriva térmica, el offset, y parámetros similares. Para llevar a cabo este proyecto, se llevará a cabo un estudio de los diferentes métodos de acondicionamiento de los sensores de gas. Además, se realizará un análisis y diseño de un sistema de suministro de energía para tales sensores, que son compuestos de un calentador resistivo y un elemento resistivo.

Abstract

This thesis consists in developing and implementing of different stages involved in gas sensor technology. New techniques and application of different methods for conditioning the signal not currently used in MOS-type gas sensors are going to be worked to power that sensors. A study of the influence of the sensor supply with thermal drift, offset, energy consumption parameters, among other parameters. A study of the different conditioning methods of the gas sensors will be carried out in this work. In addition to this, an analysis and design of a power supply system for such sensors has been done. This analysis depends on resistive heater and sensor heater.

Index

1. State of the art

1.1. Electronic nose

Electronic noses are electronic systems which can detect some substances in different gases, in other words they are devices which can detect some odours, using normally arrays of sensors with the aid of a computer or a microcontroller that allows to classify sensor data. In recent years, electronic noses are being used in different areas of study such as food and drink industries [1],[2], or health industry [3], among others. These electronic systems can be made with different kind of sensors that are sensitive to different types of substances and these sensors present different behaviours (resistive sensors, capacitive sensors, optical sensors, among others) [4, pp. 79–104]. This work covers Metal Oxide Semiconductor (MOS) gas sensors, in order to improve the analysis of current electronic noses.

1.1.1. MOS-type gas sensor

Metal Oxide Semiconductor type gas sensors are made of SnO_2, ZnO, FE_2O_3 or WO_3, which increase their conductivity in presence of some reducible gases such as H_2, CO or H_2S, at temperatures of 200-500 ºC

Inside the atmosphere (with air clean, that mean approximate 21% of the air is O_2), some oxygen atoms are adsorbed by the metal oxide surface of the sensor, these atoms trap free electrons from the semiconductor surface, because their high electron affinity, that reaction creates a potential barrier at the grain boundaries, this potential barrier work as the scattering centre for conducting electrons as can be seen in the Figure 1, in other words, resistivity of the sensor increases.

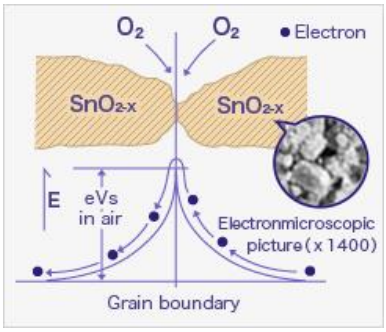

Figure 1: Grain boundary in air clean [5]

In presence of some combustible gas or reducing gas oxidation of these gases is created with oxygen occurs at the surface of sensor. This makes the density of adsorbed oxygen on the metal oxide surface decreases, and the potential barrier is reduced, making that electrons flow through the potential barrier more easily than before, that means the sensor decreases its resistance proportionally to the concentration of those combustible gas or reducing gas, as it is show in the Figure 2 [4, Sec. 4.3.1], [5].

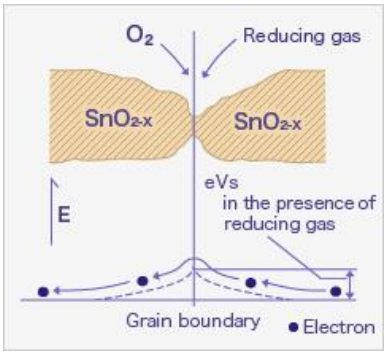

Figure 2: Grain boundary in air with some combustible or reducing gas [5]

As I said before, MOS type gas sensors need to work at temperatures of 200-500 ºC, this is achieved thanks to a resistance which acts as a sensor heater, this heater has different terminals than the sensor, as Figure 3 shows, for that reason, two different power sources are needed, one for the heater resistance and another for the sensor resistance.

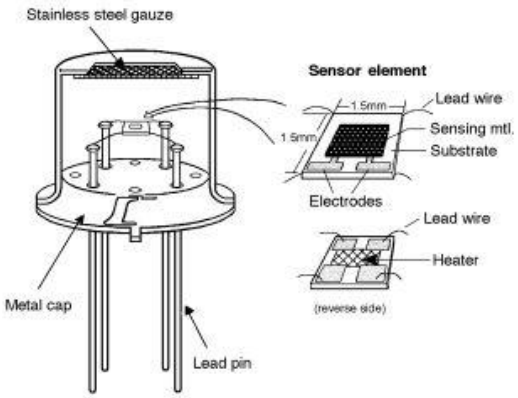

Figure 3: Structure of the sensor TGS2610 by Figaro [6]

This heater resistance normally is powered by a DC voltage, but it can be powered by AC voltage according to the datasheet, in addition, one of the problems is that these sensors need period before use it. this time normally is around 24 hours, that makes difficult use these sensors in a mobile device or a quickly turn on device with that sensors with good results.

Other problem of this type of sensors is the value of the resistance given by datasheet is unprecise (normally between 10 kΩ – 100 kΩ in air clean) [7], [8] to get a general reference, due to the temperature of the sensor is changing, because normally there are not any control of the temperature of the heater, for this reason the value of the resistance of the sensor can change each measure when the sensor is measuring air clean [9]. Although these changes of temperature are not fast, due to that a reference resistance value is needed to get it occasionally (when a measure is taken, a reference with air clean normally is taken before and after) [10]. These changes make that electronic circuits which are used to adapt the signal of these type sensors are simple and range of values choose to the sensor resistance are not optimized to a small range, for this reason, resolution of the signal given by measure normally are not good enough.

Last problem is low power that sensors are able to withstand, (which is about 15 mW), for this reason, this type of sensor is not able to use currents greater than 0.38 mA in the worst case (100 kΩ) making that noise in the signal has some importance.

1.2. Signal conditioning circuits

1.2.1. Voltage divider

The main electronic circuits used to MOS type gas sensors and recommended by the companies that market these sensors is to use a voltage divider with the resistance of the sensor such as Figure 4 [7], [8]. Where R_H is the heater resistance, R_S is the resistance of the sensor, and V_{RL} is the output voltage.

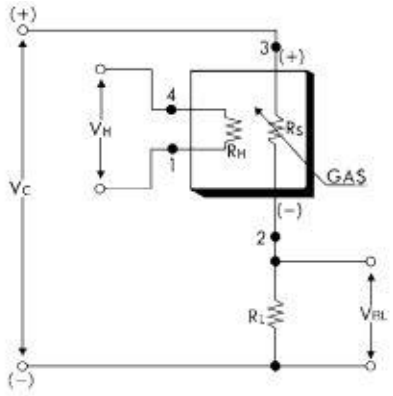

Figure 4: Voltage divider [7]

The drawback of this circuit is the low range of the output voltage give a low precision in the results obtained. Second problem of it is the output signal is not linearly proportional to the resistivity of the sensor changes, as equation 1 shows.

$$V_{RL} = V_C \left(\frac{R_L}{R_S + R_L} \right) \quad \textbf{(1)}$$

1.2.2. Wheatstone bridge

Another common conditioning circuit for resistive sensors is the Wheatstone bridge. This electronic circuit is formed for two voltage dividers, one of that, with only resistors and the other as showed in section 1.2.1. In this case, output voltage is a differential voltage between both voltage divider as Figure 5 shows, where R_S is the resistance of the sensor.

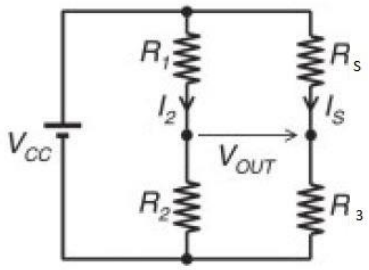

Figure 5: Wheatstone bridge

The behaviour of the output voltage of this circuit has the following equation.

$$V_{OUT} = V_{CC} \left(\frac{R_3}{R_S + R_3} - \frac{R_2}{R_1 + R_2} \right) \quad \textbf{(2)}$$

The advantage of this circuit versus voltage divider is that the offset voltage create by voltage divider is deleted, making that a bigger gain of the output using an amplifier than in voltage divider can be used doing that the precision of Wheatstone bridge is bigger than in voltage divisor as Figure 6 shows [4, Sec. 5.2.1.2].

Furthermore, in this topology can be provided temperature compensation, to sensors which their resistances change by temperature.

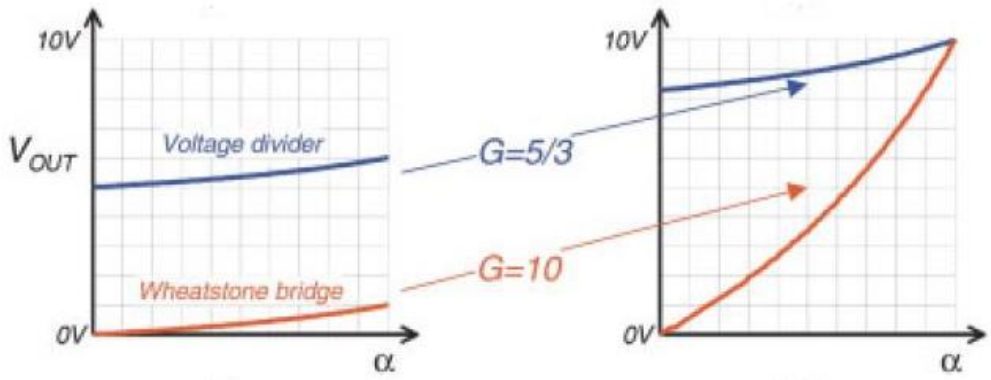

Figure 6: Output of Wheatstone bridge vs Output of voltage divider [4, Fig. 5.2]

1.2.3. Generalized Impedance Converter

Generalized Impedance Converter (GIC) is an electronic design which is able to simulate different frequency-dependent resistances as inductors or capacitors. This design is implemented using two operational amplifiers and five passive electronic components as it can be seen in figure 7.

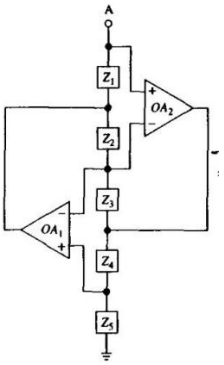

Figure 7: Generalized Impedance Converter [11, Fig. 4.13]

The behaviour of this circuit depends on the impedance of all passive electronic components, which is presented in equation 3. Depending on the position of these components and the values of impedance of them an inductor can be simulated using only resistances and capacitors, as Figure 8 shows [11, Sec. 4.3].

$$Z_{GIC} = \frac{Z_1 Z_3 Z_5}{Z_2 Z_4} \quad \textbf{(3)}$$

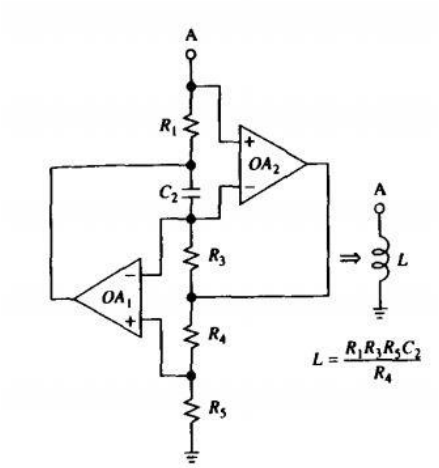

Figure 8: Inductance obtained using resistors and capacitors [11, Fig. 4.15]

With the aid of this design, a variable capacitance depending on a variable resistance can be simulated with the circuit which is in figure 9, this together with the astable operation of the timer 555 is able to make an output square wave depending of value of a resistance [12]. The simulation of the capacitor is presented in Figure and it has a capacity obtained in equation 4.

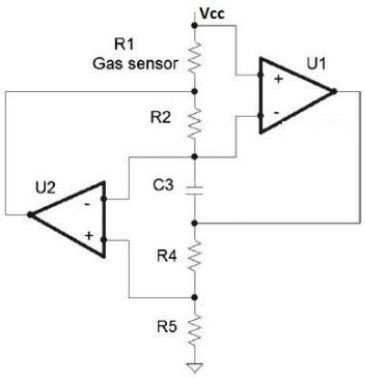

Figure 9: Capacitance simulated with a GIC

$$C_{GIC} = \frac{C_3 R_2 R_4}{R_{1,sensor} R_5} \quad \textbf{(4)}$$

The goal of this design is to replace the capacitance in a design to use the astable operation of timer 555, that is show in Figure 10, which give an output square wave frequency dependent of a capacitance following equation 5 [13].

$$f_{out} = \frac{1.44}{(R_A + 2R_B)C} \quad \textbf{(5)}$$

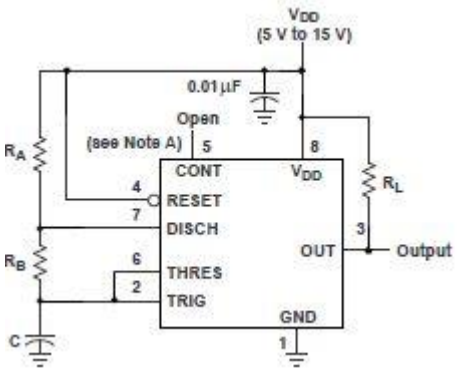

Figure 10: Astable operation of timer 555 [13]

This circuit has some advantages over previous signal conditioners. First advantage is that the frequency of the output signal is linearly dependent of changes in the sensor resistance, as equation 6 shows.

$$f_{out} = \frac{1.44R_{1,sensor}R_5}{(R_A + 2R_B)C_3R_2R_4} \quad \textbf{(6)}$$

1.2.4. Anderson loop

Anderson loop is a measurement circuit topology which is based on active subtraction of two differential voltages created by one current, which pass through by the sensor resistance and reference resistance. Normally it is made using a current source that power the sensor and reference resistances in serial, to both resistors have the same current, and their differential voltages are subtract with a dual-differential subtractor [13], [14], which is six-terminal (4 inputs terminal and 2 output terminal) to obtain a new voltage that depends of equation number 7.

$$v_{out} = A_1 v_1 - A_2 v_2 \quad \textbf{(7)}$$

Where A_1 and A_2 are gains apply by the dual-differential subtractor and v_1 and v_2 are voltages between its inputs. The basic schematic of the Anderson loop is shown in Figure 11.

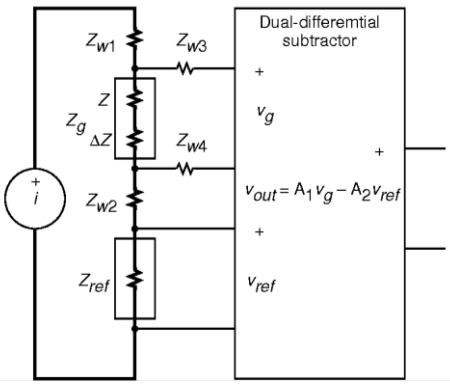

Figure 11: Anderson Loop [14, Fig. 2]

This circuit has some benefits against other circuits, one of principal benefits against others is this circuit can be implemented to more than one sensor as Figure 12 shows.

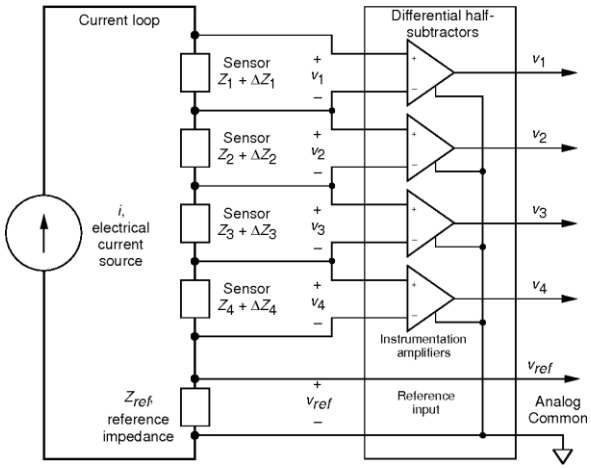

Figure 12: Anderson Loop to four sensors [14, Fig. 4]

Furthermore, this topology has an output voltage which is a linear function of sensor resistance changes, and this output is not affected by random changes in wire and connecting resistance. Moreover, power dissipation of that circuit is divided by 4 to obtain similar outputs voltages in a Wheatstone bridge. As Wheatstone bridge this circuit can be provided temperature compensation.

However, a current source is needed to power the loop of the circuit, when the other topologies only need a voltage source which is easier to find than a current source, In addition to this, in this circuit is needed an active subtractor which is made with differential amplifier or with instrumentation amplifier, which make this topology more expensive than a Wheatstone bridge or a divisor voltage.

2. Heater resistance

This section addresses how sensor respond to different kind of power in the heater of the sensor, which function is explained in the section 1.1.1.

To carry out this study, the system of data acquisition, is made up of a computer with LabVIEW software installed to control and save data obtained from a multimeter Agilent 34401A, which are connected by GPIB, and the multimeter is connected with the sensor in study. The heater of the sensor is powered by a function generator Agilent 33120A. This system was connected in two ways, one to measure the resistance of the sensor, when is powered only the heater resistance of the sensor, and the other way to measure the current which flows though the heater, how Figure 13 shows.

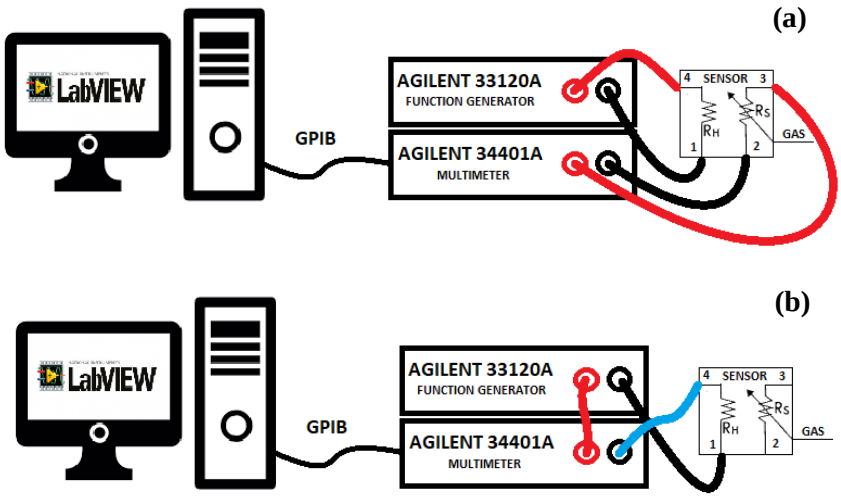

Figure 13: a) System to measure the resistance of the sensor. b) System to measure the current of the heater

To manage this system a program in LabVIEW has been developed, that is the development environment and system design platform for a visual programming language from National Instruments, because this language is fast and simple to develop programs using the GPIB connection and in this case the device Agilent 34401A has a library to manage the device from this platform easily.

In computer, the program developed in the environment of LabVIEW, or also called vi file, was running which capture the data through the Agilent 34401A each approximately 2 seconds and these data are stored in a .csv file, that can be read by different programs such as Excel or Matlab to process all data taken, and this data is plotted in a graph. Furthermore, what type of measure h taken can has been selected in this program, in a dropdown menu in the program all that characteristics can be shown in Figure 14 and in the code program in the Annex I.

As it has been said before, all data are stored in a .csv file, this type of file was chose because create and write this type of files are very easy and can be read with the program from the Windows Office package excel, although are not very optimized in size, but in this case the size of each measure has about 3600 sample the longest measure taken, which is acceptable for this type of files.

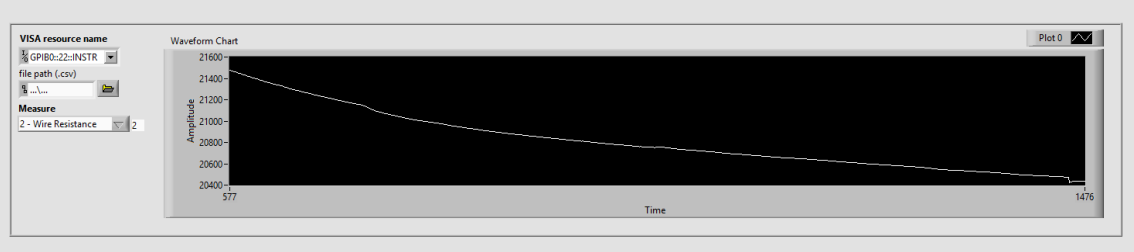

Figure 14: User interface of the program in LabVIEW

In this study was selected two sensors of Figaro company, which are called TGS2600 and TGS2610, these sensors will be used to all the measures that are made in this study. These sensors were selected because some volatile substances make react to both sensors, and with that characteristic is easier make some samples to measure with both sensors than if sensors have not any substance which make react them.

With this system, different powers to the heater are going to be studied, these different powers are going to be studied just when the power starts in the heater resistance, and with, at least, 24 hours applying some power in the heater resistance. First power which has been studied is constant power at 5 volts, which is the used by the fabricant to test these sensors. The other powers which are going to be studied are power the heater resistance with a square wave or with a sine wave both with 5 volts peak to peak and with 2.5 volts of offset, with different frequencies. In any power are negative voltages because in the cautions of these sensors [6] is indicated that the sensors have polarity, and an incorrect polarization of the power may cause deterioration to the sensor.

2.1. Results

In this section the transient behaviour of each sensor resistance. That transient starts when the power on its heater sensor is turn on, until the sensor resistance starts to arrive to its working resistance value when is measuring air clean, has been studied. Besides, the current which flows through the heater resistance has been measured too. Moreover, the stability of the value of the resistance was measured before waiting at least 24 hours since the heater was turn on, but after taking these measures, the type of the waveform of the heater of the sensor do not increase or reduce the stability of the sensor resistance, only affect in the value of the resistance which increase when a square waveform is used.

2.1.1. TGS2600

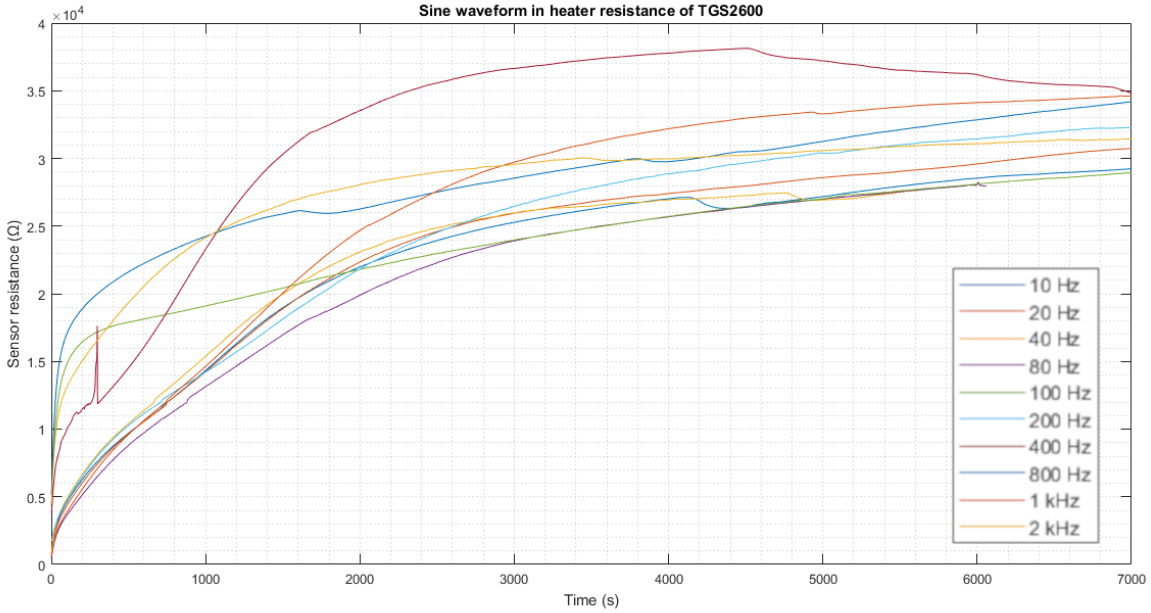

Figure 15: Transient behaviour of sensor TGS2600 when a sine waveform is used in the heater resistance

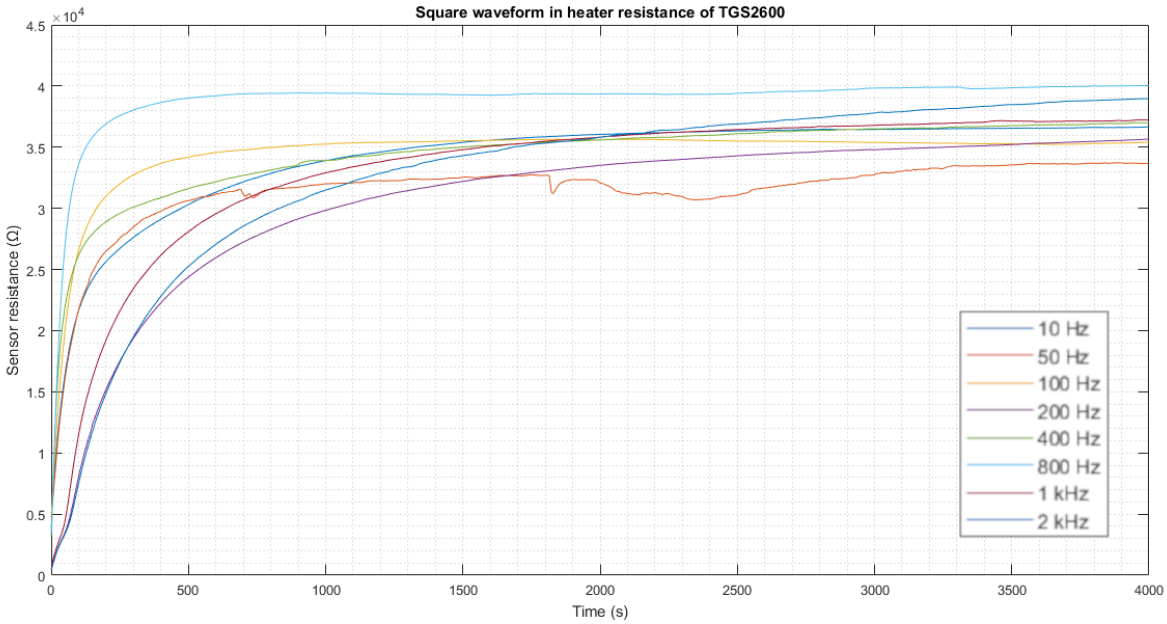

Figure 16: Transient behaviour of sensor TGS2600 when a square waveform is used in the heater resistance

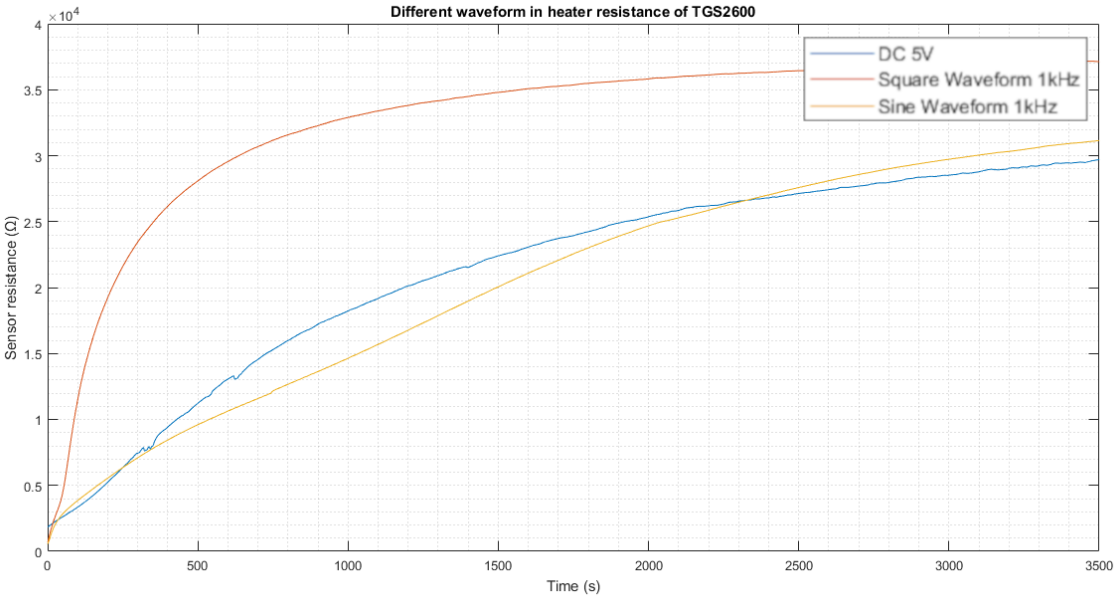

Figure 17: Transient behaviour of sensor TGS2600 when the heater resistance is powered by different type of waveform

The behaviour of the sensor resistance is presented in the above figures, when the heater resistance was powered by different waveform. Figure 15 shows the resistance sensor when the heater resistance is powered by a sine waveform with 5V peak-to-peak and with 2.5V of offset, because the company that made the sensor indicates that in the sensor there is a polarity in both resistances. In this case, there are not any logical correlation between the frequency and the slope of the change of the sensor resistance. The same happens in Figure 16, which shows the value of the sensor resistance when the heater resistance of the sensor is powered by a square waveform with different frequencies. Nevertheless, Figure 17 shows a that the slope of the change of the sensor resistant when the heater has been powered. In this way, the sensor resistor increases its value faster when a square waveform is used instead of a sine waveform or a continuous voltage. This fact allows that the sensor is ready to use faster than in other cases. that means that when square waveform is used in the heater resistance, the sensor will be ready to use faster than using a sine waveform or a constant voltage.

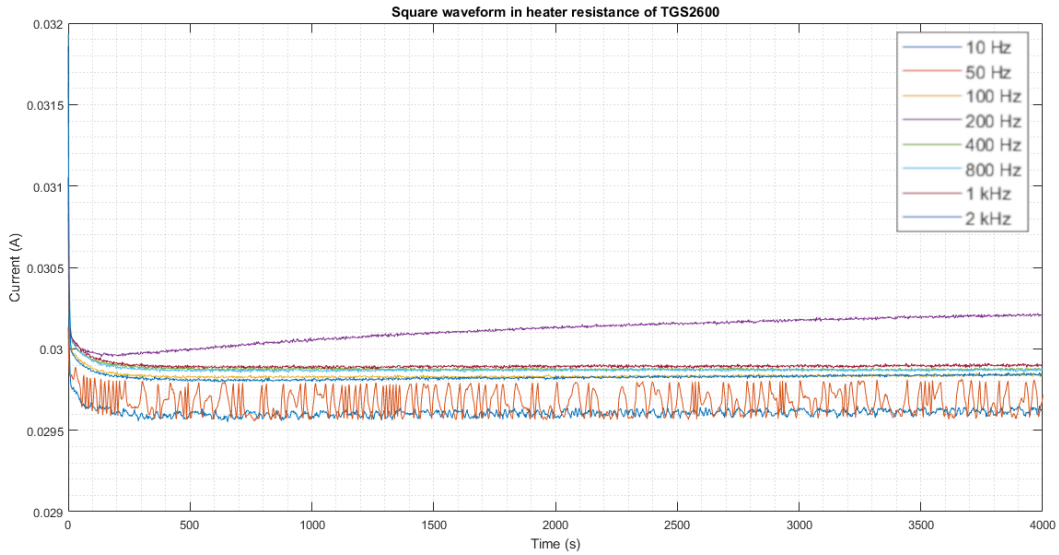

Figure 18: Transient behaviour of the heater resistance of the sensor TGS2600 it is power by a square waveform

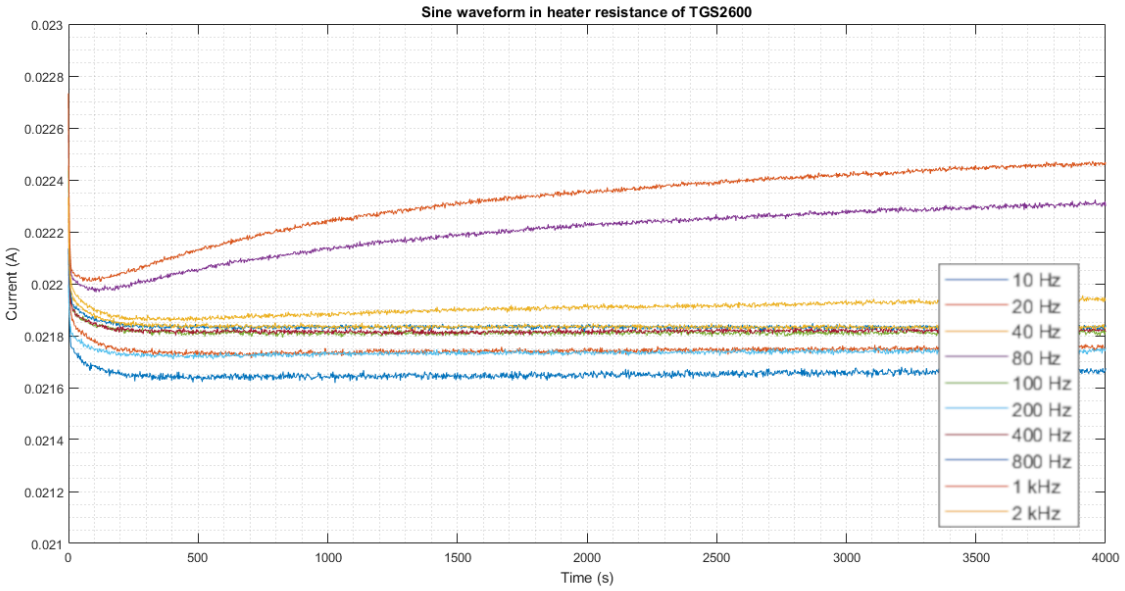

Figure 19: Transient behaviour of the heater resistance of the sensor TGS2600 it is power by a sine waveform

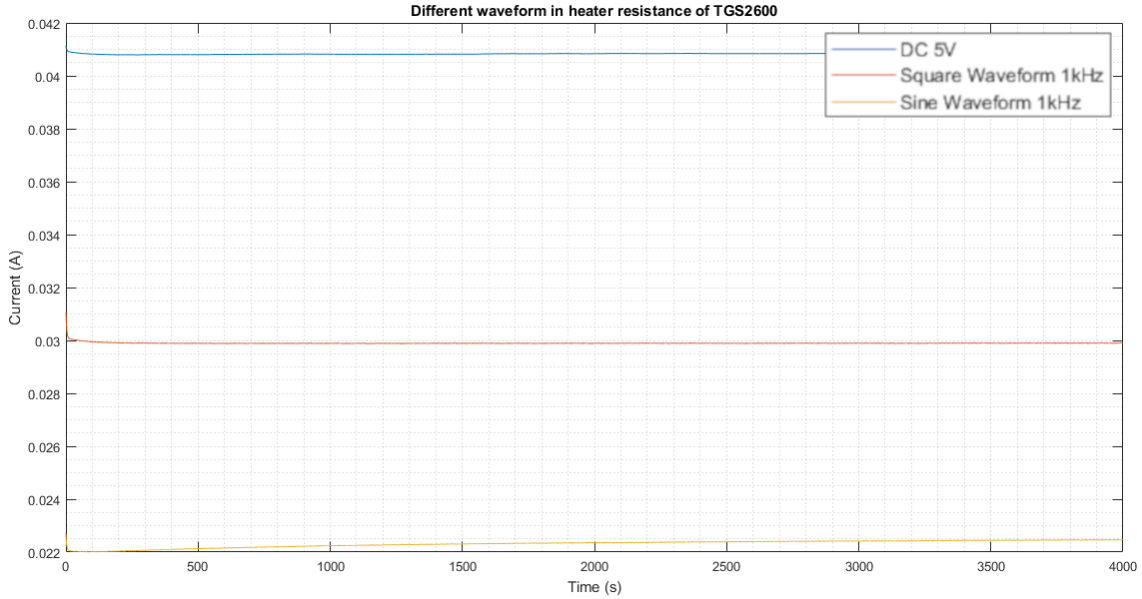

Figure 20: Transient behaviour of the heater resistance of the sensor TGS2600 it is power by different type of waveform

In last 3 figures the current of the heater resistance using different waveforms types and different frequencies do not give much information, only from this data the value of the heater resistance can be calculated. Besides in the Figure 20 is confirmed that the value of the heater resistance do not change caused by the power chosen.

2.1.2. TGS2610

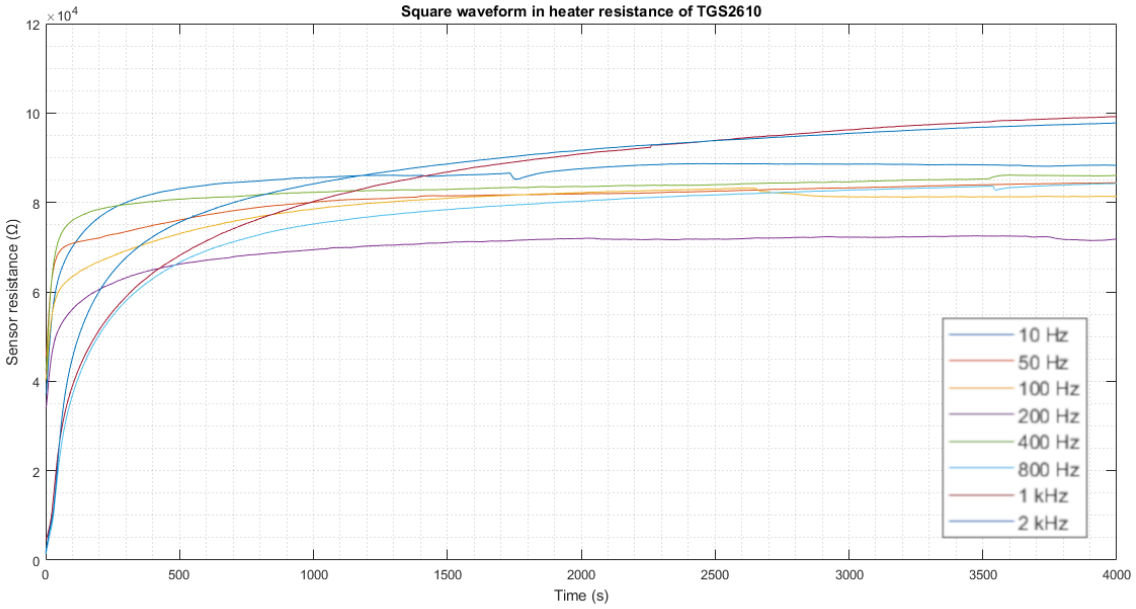

Figure 21: Transient behaviour of sensor TGS2610 when a square waveform is used in the heater resistance

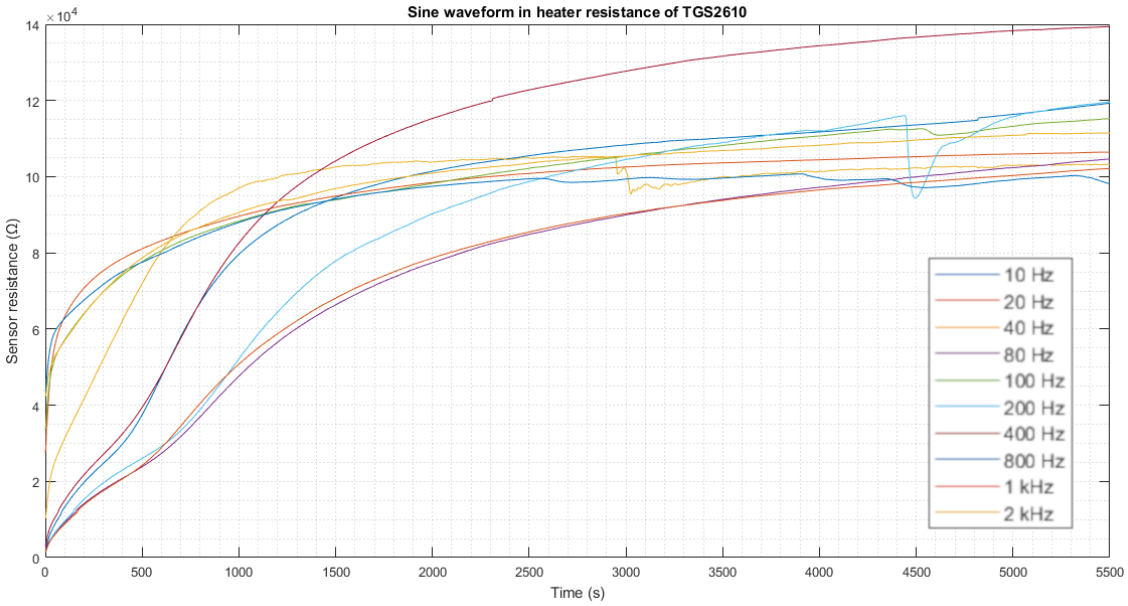

Figure 22: Transient behaviour of sensor TGS2610 when a sine waveform is used in the heater resistance

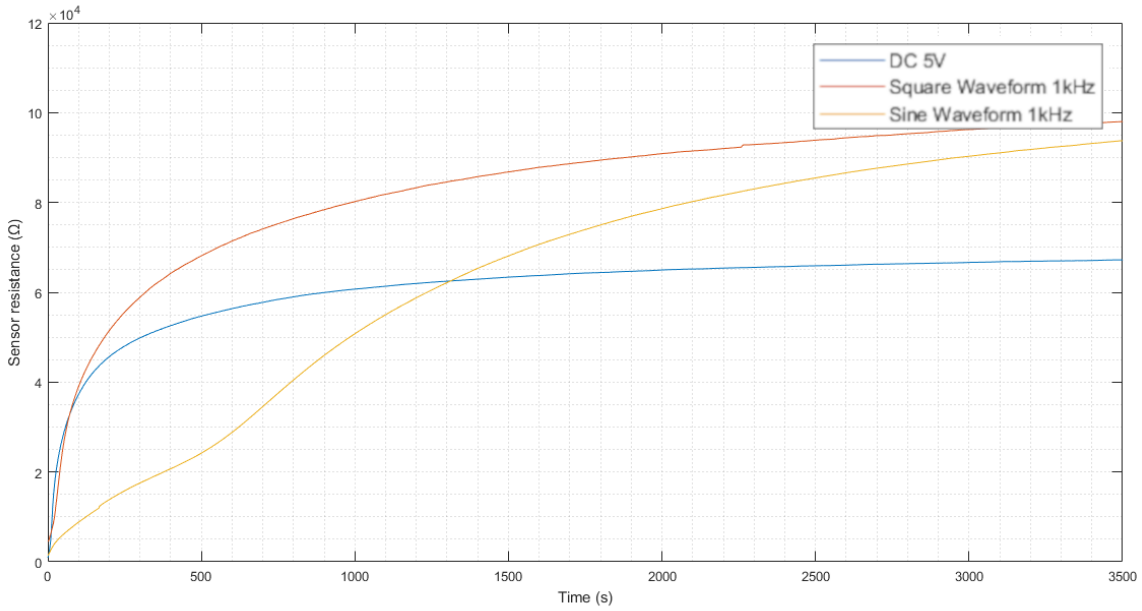

Figure 23: Transient behaviour of sensor TGS2610 when the heater resistance is powered by different type of waveform.

In the sensor resistance of the TGS2610 happens a similar situation than in the sensor resistance of the TGS2600, but a new characteristic appears in the Figure 23, which is that in the beginning, the transient of the changes of the sensor resistance has a less slope when the heater resistance is powered by a sine waveform, but there are a moment when the slope when the heater resistance is powered by a continuous voltage decrease before arrive to the final value, and in this moment the slope of the sensor resistance using the sine waveform in the heater resistance is greater than the other, and for this reason the this slope of the sine waveform made arrive faster to the sensor resistance to its final value.

The graph of the currents is not here because is similar to Figure 18, Figure 19 and Figure 20, and they do not contribute to add any information. Others graphs that could have been interesting, are the transient of the behaviour of the sensor resistance when is in its working value when is measuring air clean, but to both sensors do not contribute to add information too, because there are not significant changes in the behaviour of the sensor resistance between use different type of waveform in the heater resistance.

3. Sensor resistance

This section has been studied four different topologies to power the sensor resistance of a generic MOS gas sensor as TGS2600 and TGS2610, among others. The first topology, which has been studied, is a voltage divider, that is the test topology of the manufacturer. Following with the most used topologies to measure resistive sensors, the Wheatstone bridge is another topology which has been studied. Another topology is based in the Anderson Loop above explained. Last topology which has been studied is based in a paper [12], that consist in create a simulated capacitate which varies linearly with the variation of the sensor resistance with a Generalised Impedance Converter and using a timer 555 create a circuit that detects changes in the sensor resistance.

3.1. Voltage divider and Wheatstone bridge

Voltage divider is the simplest topology to create a sensor system to a resistive sensor, how is explained in the section 1.2.1 how works, and the Wheatstone bridge is an evolution of voltage divider, as can be seen in the section 1.2.2 Wheatstone bridge use a voltage divider to works, for this reason are going to be designed together.

3.1.1. Design

In the case of the design of voltage divider to these sensors only needs choose a load resistance (R_L in Figure 4). To choose that resistance, first is take into account was datasheets of different sensors which have been used [7], [8], where indicates that the load resistance used to a voltage divider with one of these sensors should be greater than 0.45 kΩ. Another thing important to choose this resistance was the sensor resistance when detect clean air, in this case this resistance can be from 10 kΩ to until a little more than 100 kΩ, that range is very big, for this reason if the load resistance is close to 100 kΩ and the sensor has a sensor resistance with clean air close to 10 kΩ, the output signal change is going to be small when the sensor resistance changes, and that made that the resolution of the measure will be worst. Consequently, the load resistance should be close to the small values of that range.

As result of the above ideas, the chosen value for the load resistance for the generic voltage divider for these sensors is 10 kΩ. Furthermore, power voltage of the circuit is going to be five volts as is indicated in datasheets of the sensors. Therefore, the behaviour of the output signal of that voltage divider is going to be as equation 8 shows, where R_S is value of the sensor resistance and V_{OUT} is the output voltage of the voltage divider.

$$V_{OUT} = 5 * \left(\frac{10.000}{R_S + 10.000}\right) \quad \textbf{(8)}$$

In this case the Wheatstone bridge is going to implement together with the divider voltage. As a result, to design the Wheatstone bridge balanced, another divider voltage must be made with the same resistance value that when the sensor is detecting clean air. If the Wheatstone bridge is balanced, when the sensor of the system is detecting clean air, the output voltage of the system must be 0 volts, but the resistance value when the sensor is detecting clean air is unknown, consequently, in the second voltage divider, a potentiometer of 100 kΩ will be placed in the same position of the sensor in the first voltage divider, which is going to modify the value of the resistance manually, before take any measure, to balance the Wheatstone bridge. The equation 9

shows the behaviour of the Wheatstone bridge, where V_{OUT} is the output voltage, R_{CA} is the resistance value of the sensor when is detecting clean air, and R_{SEN} is the value of the sensor resistance.

$$V_{OUT} = 5 * \left(\frac{10.000}{10.000 + V_{SEN}} - \frac{10.000}{10.000 + R_{CA}} \right) \quad \textbf{(9)}$$

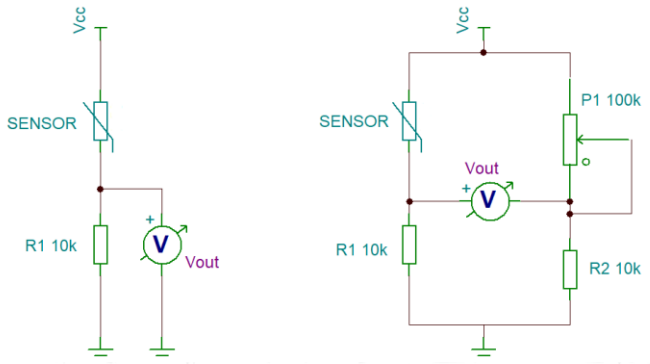

Figure 24: Final design of the voltage divider and of the Wheatstone bridge

In this design, to store the measure is necessary use to an Analog to Digital Converter (ADC), and in this case is chosen the ZSSC5101, which normally is used to measure two magnetoresistive bridges sensors. As Figure 25 shows, the typical application [16] of this integrated circuit one of their magnetoresistive bridge sensors is rotated 45 º than the other to obtain how many degrees is rotated the magnetic field measured to respect this sensors, this is because with this position of the sensors is obtained, with one of theirs, a measure correlated with the sine of the angle of the magnetic field, and with the other sensor, its measure is correlated with the cosine of the angle. For this reason, the output of the ZSSC5101 is the angle created with the sine and the cosine measured. Furthermore, this integrated circuit separates the power from the digital part of the analog part, that is important, because if both powers are together, the digital part can add noise to the analog part and that worsens the measure.

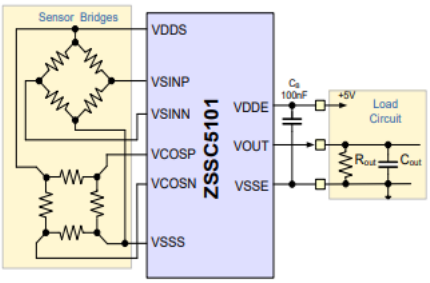

Figure 25: ZSSC5101 typical application circuit [16]

This integrated circuit has been chosen because the similarity between the gas sensor system in deigned before with a magnetoresistive bridge sensors, furthermore ZSSC5101 has two channels, being able that can measure two sensors at the same time only replicating the Wheatstone bridge.

3.1.2. Simulation

OrCAD Capture has been used to simulate these circuits. The behaviour of both circuits has been confirmed using Bias Point simulations. The value chosen to the potentiometer resistance is 100 kΩ. From these simulations, output voltage is obtained, and with these data are created a graph with Excel by Microsoft Office and they are compared with the equations 8 and 9.

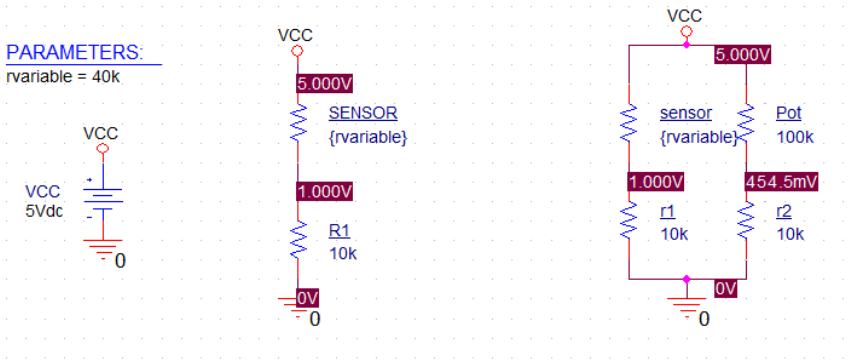

Figure 26: Schematic of simulation of both circuits

Simulations made with different value of the sensor resistance confirms that both circuits work as equations show. With the data obtained in the simulations is made a graph, which shows the main characteristic of the Wheatstone bridge, that is delete the offset voltage when the sensor is detecting clean air (in this case the value of the sensor resistance taken to the sensor when is detecting clean air is 100 kΩ). Figure 27 shows this graph.

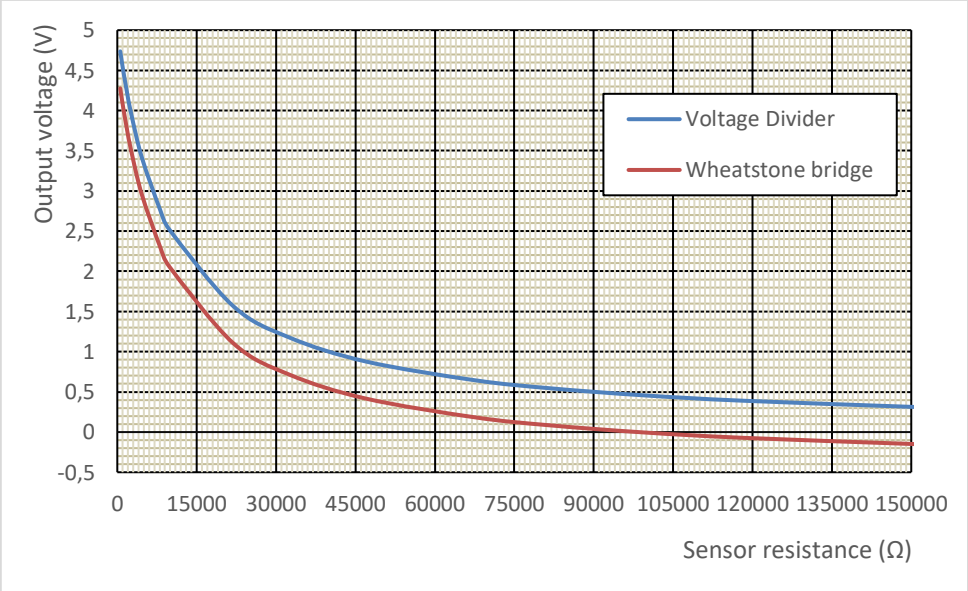

Figure 27: Graph with simulation data

3.1.3. Implementation

The design layout is created using the free software EAGLE 8.6.0 by Autodesk. This is the program most used for making Printed Circuit Boards (PCB) of two layers, with Altium Designer Program.

The first step to make the layout of the design is make a list with all components, that are necessary to make the design and looking for they in the distributor who are you going to buy them, because shape and package of each component must be known.

Once the components for the design have been chosen, their pin pads and model of each package must be in any library of the program, for this reason, all models will be looking for in all libraries of the software and models which are not in, they will be stored in a library which will be created. In this case only three components are not in any library of the software, these are the model of potentiometer, the model of ZSSC5101 and model of the socket SR6 by Figaro to family of TGS24XX and TGS26XX gas sensors.

To create any component in a library of Eagle is needed create a symbol to use it in the schematic of the design and the model of the package to use it in the layout of the design, Figure 28 shows three models of the package creates to the three components which did not have any model in any library of the software. In Figure 28, the potentiometer which is show is a rotatory potentiometer which can withstand much power this is because is the only type of potentiometer that was founded in the distributor.

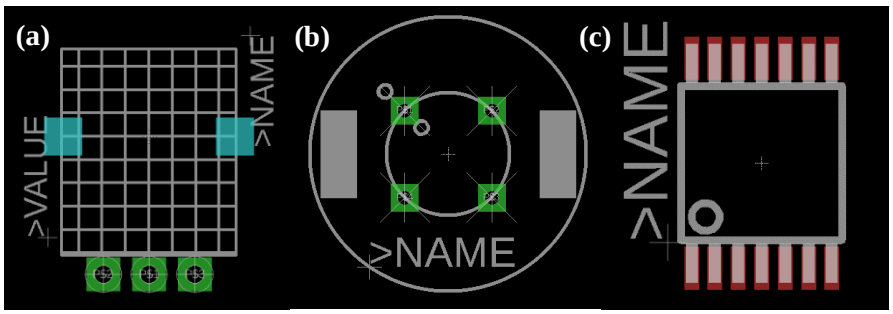

Figure 28: a) Model of the package of the potentiometer. b) Model of the package of the socket SR6. c) Model of the package of the ZSSC5101

With all models of components necessaries to build the PCB in some library, the schematic of the design is made. Figure 29 shows the schematic of the design, where jumper JP1 and JP2 is to choose which design wants measure between the voltage divider or Wheatstone bridge, besides it shows that the power of the heater resistance is separate from the whole design (HEAT pins), moreover a capacitor is between the digital signal wire and digital power of digital part, that is because is needed to correct behaviour of the ZSSC5101. In addition, the digital wires cross each other because a position of the digital connections is needed to connect this design to SSC Communication Board V4.1 by IDT. This Communication Board (SSC CB) is needed to communicate with the ZSSC5101 because this integrated uses a digital communications calls OWI, which is a communication through only one wire, and to create the communication between the integrated and one computer is needed this interface.

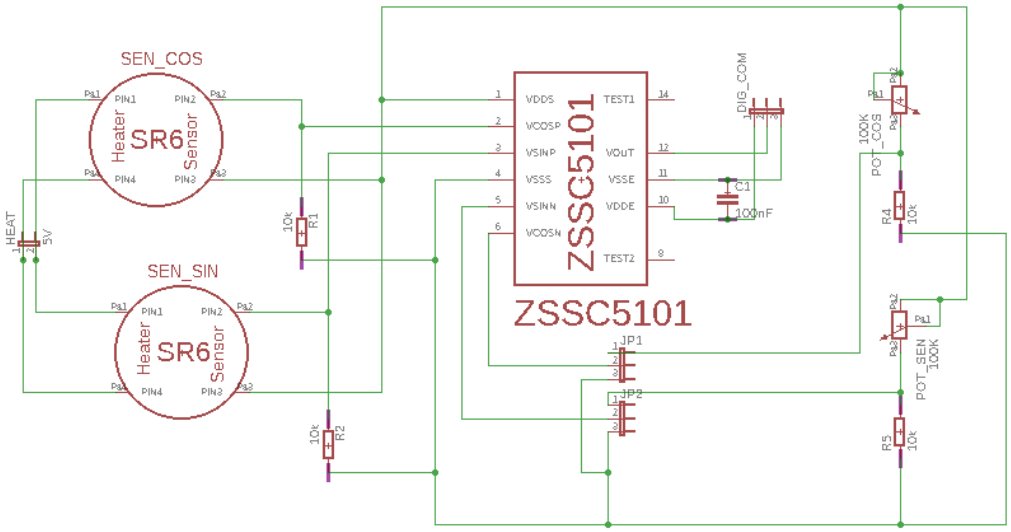

Figure 29: Schematic of voltage divider and Wheatstone bridge design

Last step with Eagle software is make the layout of the PCB, in this case, a PCB with two layers is chosen to make easier the routing of this. Figure 30 shows the result of the layout of the PCB. As the layout shows, the digital part has a ground plane surrounding the digital signal of the ZSSC5101, this is done to improve the integrity of the digital signal, creating a return path with low impedance.

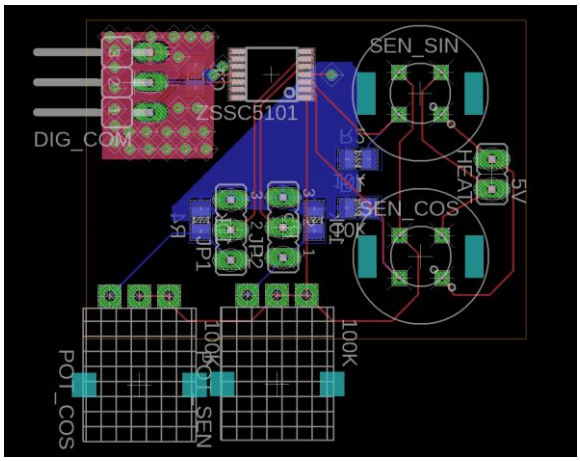

Figure 30: Layout of voltage divider and Wheatstone bridge design

With the layout finished, the PCB layout is printed in copper clad double sided FR4 fiberglass board with a milling machine. After that all components are welded by hand to the PCB. Figure 31 shows the result of the PCB of the design.

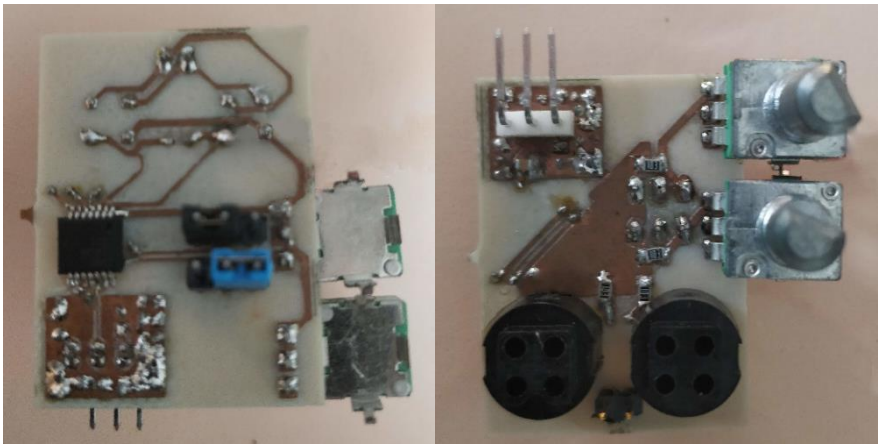

Figure 31: PCB of design of voltage divider and Wheatstone bridge

3.1.4. Problems and solutions

In this design, there was a problem with the communication between the ZSSC5101 and the computer trough the SSC CB. This communication was tried to do using first a LabVIEW example to the D2XX drivers created by FTDI chip[1] which communicates with SSC CB, but did not detect the ZSSC5101, for this reason it was impossible make the communication with LabVIEW. Owing to this program did not work, the communications between the computer and the ZSSC5101 was tried using commands that are given in a spreadsheet called "SSC CB Command Syntax for V4.x Communication Boards" in the official web page of the SSC CB[2], in this case, the supply voltage to the ZSSC5101 was turned on, but the communications with it was not possible did it. After testing these methods to create the communications, this topic was asked to the IDT company, but they did not answer it, due to this, the solution taken was use another platform to take the data. This platform will be the same for all and it will be discussed in the section 3.4 to use this data acquisition board is needed have a wire in points which are going to be measured, and to use a power supply which are not from the ZSSC5101 is needed other two wires, for this reason wires needed are soldier to the PCB where are necessaries.

3.2. Anderson loop

This second design is based on the Anderson loop that has been explained in the section 1.2.4, but a current power supply is needed to use this topology, and in the laboratory only are voltage power supply, for this reason a voltage-controlled current source has been created to power the Anderson loop.

3.2.1. Design and simulation

The first part to design is the voltage-controlled current source that has been based in a characteristic that the Generalized Impedance Converter (GIC) have when all passive elements of it are resistors, which is that the current that flows through the resistor R_5 is the same than the

[1] http://www.ftdichip.com/Support/SoftwareExamples/CodeExamples/LabVIEW.htm
[2] https://www.idt.com/products/sensor-products/sensor-signal-conditioners/ssc-cb-ssc-communication-board

current which flows through the resistor R_4, and the voltage between the pins of the resistor R_5 is the same than the reference voltage of the GIC such Figure 32 shows [17], [18].

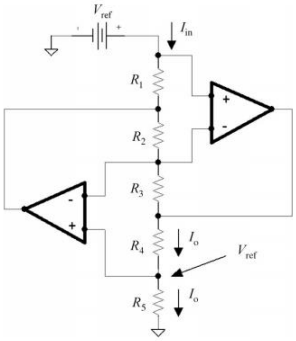

Figure 32: Constant current source to resistive elements create with a GIC [18, Fig. 3]

The first step to design this GIC is to selecte how many currents should be provided by the current source. In the first instance, 1 mA is chosen. To choose resistance R_5 and voltage reference of the GIC are some restrictions which are found in different paper, in the equation 6 of the paper [18] appears the first restriction. The first restriction is the equation 11 of this document.

$$V_{sat_{Op.Amp.}} \geq \left(1 + \frac{R_4}{R_5}\right) * n * I_{ref} = \left(1 + \frac{R_{sensor_{max}}}{R_5}\right) * I_o \quad \textbf{(10)}$$

$$Where \rightarrow R_4 = R_{sensor_{max}} \quad \& \quad I_{ref} = I_o$$

$$R_5 \geq \frac{R_{sensor_{max}} * I_o}{V_{sat_{Op.Amp.}} - I_o} \quad \textbf{(11)}$$

Where $V_{sat_{Op.Amp.}}$ is the saturation voltage of the operational amplifiers of the GIC, $R_{sensor_{max}}$ is the maximum value of the sensor resistance, which is placed in the same position of R_4, and the others variables are those shown in Figure 32. The second restriction is the equation 13 in [18], and it is the equation 13 of this work.

$$m < \frac{V_{sat_{Op.Amp.}}}{R_{s_{max}} * I_o} - \frac{R_4}{R_{s_{max}}} \quad \textbf{(12)}$$

$$Where \rightarrow m * R_{s_{max}} = R_{5_{max}} \quad \& \quad R_4 = R_{sensor_{max}}$$

$$R_{5_{max}} < \frac{V_{sat_{Op.Amp.}} - R_{sensor_{max}} * I_o}{I_o} \quad \textbf{(13)}$$

The last restriction is obtained combining equation 12 and 13 such as is presented in equation 14.

$$V_{sat_{Op.Amp.}} > I_o * (R_{sensor_{max}} - 1) \quad \textbf{(14)}$$

With above restrictions and the output current chosen is time to make the design. First of all, knowing the maximum value of the sensor, that is of 100 kΩ, this produce a maximum value of 100 V. Obviously this voltage is very huge to the power supply that are in the laboratory, the

(15)

range of the values of the sensor resistance is decrease to from 0.5 kΩ to 40 kΩ and for that values the restriction are as follows.

$$V_{sat_{Op.Amp.}} > 40V \rightarrow V_{sat_{Op.Amp.}} = 45V$$

$$0.889\Omega \leq R_5 < 5k\Omega \rightarrow R_5 = 4.7k\Omega \quad \textbf{(16)}$$

$$V_{ref} = R_5 * I_o = 4.7V \quad \textbf{(17)}$$

The other resistors are selected using the tool of simulation OrCAD Capture to obtain values which make the circuit works properly, but taking into account that R_3 must have a high value to assure good efficiency between the upper operational amplifier output current and the current source [18]. With a R_3 with a resistance value of 47 kΩ, this is because is close to the maximum value of the resistance sensor, the value of resistances of R_1 and R_2 have been modified to achieve, in the lower values of the range, a properly behaviour of the GIC.

Before selecting the value of R_1 and R_2, the operational amplifier (Op. Amp.) of the GIC is selected. In order to select the Op. Amp. the equation 15 is considered and, if it is possible, an Op. Amp. with a small input offset current or with a high input resistance value should been chosen. In this case, the Op. Amp. selected is the OPA454 by Texas Instruments which can withstand from 10 V until 100 V of power voltage, and the input offset current can be up to 0.1 µA at 25 °C [19] which is an input offset current sufficiently low to the properly work of the GIC.

After the Op. Amp. to the GIC was selected, the schematic is created of the GIC in OrCAD Capture with the PSpice models of components of the GIC. With the method above mentioned the values of resistances of R_1 and R_2 are obtained, and these values are 3.3 kΩ to both, as Figure 33 shows.

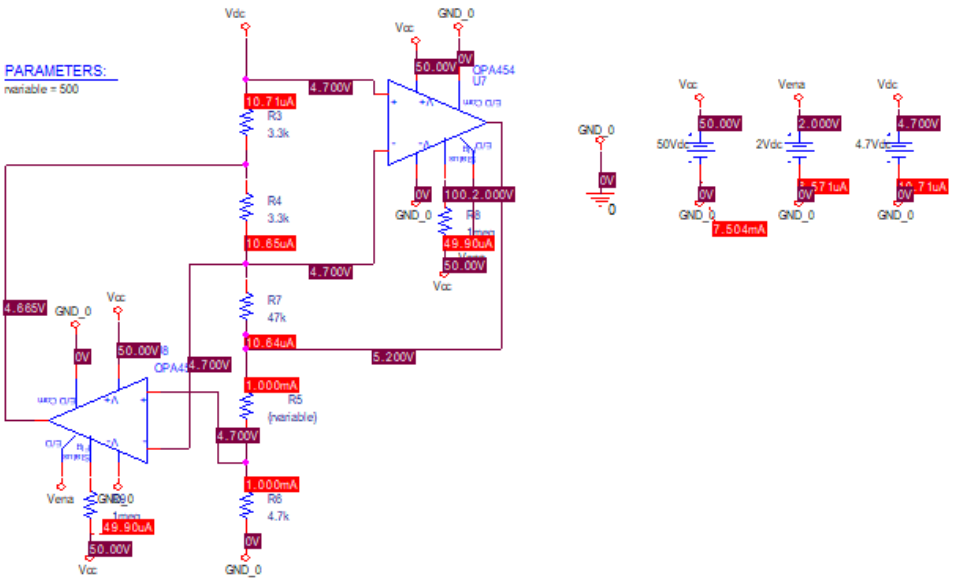

Figure 33: Results of simulation of GIC with the value of the sensor resistance equal to 500Ω

This design was not implemented because two reasons, it does not accomplish with the range laid before of the values of the sensor resistance, which is from 500 Ω to 100 kΩ, besides this type of

sensors only can dissipate 15 mW of power, and with this current in the worst case the sensor dissipates 40 mW. Owing to this, the current supply was decreased until 0.1 mA, and the range of the value of the resistance of the sensor was restored to the first values between 500 Ω until 100 kΩ. With this change all restrictions were recalculated with the following results.

$$V_{sat_{Op.Amp.}} > 10 \;\rightarrow\; V_{sat_{Op.Amp.}} = 15V \tag{18}$$

$$0.66\Omega < R_5 < 50k\Omega \;\rightarrow R_5 = 33k\Omega \rightarrow V_{ref} = R_5 * I_o = 3.3V \tag{19}$$

For this design the value of resistances R_1, R_2 and R_3 were not changed, because keeping these values, in the lower part of the range of the values of the sensor resistance the design continues working properly. Nevertheless the Op. Amp. of the design was changed by the OPA202 due to this last Op. Amp. has less input offset current and less input offset voltage, which can be up to 150 pA and 200 μV respectively, and its supply voltage in single supply is from 4.5 V to 36 V [20].

Once the current source is designed, it is time to design the Anderson loop. In this topology, the differential voltage of the sensor resistance is subtracted to the differential voltage of a reference resistor. Both are powered by the same current to obtain a voltage which only depends on the variation of the sensor resistance, as equation 21 shows

$$V_o = A_1 * v_1 - A_2 * v_2 = A_1 * I_o * R_{sen} - A_2 * I_o * R_{ref} = I_o * \left(A_1 * R_{sen} - A_2 * R_{ref}\right) \tag{20}$$

$$If\ R_{sen} = R_{sen_0} * (1 + \alpha) \;\;\&\;\; A_1 * R_{sen_0} = A_2 * R_{ref}$$

$$V_o = I_o * A_1 * R_{sen_0} * \alpha \tag{21}$$

But in this case the sensor resistance decreases its value, this produces a negative α and make that the output voltage lead to a negative voltage, this makes that a negative power supply to the Op. Amp., on account of this, in this design the value of the reference resistor is subtracted to the value of the sensor. After this change in the Anderson loop the equations of the circuit are the following.

$$V_o = A_2 * v_2 - A_1 * v_1 = A_2 * I_o * R_{ref} - A_1 * I_o * R_{sen} = I_o * \left(A_2 * R_{ref} - A_1 * R_{sen}\right) \tag{22}$$

$$If\ R_{sen} = R_{sen_0} * (1 + \alpha) \;\;\&\;\; A_1 * R_{sen_0} = A_2 * R_{ref}$$

$$V_o = -I_o * A_1 * R_{sen_0} * \alpha \tag{23}$$

As it is indicated in equations 10 and 12 the sensor is placed in the position of R_4 of the GIC, and to the reference resistor has been place a characteristic of this GIC has been considered. This characteristic is that R_4 and R_5 have powered by the same current because of the reference resistor has been place in the position of R_5. The differential voltage of the reference resistor is currently a single-ended voltage, due to this a differential voltage measure is not necessary in this case and to apply the gain A_2 is only necessary to create a non-inverter amplifier which has been created with the same Op. Amp. of the GIC (OPA202), with a gain between 1 to 4.5 which is controlled by a potentiometer in the position of R_1 in the circuit (Figure 34). The behaviour of the voltage output of this circuit follows the equation 24 [21], for that reason the resistance selected to R_2 has a value of 1 kΩ and the potentiometer R_1 position have a maximum value of 3.5 kΩ.

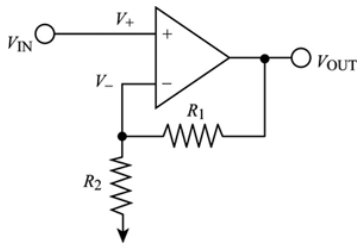

Figure 34: Non-inverter amplifier

$$A_{non-inverter} = \frac{R_1 + R_2}{R_2} \quad \textbf{(24)}$$

The differential voltage of the sensor has been measure with an instrumentation amplifier which must have a small input bias current to the GIC continues working properly. For this reason, the instrumentation amplifier selected to measure the differential voltage of the sensor is the INA188 with a maximum value of input bias current of 2.5 nA, and it is a Rail-to-Rail allowing a values close to 0 V in the output [22].

the INA188 has been used to compose the active subtractor, mainly due to it is a Rail-to Rail instrumentation amplifier, which is powered by the same voltage than all Op. Amp.

The last step of this design is to create a differential Low Pass Filter with a cut-off frequency close to 50 Hz, because the sensor changes slowly, and the noise should be deleted by the grid circuit in the measure. This design filter is created, in the software TINA by Texas Instrument for drawing a schematic and using the tool to make the diagram bode, the behaviour of the filter in differential mode and common mode has been studied. This filter has been designed following a paper focus on the design of differential filters of first and second order. To simplify the filter, and because is enough to this application, the filter is a first order passive filter. Using the equations of the paper [23] the values to the filter are showed in the schematic of the Figure 35, and this filter has a cut-off frequency of 48.04 Hz in both modes such as show the Figure 36.

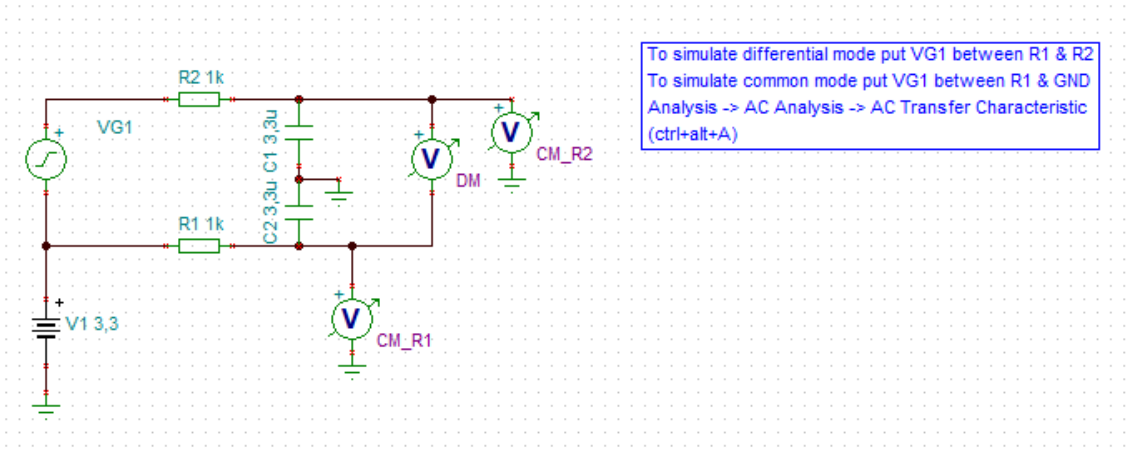

Figure 35: Schematic to get bode diagrams of the filter

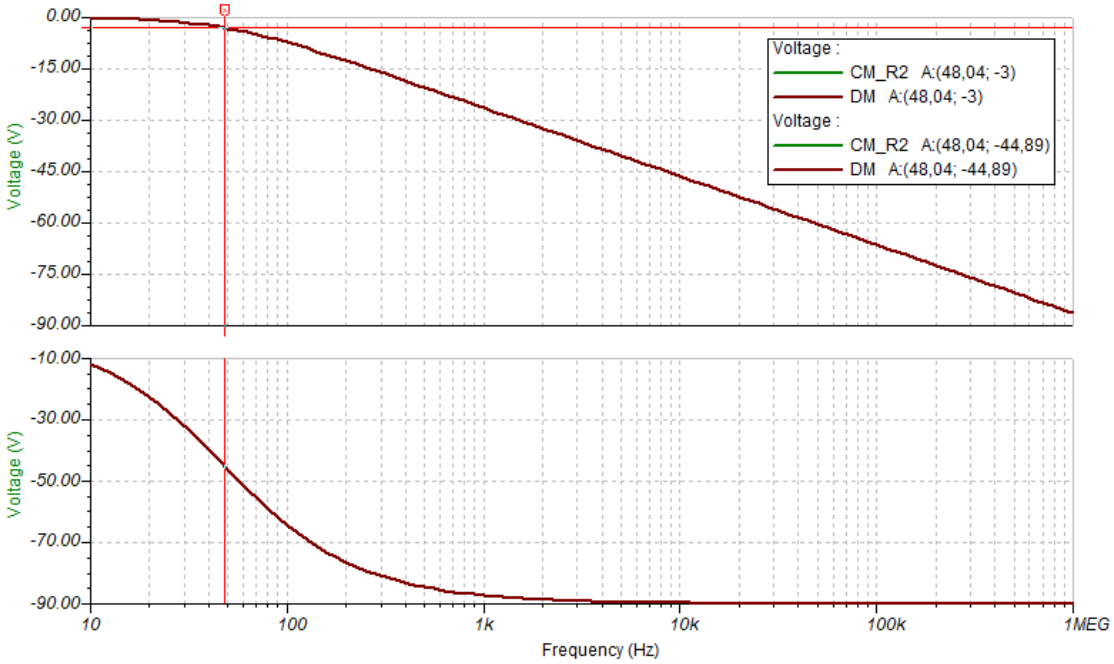

Figure 36: Bode diagram of common mode and differential mode of filter

The last step of this design to check that this works properly. All stages of the design are put together in the same simulation in the software OrCAD Capture as Figure 37 shows. Results of simulations are compared with the equation 23 to check the correct behaviour, and in Figure 38 can be observed the results are correct for the range of working. The range of the sensor resistance can increase up to 300 kΩ only growing the voltage which power Op. Amps. and instrumentation amplifiers up to 36 V and growing the gain of the reference resistor amplifier.

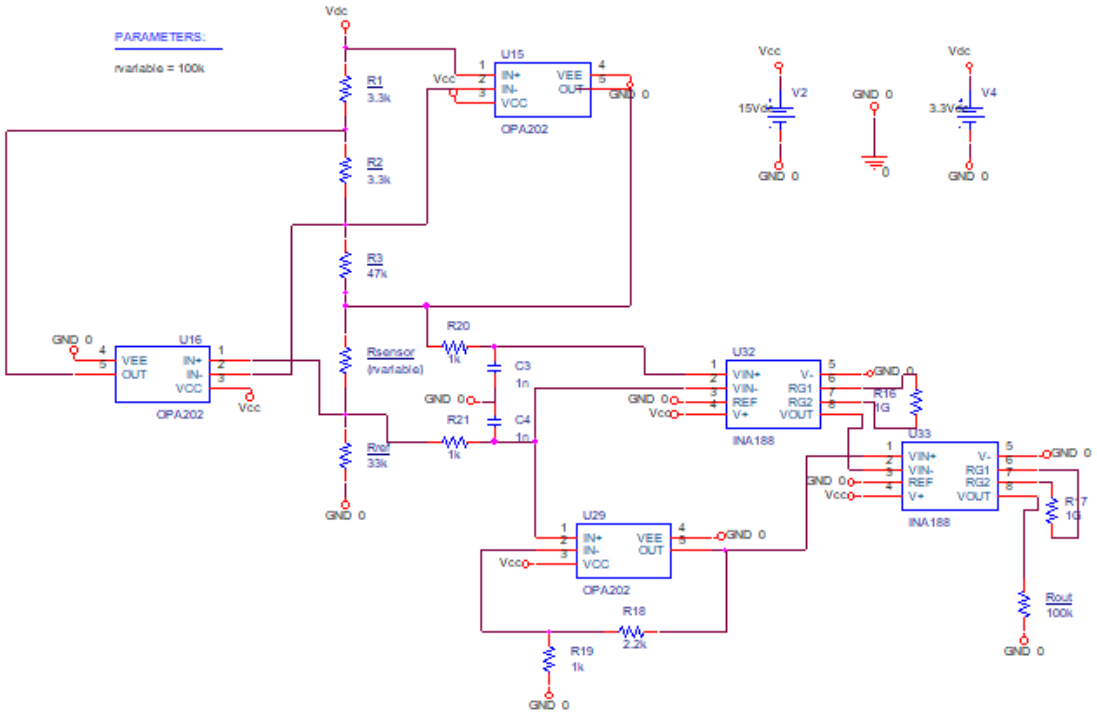

Figure 37: Schematic of design made in OrCAD Capture

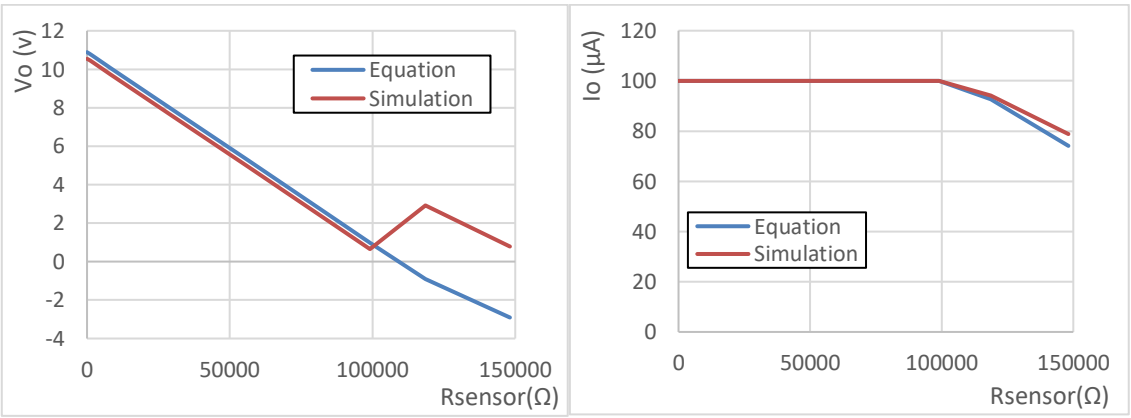

Figure 38: Results of simulation compared with the values of the equations of voltage output and current output of GIC

3.2.2. Implementation

The layout of this design has been made using the same software than the voltage divider and Wheatstone bridge design, that is Eagle 8.6.0 by Autodesk. As in the before design, the first step is to make a design of the components which are not in any library. In this design, five components are not in any library, these five components are the OPA202, the INA188, two different terminal bocks that are going to be used, and the potentiometer.

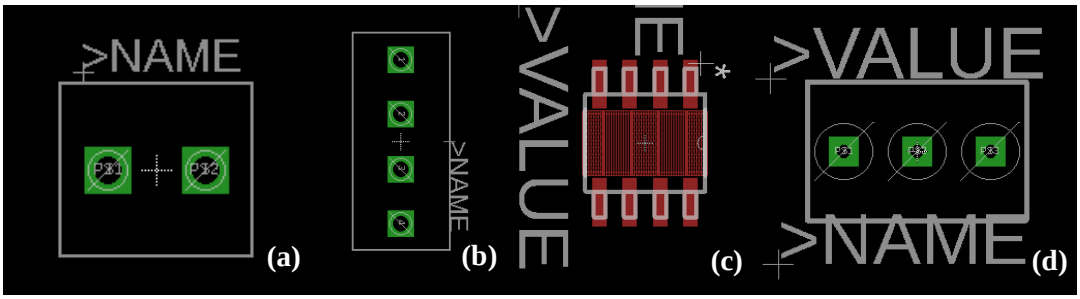

Figure 39: a & b) Model of the package of different block terminals. c) Model of the package of the INA188 and OPA202. d) Model of the package of the potentiometer.

With all models of all necessaries components, the schematic of the design has been made. As Figure 40 shows the block of two terminals is to power the heater of the sensor, and in the block of four terminals are both voltage inputs (3.3 V and 15 V), the ground of the circuit, and the output voltage. In the Figure 40 is indicated each stage of the design with different colours to make is easy to understand.

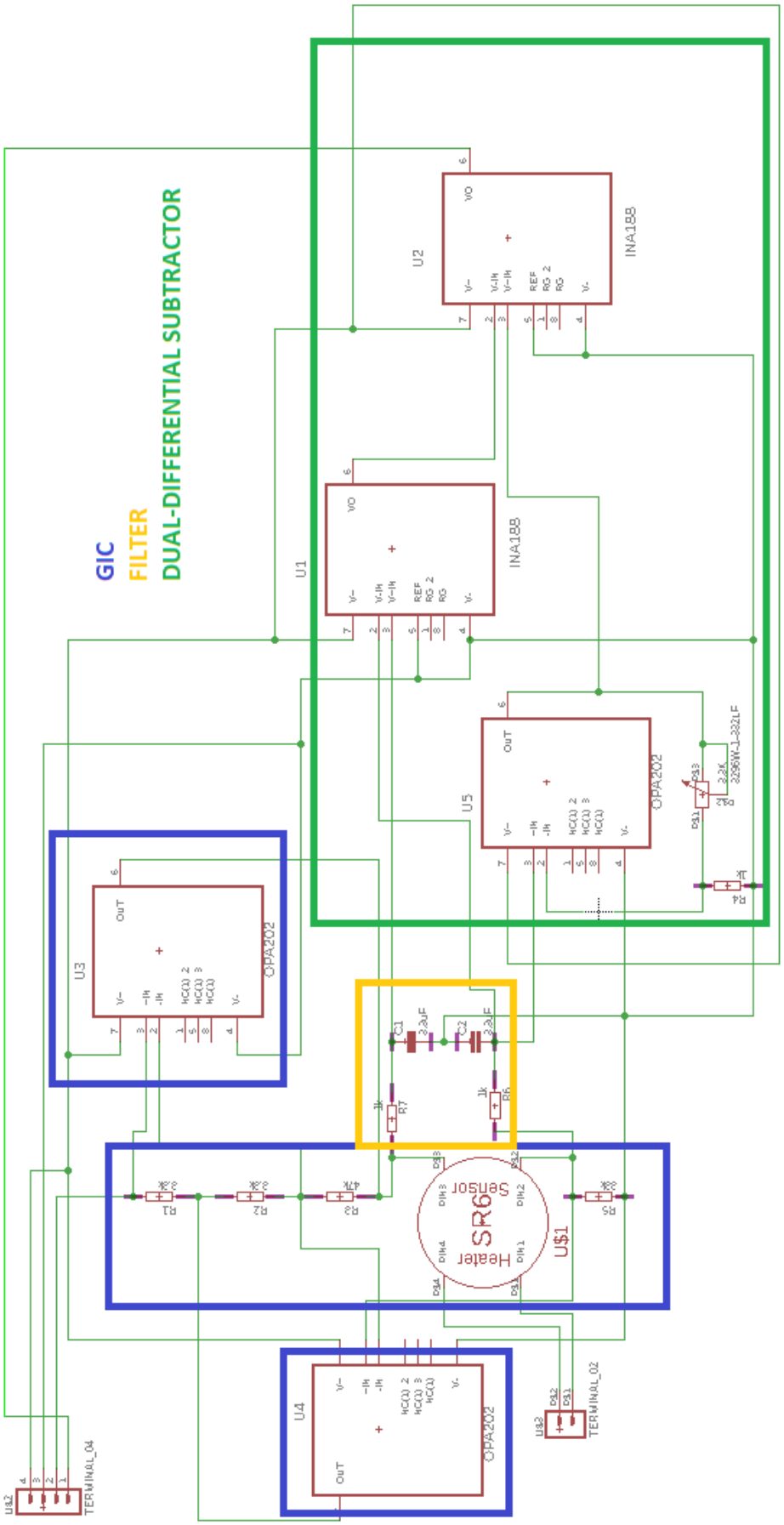

Figure 40: Schematic of Anderson loop design, with each stage of the design indicated

Based on this schematic, and with the same software, the layout of the design is made with two layers.

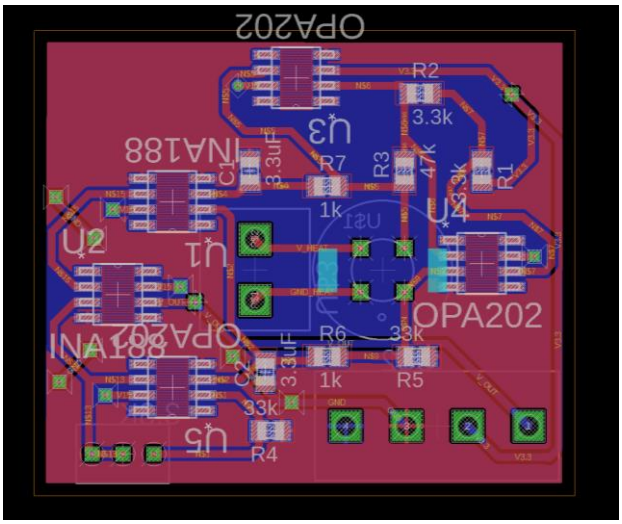

Figure 41: Layout of Anderson loop design

Once the layout was made, the PCB is fabricated, and all components are welded by hand obtaining the PCB of the Anderson loop design finished. Figure 42 shows the finally results of the PCB of this design.

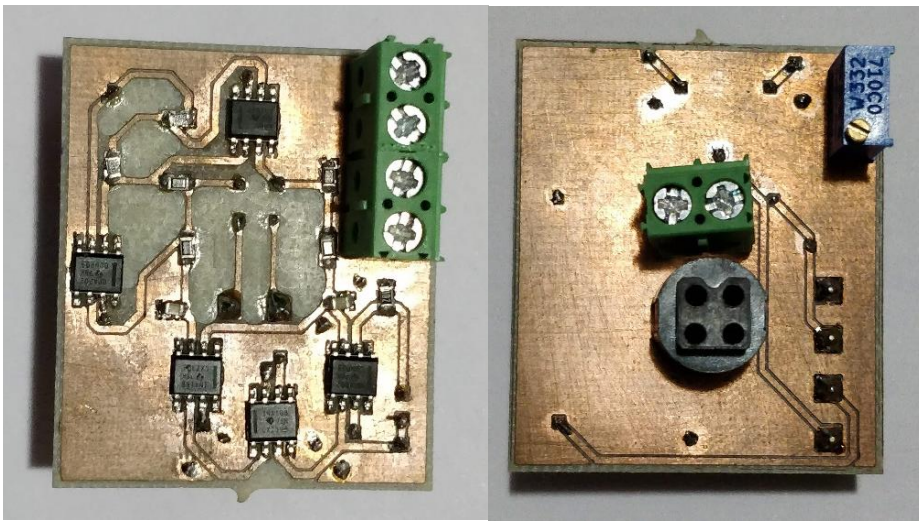

Figure 42: Both sides of the PCB of Anderson loop design

3.3. Timer 555 and pseudo capacitance

This design is based on a paper [12], and it consists in creating a pseudo capacitance which has a linear variation with the sensor resistance using a GIC explained in the section 1.2.3. With this pseudo capacitance, the astable mode of a timer 555 is used to create a square signal whose frequency depends on the sensor resistance.

3.3.1. Timer 555

Timer 555 is an integrated circuit whose principal function is to create pulses of temporization with a great precision, also it can be an oscillator as it has been used in this application. This integrated circuit (IC) has three working modes, which are monostable, bistable and astable modes [24].

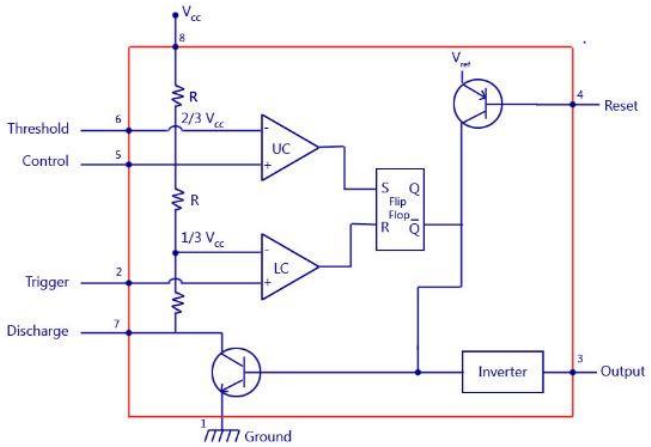

Figure 43: Block diagram of 555 Timer IC

In this design only the astable mode has been used, and this mode consist on charging and discharge a capacitor between 1/3 Vcc and 2/3 Vcc. The time of charge and discharge depends on two resistances and a capacitor. To implement this mode is necessary use the circuit which is presented Figure 10. In this design the capacitor "C" has been the GIC circuit simulating a capacitor. The output signal of this circuit is a square wave whose frequency follows equation 5.

3.3.2. Design

The circuit presented in paper [12] has been rendered to study this mode of working, the timer 555 has been used as an integrated circuit, and the operational amplifier OPA202 compose the Anderson loop design in the section 3.2. Another change between this design and the design of the paper is the range of the sensor resistance, in the paper the range is between 0.5 kΩ to 30 kΩ, but in this design is between 0.5 kΩ to 100 kΩ, changing the maximum output frequency which is around 20 kHz following the equation 25.

$$f_{out} = \frac{1.44 * R_{sensor} * R_5}{3 * R_a * C_3 * R_2 * R_4} \quad \textbf{(25)}$$

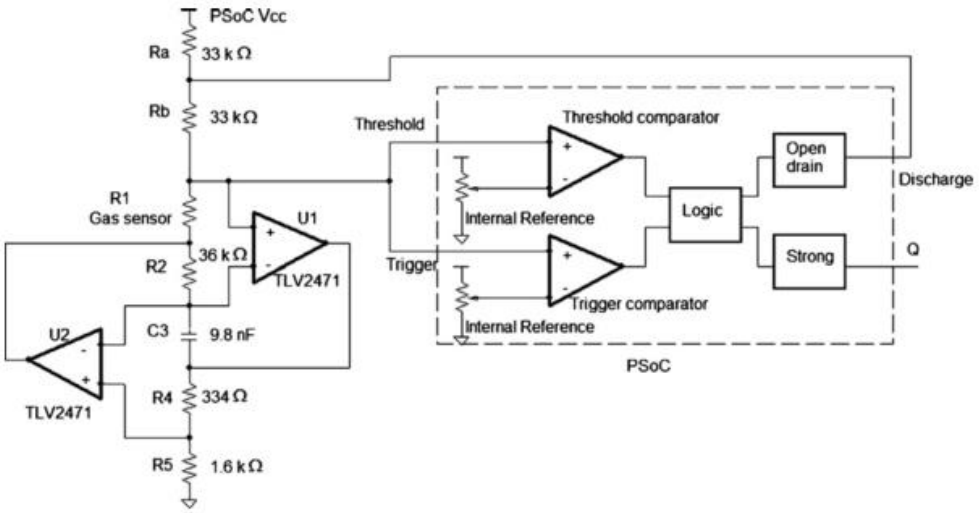

Figure 44: Design made in the paper [12, Fig. 3]

As it is a design from a paper, any simulation of it was not made. For this reason, the following step of this design is to make the PCB with the paper's design.

3.3.3. Implementation

The first step to the implementation is to choose all components necessaries to the design, founded in the distributor have a package model all of them in the PCB design software which in this case as in the above designs is the EAGLE 8.6.0. In this case, only is needed to create a package model of a block of three terminals, all other components were made for using in the other designs.

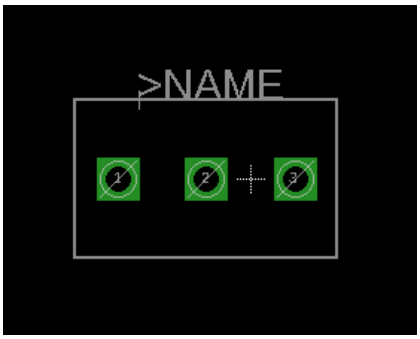

Figure 45: Package model of block of three terminals

Second step of the implementation is to create the schematic of the design in the EAGLE, because this has been a route to follow when the layout of the design will be made. As it is shown in this design the 555 timer selected is the TLC555 by Texas Instrument which has very low power consumption [13] besides the TLC555 has the output maximum frequency 2 MHz which is enough to this design. Moreover, in the block of figure 45 the three terminals are the input voltage, the ground of the circuit and the output voltage of the circuit, and as similarly to the above design the power of the heater of the sensor is separated from the others.

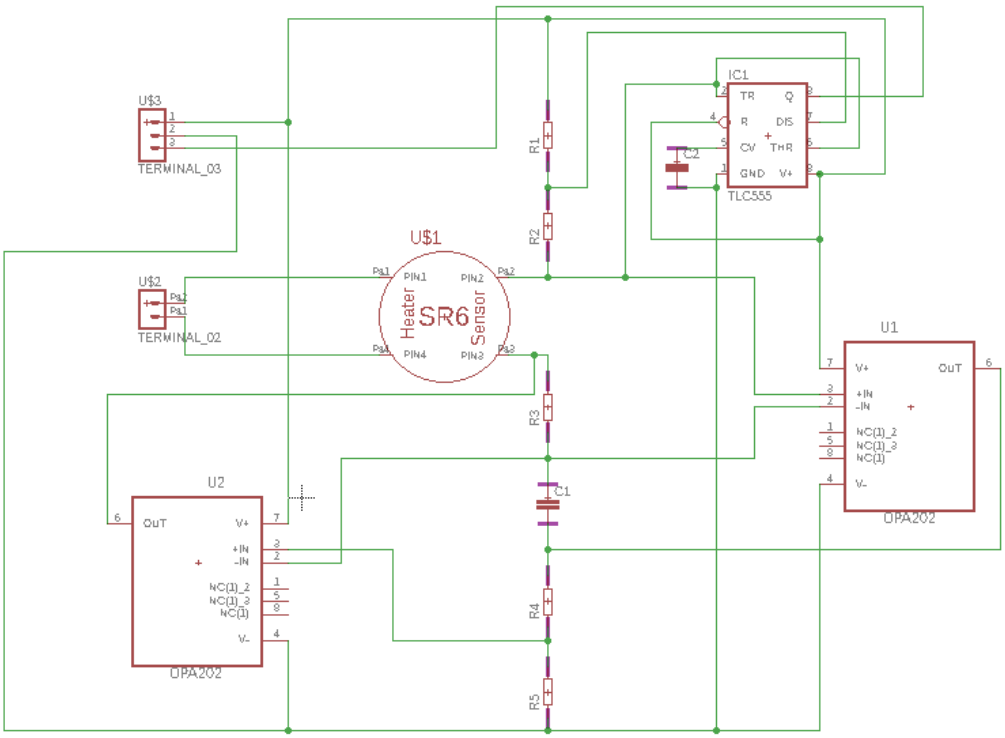

Figure 46: Schematic of the 555 timer design

Once the schematic had been made, the layout of the PCB of the timer 555 design was created based on this schematic.

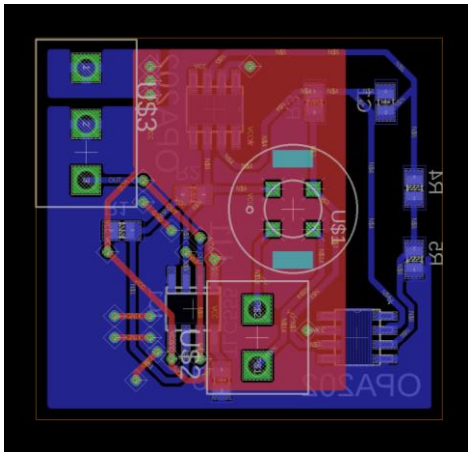

Figure 47: Layout of PCB of 555 timer design

To finalize the implementation of the design, the PCB was routed, and all components were welded by hand, obtaining the result, that is showed in the Figure 48.

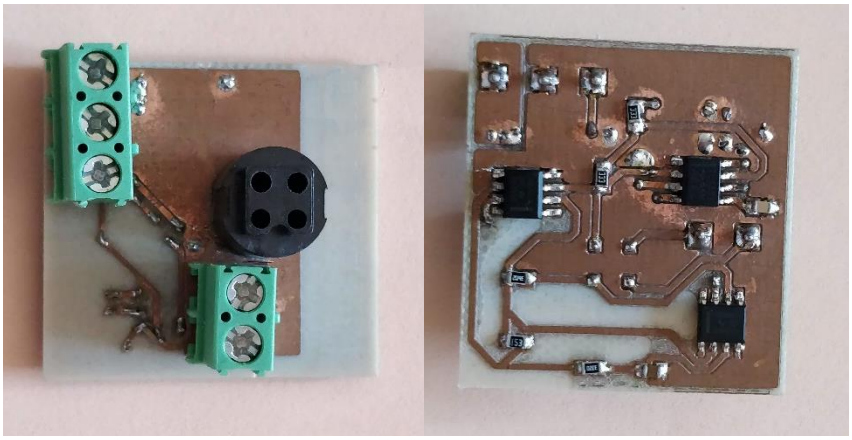

Figure 48: Final result of PCB with the 555 timer design

3.3.4. Problems

In this design, some problems were founded. First was that the voltage to power the Op. Amp. and the timer 555 with the GIC were different in the design of the paper because of a misunderstanding they are together in the design. This problem was solved separating both sources cutting the power plane by the centre and welding a wire in the subplane which does not have any terminal, as Figure 49 show.

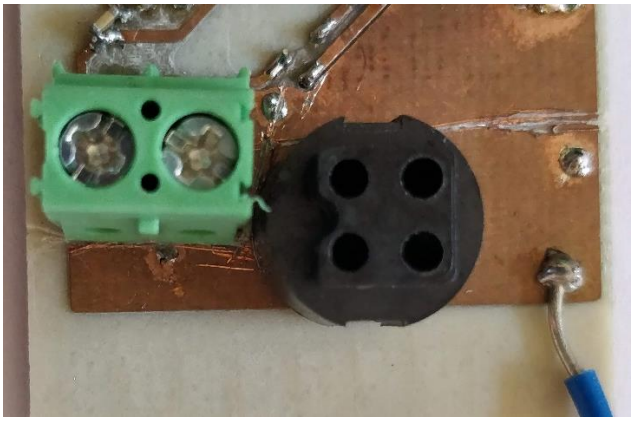

Figure 49: Cut made in the power plane

With both power planes separates the following problem was that the integrated circuit TLC555 needs a minimum input voltage of 5 V, and in the paper a PSoC simulating the behaviour of a timer 555 is used, whose input voltage is 3.3 V. This problem is easy to solve by increasing both voltages, the voltage of the GIC and the TLC555 to 5 V and the voltage to power Op. Amps. to a value greater than 6.043 V following the equation 2 of the paper [12], due to the value of the voltage power to Op. Amps. selected is 10 V.

After these changes were made, other problem appeared, when the design was tested. If in the position of the sensor are a resistor bigger than 80 kΩ, a glitch appears in the output signal. For example with a resistance of 82 kΩ, the signal oscillates at 240 kHz during 70 μs, and after that output signal does not oscillate during 36 μs, and it starts to oscillate again during 70 μs repeating this process all the time. For this reason, this design has been redesigned.

3.3.5. Redesign

This design should work, because is made with the equations given in the paper [12], this redesign has been made with the help of the electronic simulation software. This design first was simulated in OrCAD Capture, but in this simulator the behaviour of the TLC555 did not work properly every time, because sometimes when the output signal is low the pin of discharge of the TLC555 did not make a short circuit with ground such as Figure 50 shows. Consequently the electronic simulation software is changed by the Tina by Texas Instruments due to all integrated circuits that are used in the design are from the same company, and this simulator has especial models to the timer 555 of the company.

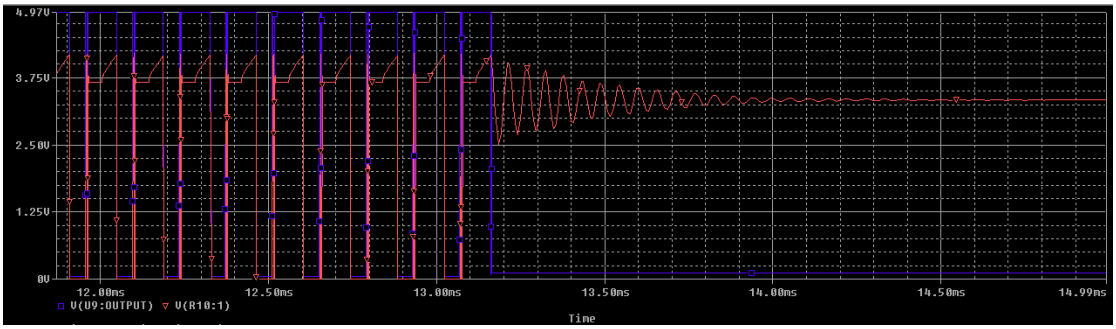

Figure 50: Simulation where the discharge voltage (Red) do not go to ground when the output signal (blue) is low level

When a simulation with a value of the resistance sensor 82 kΩ is made, the results confirm that the circuit do not works properly, and that the equation 2 of the paper [12] is not correct to all cases, because they only take into account the Op. Amp. of the GIC which have between its input the gas sensor and the R_2 to calculate this equation, but as Figure 51 shows the other Op. Amp has in its output a value close to 10 V.

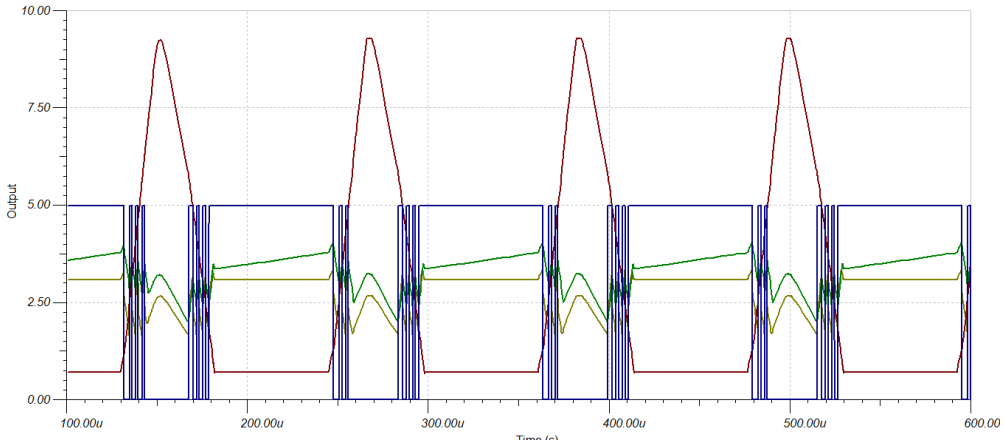

Figure 51: Simulation of the design with 82kΩ as value of sensor resistance

The first test that was made to correct the error was changing the R_5 by the C_3 of the circuit of the Figure 44, with this change the behaviour of the circuit should not change, due to the impedance of the GIC did not change, as equation 3 shows. With this change, the output voltage of the Op. Amps. decrease as Figure 52 shows, yet the frequency of the output signal is to high.

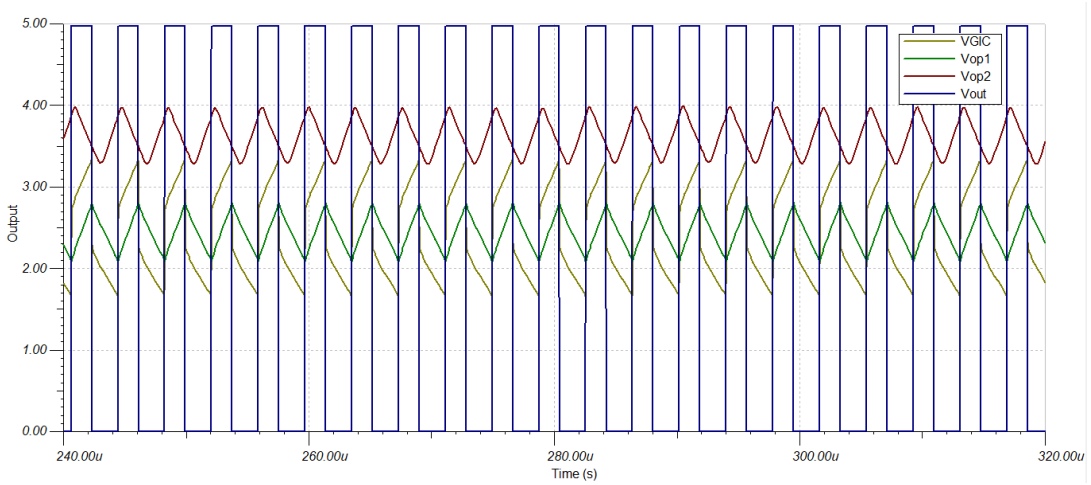

Figure 52: Simulation of the design with R_5 and C_3 changed position and with the value of the sensor resistance as 82kΩ

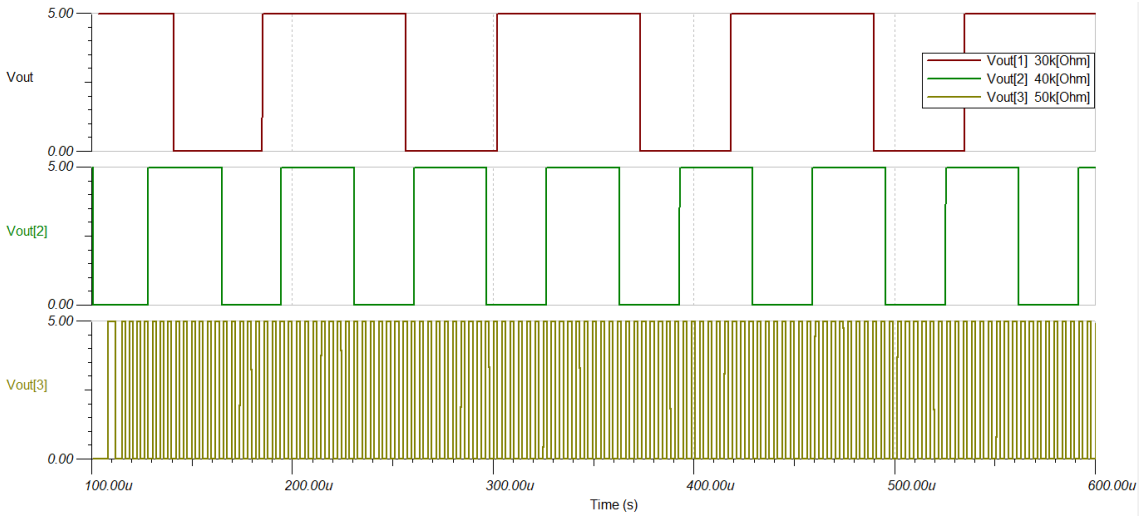

Figure 53: Simulation of modify design using 3 different values of sensor resistance

Figure 53 shows that the frequency of the output has increased very fast between the value of the sensor resistance of 40 kΩ to 50 kΩ. That is corrected when the value of the capacitor C_3 is grow at the same time that the value of the R_5 is grow too. Finally, the solution obtained is to change the positions of C_3 and R_5 and to grow their values until 33 nF and 15 kΩ as Figure 54 shows.

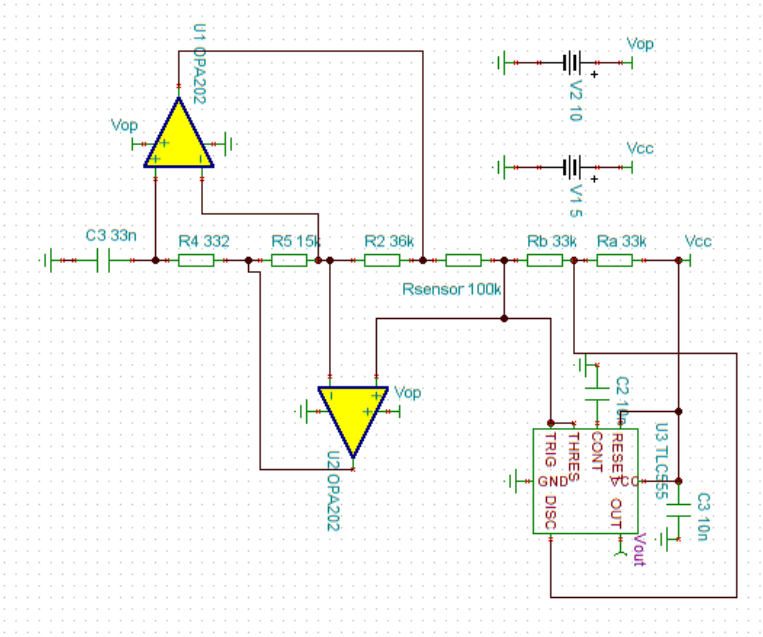

Figure 54: Final schematic of the timer 555 design

The last step is simulating different values of sensor resistance, to see if the design works properly, Figure 55 shows that meanwhile the value of the resistor is lower 40 kΩ, the output frequency has the same behaviour than the equation. If the sensor resistance has a value greater than 40 kΩ, the frequency in lower in the simulation than the calculated by equation 25, this is due to that the Op. Amps. have single supply but considering this error the design can be used.

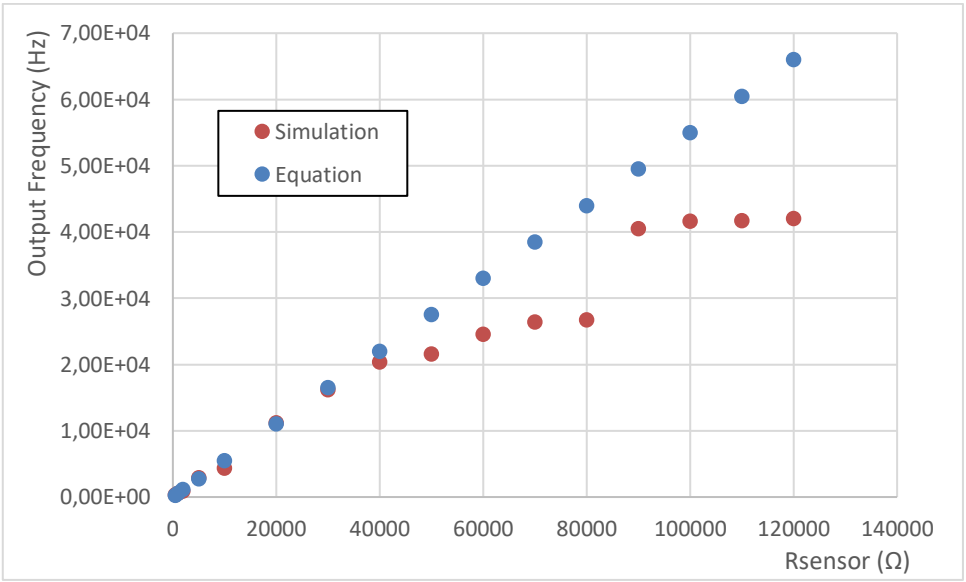

Figure 55: Comparation of the simulation of the output frequency of the new design, with its equation

As before the design did not work properly, the new design is implemented in the same PCB that the previous one. It was only needed to change two components with the same package model. In this test was discovered that if the GIC and the TLC555 are powered by 5 V another glitch, which is not in any simulation, appears as Figure 56 shows.

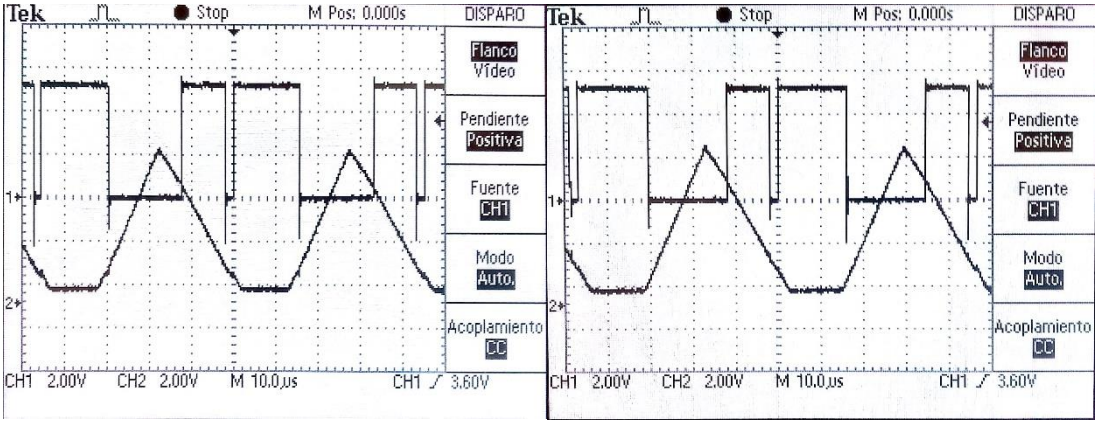

Figure 56: Output signal and output voltage of Op. Amp.U2 of Figure 45 of new design when the GIC and the TLC555 are powered by 5V, with value in the sensor resistance of 82kΩ (left) and 100kΩ (Right)

This glitch was avoided by increasing the voltage which powers the GIC and the TLC555. Consequently, the voltage that power Op. Amps. was increased in order to Op. Amps. do not saturate. This design starts to work properly when the voltage of GIC is greater than 6.1 V, as Figure 57 shows.

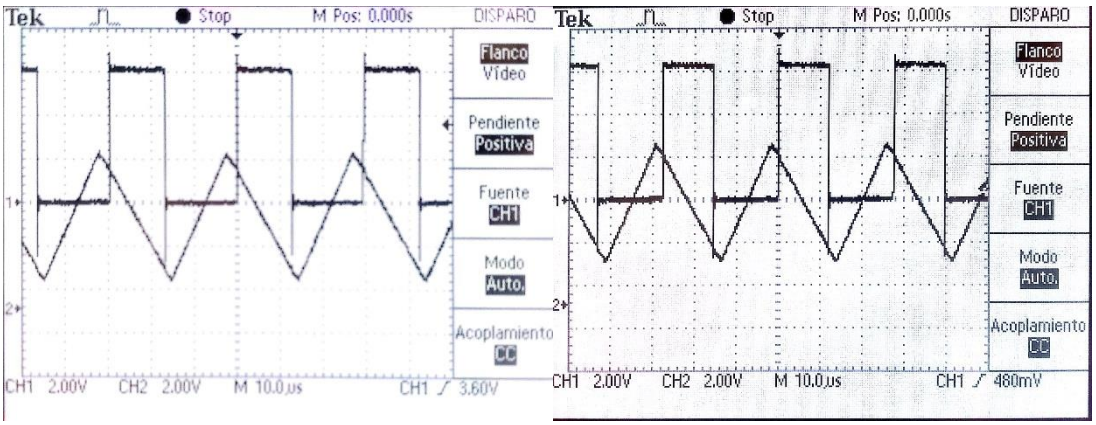

Figure 57: Output signal and output voltage of Op. Amp.U2 of Figure 45 of new design when the GIC and the TLC555 are powered by 6.1V, with value in the sensor resistance of 82kΩ (left) and 100kΩ (Right)

Finally, the voltage to power the GIC and the TLC555 has been 9 V and the voltage to power the Op. Amps. has been 15 V, because both voltages are standard voltages. With these voltages the behaviour of the design is showed in the Figure 58.

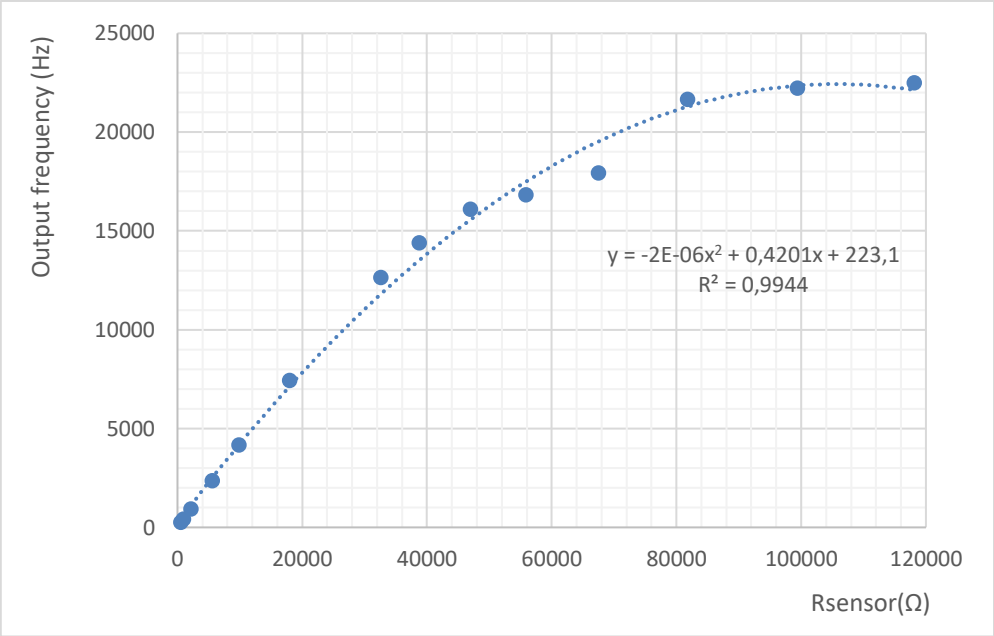

Figure 58: Real behaviour of the design

As Figure 58 shows the behaviour of the design is lineal with the sensor resistance between 500 Ω to 40 kΩ as the paper [12] shows. But when the sensor resistance is bigger than 40 kΩ, the output frequency is not enough to maintain the linearity of the system. This could be because of two reasons: firstly, the Op. Amps. need negative voltage, and secondly Op. Amps. do not have a linear response in this frequency. But although the linearity of the system is breaking in the higher frequency response, the behaviour of this sensor can be represented with the equation which is in the figure with an acceptable error.

3.4. Data acquisition system

To compare these different designs are needed any system to record the output signal of each design, for this reason a digitalization of the output signal is needed. This digitalization of the signal has been made with the integrated circuit ZSSC5101 in the beginning. This integrated circuit is used as signal conditioner to magnetoresistances bridges, which are similar to the Wheatstone bridge made with this kind of sensors. But the communications with this integrated circuit was difficult and it could have been used only to the first design because it provides a power voltage to the analog circuit of 5 V. If this circuit was used, it would needed to weld this component to each design. For that reasons this integrated circuit was not used.

A system which does not need to be weld was looking for, besides this system must measure voltages greater than 10 V because the Anderson loop design needs it. Furthermore, this system must to have a sample rate greater than 50 kHz to measure properly the output signal of the timer 555 design. Taking all these terms into account, and looking for a cheap system, the Red Pitaya STEMlab 125-14 board was selected. It is a board that is managed by a processor dual core ARM cortex A9 inside of a FPGA Xilinx Zynq 7010 SoC, moreover it has two Analog to Digital Converter (ADC) of 14 bit, which each one can work in two different ranges of voltage measurements, one voltage range is between -1 V to 1 V with a minimal voltage sensitivity of 0.122 mV and, and the another is between -20 V to 20 V with a minimal voltage sensitivity of 2.44 mV [25]. These ADC are connected with a FIFO memory using the protocol AXI which

write the FIFO when an trigger event occurs. These ADC can work with different sample rates that Figure 60 shows [26].

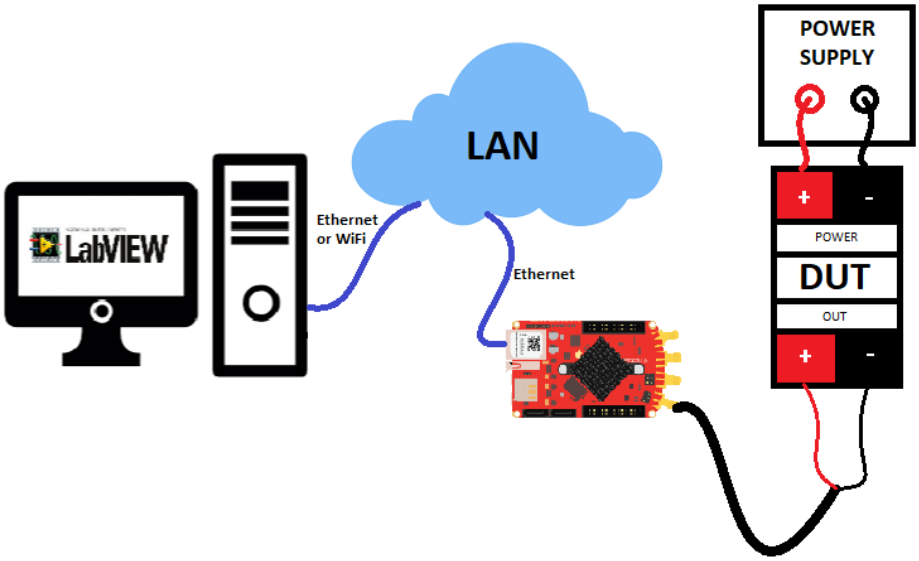

Figure 59: Acquisition system used

Sampling Rate	Time scale/length of a buffer
125 MS/s	131.072 us
15.6 MS/s	1.049 ms
1.9 MS/s	8.389 ms
122.0 MS/s	134.218 ms
15.2 kS/s	1.074 s
7.6 kS/s	8.590 s

Figure 60: Sampling rates available to each ADC of the Red Pitaya board

Unfortunately. this board has a problem. The board works like an oscilloscope, which means that ADCs write a memory buffer when a trigger event occurs. However, to use it in this project, this board should work like continuous acquisition system. This problem was solved using the project made by Nils Roos which made a new configuration of the FPGA to create new channel that connects the ADC directly with the main memory, and to create a Direct Memory Access (DMA) which is used to allow that user will be able to read the main memory [27]. This project was created to the Operative System (OS) of Red Pitaya 0.92v or 0.94v but when the Red Pitaya STEMlab 125-14 board was received it works with the OS of Red Pitaya 0.96v, for this reason in a new microSD card the old OS was installed, this old OS was founded in the repositories of Red Pitaya[3]. In this case the OS chosen was the version 0.94-RC8, all these OS are based on a linux OS using the Linaro Proyect. Using this OS, and using software WinSCP, files given by Nils Roos are copied into the memory of the Red Pitaya, these files are two, the first modify the FPGA creating the changes previously indicated, which is stored in the folder ~/tmp, and the another file is a program which can store in a file all data of ADCs or can create a communication TCP or UDP with another computer and send all data through it like the user wants. The following step

[3] http://downloads.redpitaya.com/downloads/

is to modify the FPGA configuration using the first file, the software PuTTy was used to send commands to the processor of the Red Pitaya board through an SSH communication and using the following commands the FPGA is configurated to work as is wanted.

```
systemctl stop redpitaya_nginx.service
cat ~/tmp/ddrdump.bit > /dev/xdevcfg
systemctl start redpitaya_nginx.service
```

The program which creates the communication with another computer is knowing how execute following the help of it that Figure 61 shows.

```
redpitaya> ./rp_remote_acquire -h
Usage: ./rp_remote_acquire [-mapqukfgrhcdes]
-m  --mode <(1|client)|(2|server)|(3|file)>
        operating mode (default client)
-a  --address <ip_address>
        target address in client mode (default empty)
-p  --port <port_num>
        port number in client and server mode (default 14000)
-q  --secondary_port <port_num>
        secondary port number in dual channel client mode (default 14001)
-u  --udp
        indicates tool should use udp transfer (default tcp)
-k  --kbytes_to_transfer <num_kbytes>
        kilobytes to transfer (default 0 = unlimited)
-f  --fname <target>
        target file name in file mode (default /tmp/out)
-g  --secondary_fname <target>
        target file name for second channel in file mode (default /tmp/out2)
-r  --report-rate
        turn on rate reporting (default off)
-h  --help
        display this usage information
-c  --scope-channel <(0|A)|(1|B)(2|AB)>
        scope channel (default A)
-d  --scope-decimation <decimation>
        0,1,2,4,..,65536 (default 32)
-e  --scope-no-equalizer
        disable equalization filter (default enabled)
    --scope-HV
        enable HV equalizer settings (default LV)
-s  --scope-no-shaping
        disable shaping filter (default enabled)
-x  --use-rpad
        use rpad kernel module for scope access (default use /dev/mem and
        assume that the top 32MB of RAM are reserved for the scope)
-l  --load-bitstream [<bitstream>]
        load specified bitstream into the FPGA during startup (default do
        nothing, default filename ./ddrdump.bit)

Examples:
./rp_remote_acquire -m 1 -a 192.168.1.1 -p 1234 -k 0 -c 0 -d 64
        connects to a server on 192.168.1.1:1234 and streams samples from
        channel A for an unlimited time (until interrupted) at 1.953MSps
./rp_remote_acquire -m file -k 1024 -c 1 -d 4 -f /tmp/out.dat
```

Figure 61: Help of the program created by Nils Roos

This help command shows some different options of the program: how can be choose the input channel of the board, or store the data into a file, among others. In this case a TCP communication has been created with different sample rates depending on the design. All these data have been read in another computer and stored in a file using different .vi in LabVIEW which are showed in the Annex II and the Annex III. Depending on the design, one .vi or another have been used. The common part of these .vi are the TCP connection, the changing of type of data, because the data received by the .vi are 16 bites signed integer in little endian ordering, but the data which are in double precision format. Due to this a conversion is needed, to obtain the gain and the offset to convert 16 bits data to double precision. The least square method [28, Ch. 14] was used to convert data, creating two vectors with different voltages of reference measured, and following the

equation 26. Where 'a' are the values of the conversion equation, X is a 2 x N matrix where the first row are the values in 16-bit signed integer and the second row is full of ones, and the Y is a vector with the value of the voltages of reference.

$$a = X^T * (X * X^T)^{-1} * Y \quad \textbf{(26)}$$

With this method, the equation to convert data in this case is the equation 27.

$$Data_{double} = 0.000722 * Data_{16bit} + 0.2665 \quad \textbf{(27)}$$

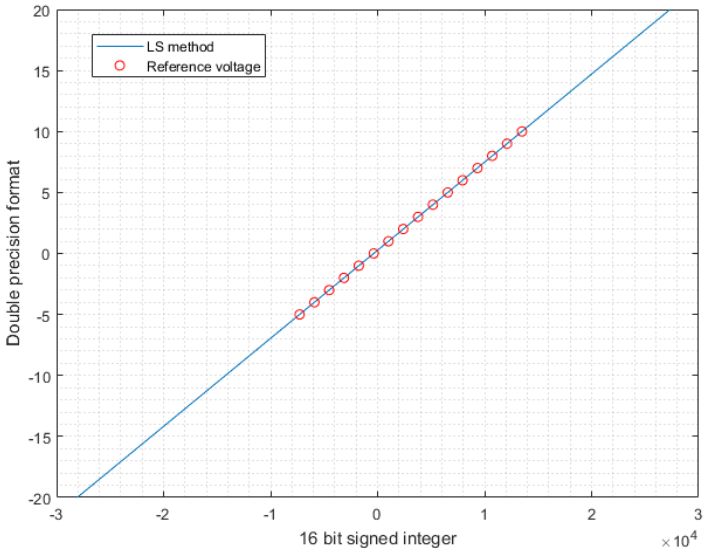

Figure 62: Graphic comparing the equation obtained with the reference points

After the conversion equation is getting, the sample rate to each topology is selected. The design that has the timer 555 needs a sample rate bigger than 50 kS/s to avoid the aliasing effect, as the Nyquist equation indicates. It is needed the double of the sample rate than the maximum frequency, and in this case, the maximum frequency that can be created by the design is close to 25 kHz. For this reason, the sample rate chosen to this design is 122 kS/s, that means that the decimation of the Red Pitaya board has been 1024 to obtain this sample rate. Consequently, the command to execute the program in the Red Pitaya has been "./rp_remote_acquire -m 1 -a 192.168.10.101 -p 1234 -k 0 -c 0 -d 1024 --scope-HV". Others designs have a very slow frequency response, for this reason is not needed a fast sample rate, but this system does not send data to the computer until the buffer of 16 kB is full. Therefore a frequency of 15.2 kS/s is chosen to get data each second. But in the .vi a down sample of this data is created making an average of each 512 points. This make that the sampling rate of the data stored are 29.6875 S/s. the command to execute in the Red Pitaya board the program necessary to these design is "./rp_remote_acquire -m 1 -a 192.168.10.101 -p 1234 -k 0 -c 0 -d 8192 --scope-HV".
Due to each design works different a different .vi have been made. The first was the design which has the timer 555, this circuit needs store all points because Fourier transform of different parts of this signal has been made to know the main frequency of the signal, that depends on the resistivity of the sensor. This resistivity depending directly on the concentration of the substance that has been measured. Therefore, in this .vi all points measured are stored in .TDMS file which is a file created by National Instruments in order to store high quantity of data. This file is easy to convert to an Excel file and it is loadable in Matlab using a free library created by Jim Hokanson too [29]. Moreover, a Fast Fourier Transform (FFT) of 1024 points is made in the program and it is showed in a graphic as control tool that the system works properly. Furthermore, some metadata about the measure is saved in the .TDMS file such as the sensor used or the temperature of the measure, among others.

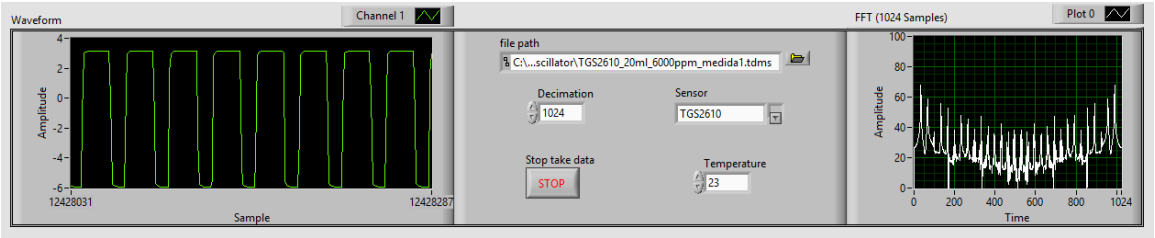

Figure 63: User panel of .vi to the design with the timer 555

The other designs are very slow as it is mention above. in this case their .vi is similar to the other .vi but the FFT is not in this one. Furthermore, a down sample is performed by the average of 512 point. All the data is stored in a .TDMS file as in the other .vi. The block diagram of both .vi are in the Annex II and in the Annex III.

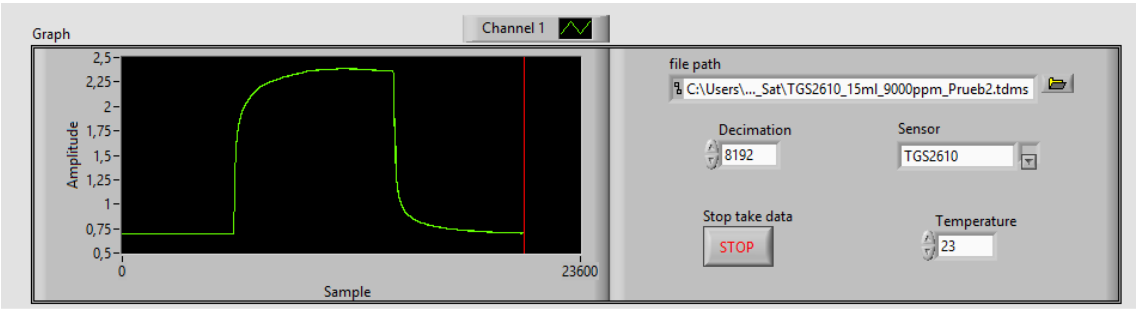

Figure 64: User panel of .vi to designs with output voltage slow changes

As Figure 65 shows, to measure with all the designs, there are some steps to follow. Firstly, the sensor needs be switching-on at least 24 hours, because it needs to be warmed up to a stable temperature. Once the sensor has a stable temperature, a measure of air clean is taken because the resistance can change for different factors such as the humidity or the ambient temperature, among others. the following step is to start the measurement of sample during at least 3 minutes, because this type of sensors are very slow, and they need some time to the sensor stabilizes. The last step is measure again air clean to the sensor goes to the rest state.

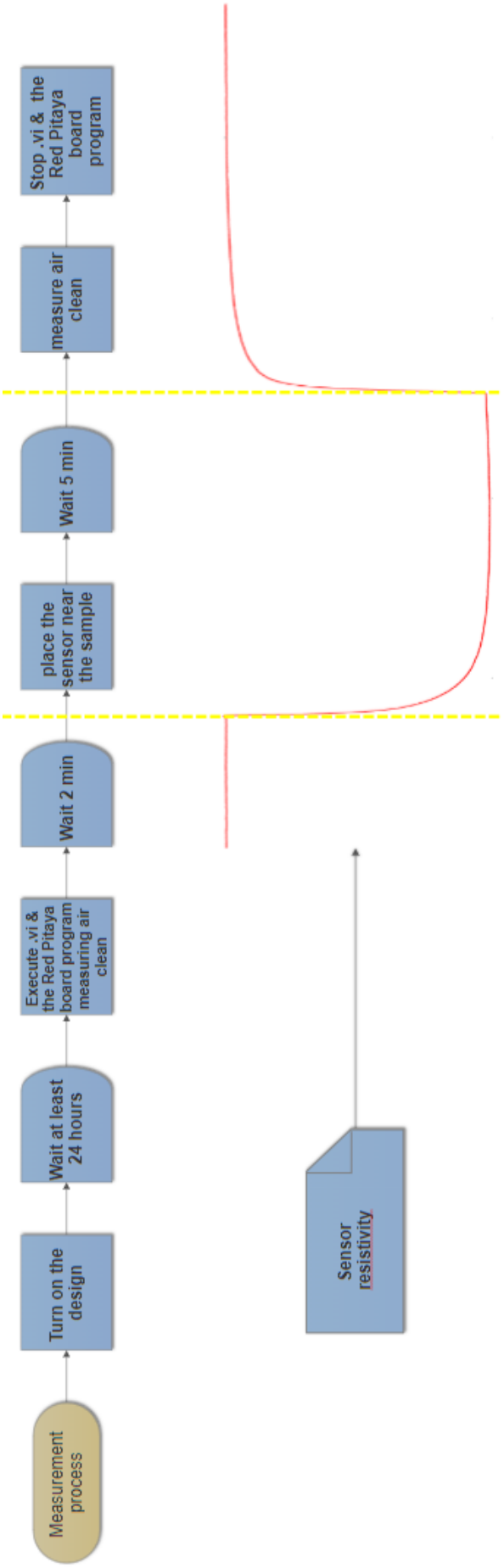

Figure 65: Measurement process steps

4. Results

The results have been getted by two sensors: TGS2600 and TGS2610. These sensors react to different substances, but some of these substances are the same for both sensors such as methane or hydrogen, among others. Considering this characteristic, a substance which both sensors react to it has been chosen to take the results, for this reason the substance chosen to measure is the ethanol absolute of Scharlau which have a density of 0.79 g/cm^3. Samples that have been measured were made by creating a dissolution of this ethanol in water with different concentrations between 500 mg/L up to 6000 mg/L of ethanol in water. The samples measured were of 2 mL of each concentration, in different vials. When the sensor was put close of the sample that vial was opened and the sensor was put into the vial, as Figure 66 show.

Figure 66: Position of the design when it is measuring a sample

One important data to each measure was the ambient temperature of the measure, this temperature was measured using a digital thermometer TES-1302 with a thermocouple type K.

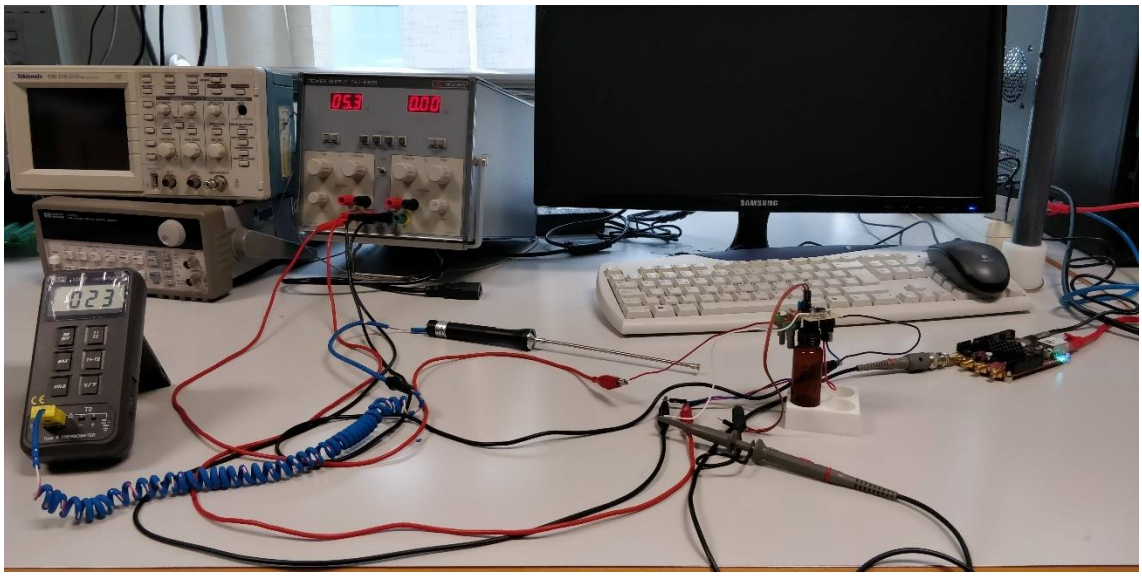

Figure 67: Complete gas sensor system working

4.1. TGS2600

All these measures were taken with a temperature between 23 to 24 °C, the followings figure shows how the output voltage changes with respect to time following the measurement process described in the section 3.4.

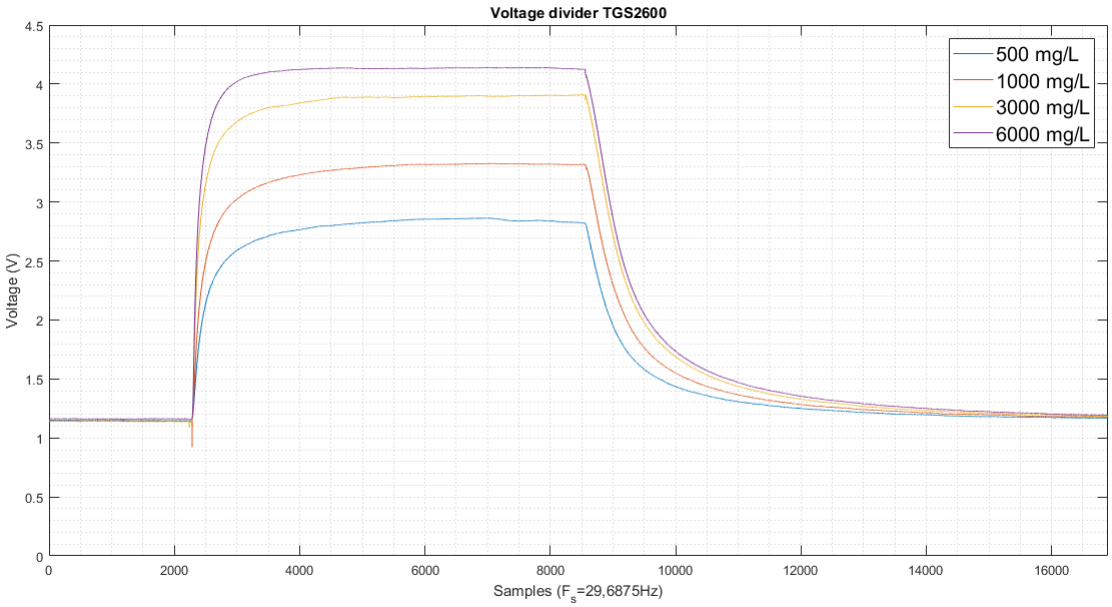

Figure 68:Voltage output of voltage divider design with the sensor TGS2600

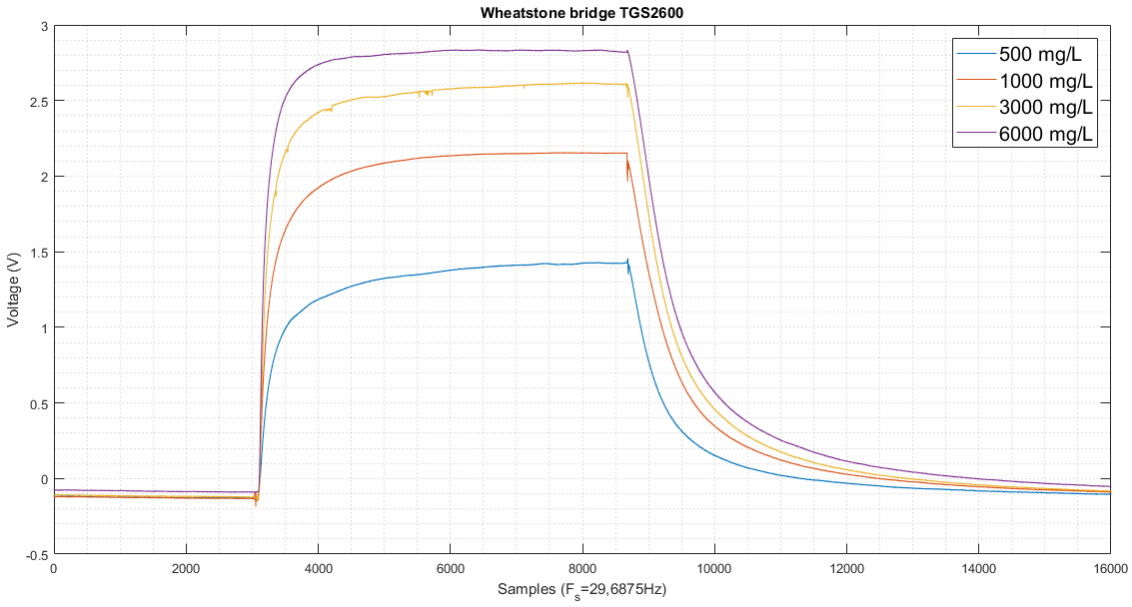

Figure 69: Voltage output of Wheatstone bridge design with the sensor TGS2600

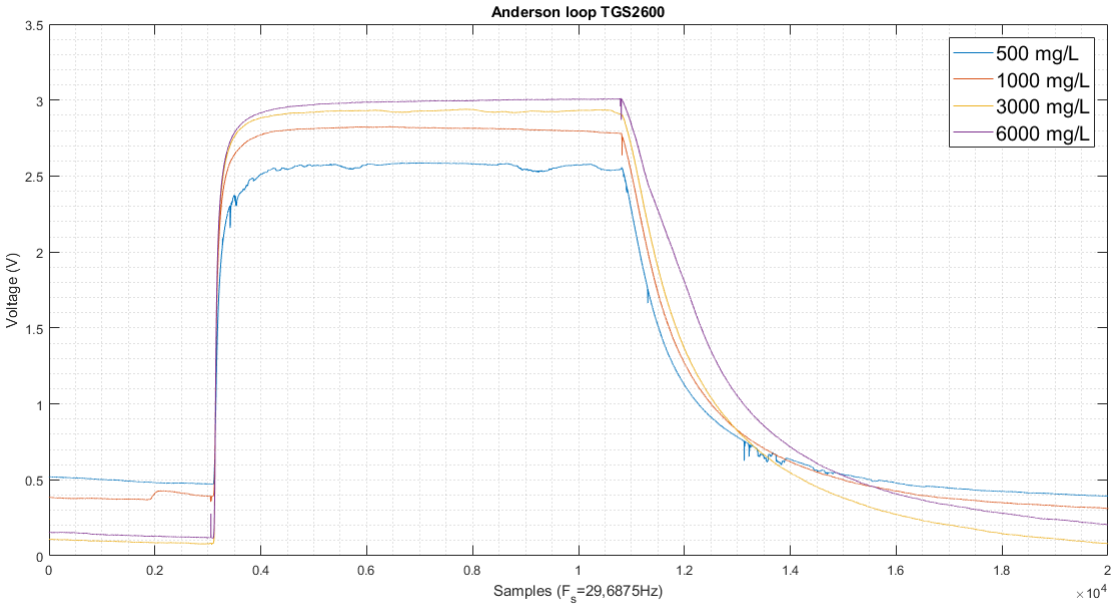

Figure 70: Voltage output of Anderson loop design with the sensor TGS2600

In the design with the timer 555 the output voltage is always in the same values, because is a digital output, the important data in this design is the frequency of this output voltage, for this reason the Figure 71 shows the output voltage during 2.1 ms when was measuring each sample and the sensor resistance was stable.

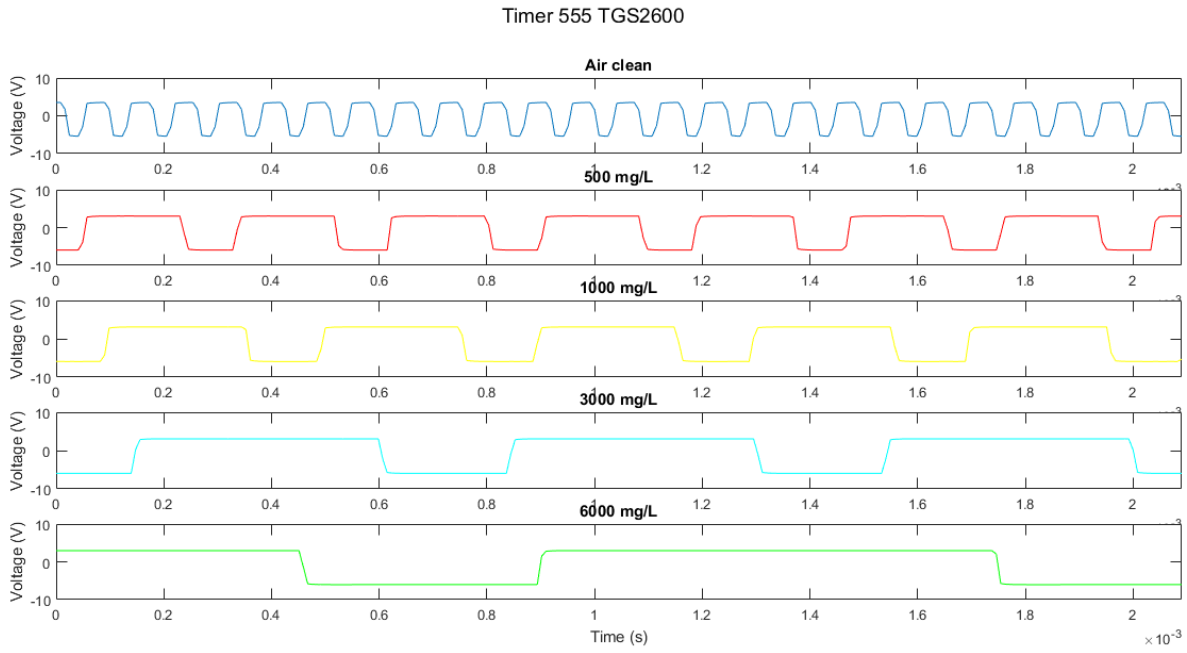

Figure 71: Voltage output of timer 555 design with the sensor TGS2600

The Figure 72 shows, in the timer 555 design, how the frequency of the output voltage change depends on the sample measured, besides it shows how the output voltage of the others designs changes depends on the sample measured too. In that figure it is confirmed the properly working of each design, because all of them are able to detect different concentrations of ethanol in the air.

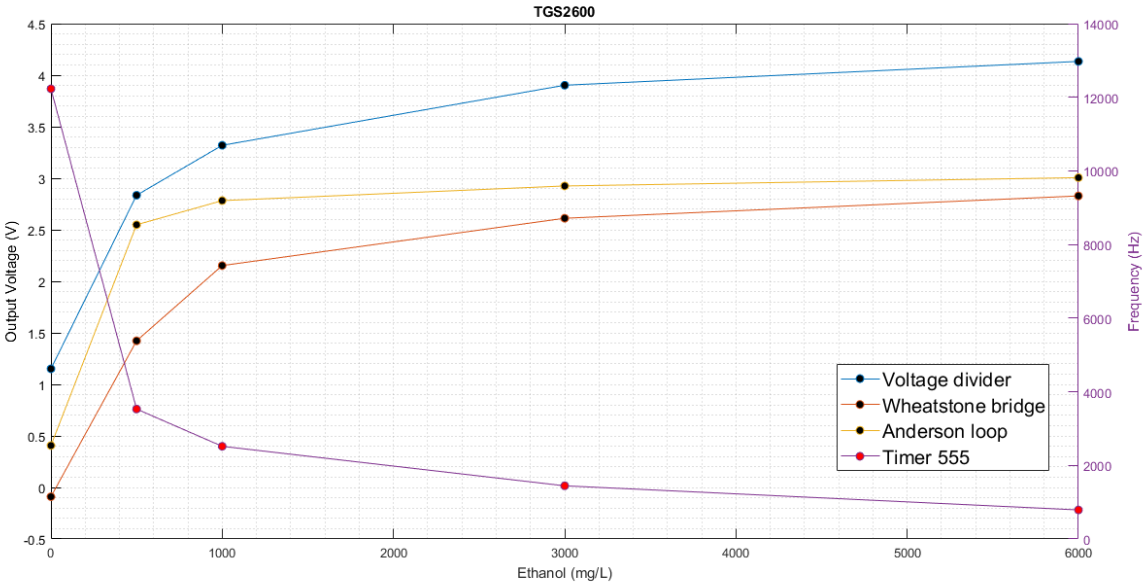

Figure 72: Magnitude of output voltage measured versus the concentration of ethanol in each sample

Another magnitude which is able to be used to detect the quantity of the substance in the air is the slope of the change of the output voltage when the sensor starts to measure a sample. However this magnitude can not measure in the timer 555 design. In this case, slope measure is the straight-line between the moment when the measure starts and the 60% of the slope, and another slope measure is the straight-line between the 60% of the slope and 90% of the slope. Figure 73 shows how obtain these slopes.

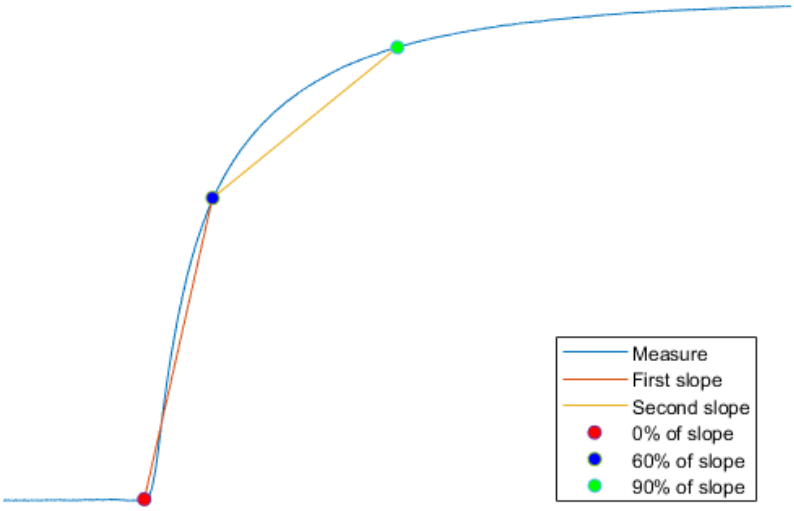

Figure 73: How obtain slopes measured

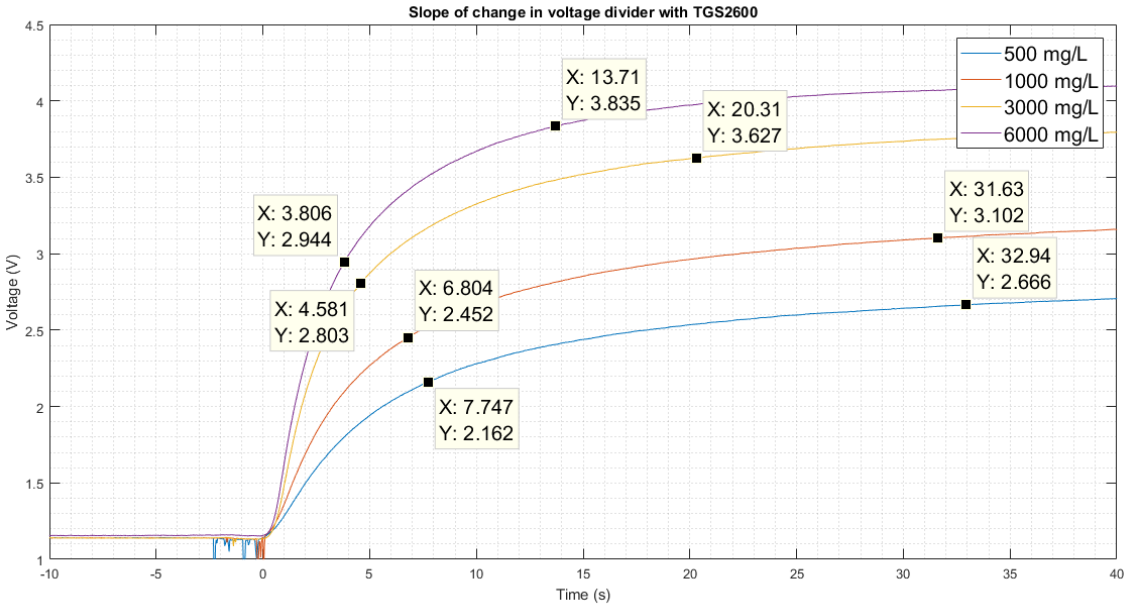

Figure 74: Slopes of voltage divider design with the sensor TGS2600 where are markers in the 60% and 90% of each slope

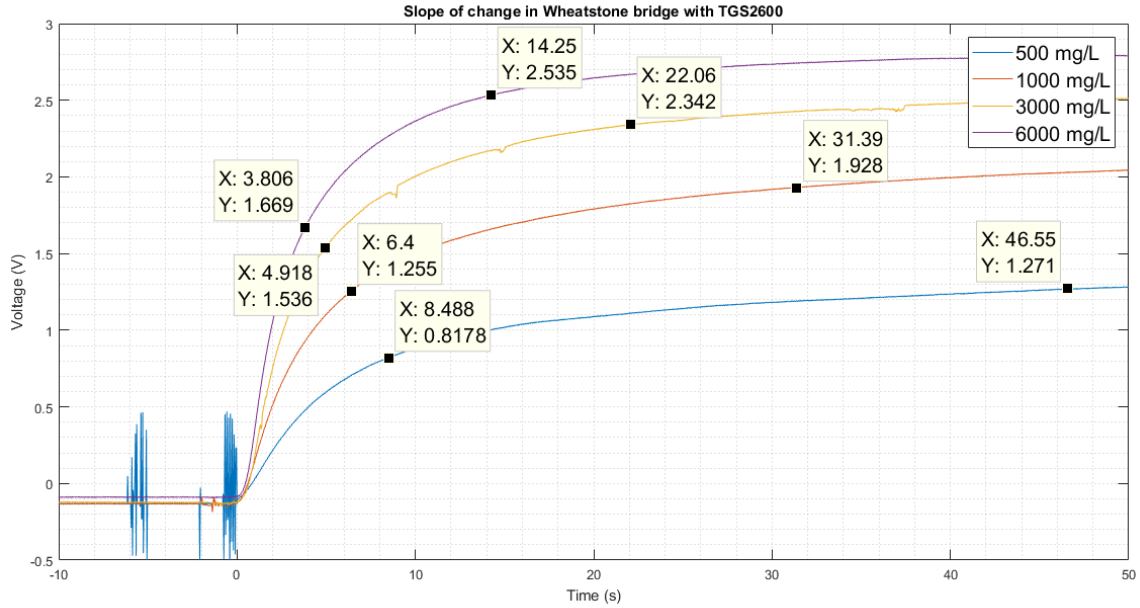

Figure 75: Slopes of Wheatstone bridge design with the sensor TGS2600 where are markers in the 60% and 90% of each slope

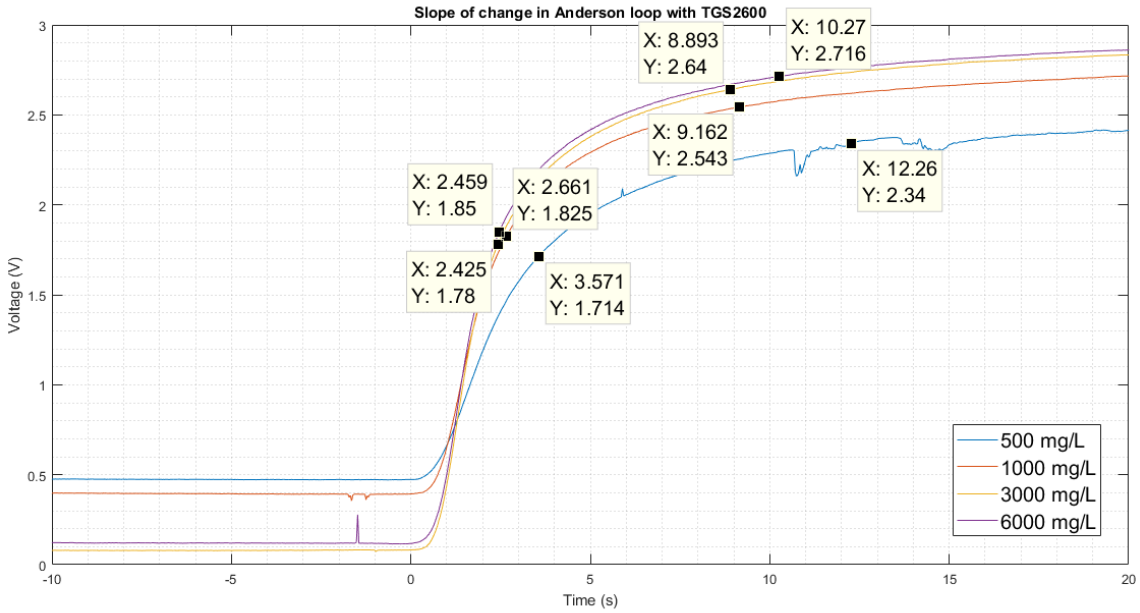

Figure 76: Slopes of Anderson loop design with the sensor TGS2600 where are markers in the 60% and 90% of each slope

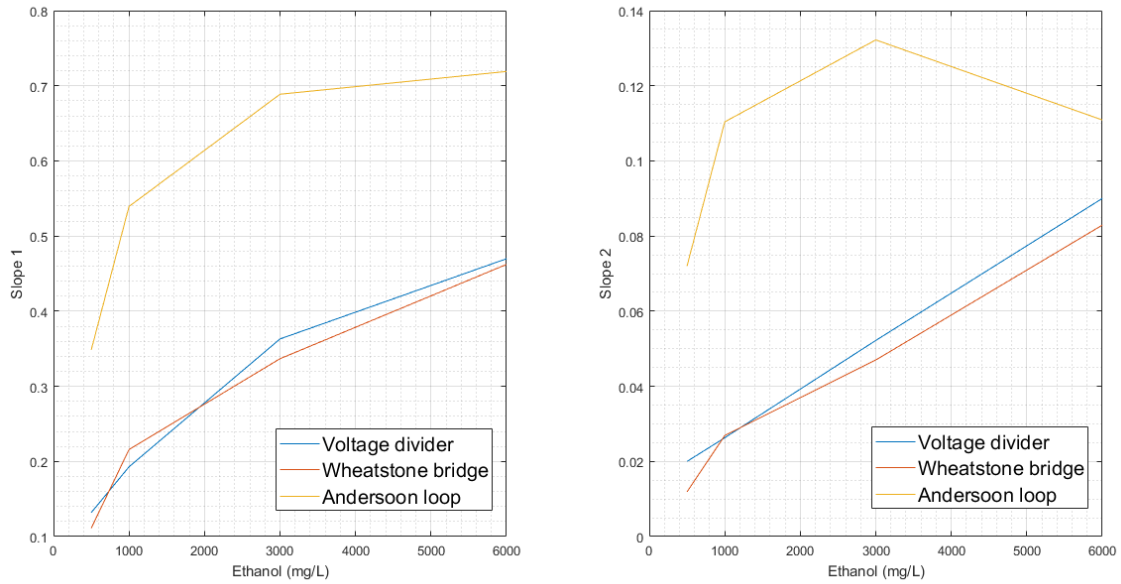

Figure 77: Slopes versus Ethanol of each design with the sensor TGS2600

As Figure 77 shows, the slopes of the voltage divider and the Wheatstone bridge design have a linear correspondence with the quantity of ethanol in the sample, especially the second slope of both. However, the first slope of the Anderson loop design has a logarithmic shape, its second slope the correspondence does not have any sense to use it.

Below FFT of all designs are shown, these graphics show the noise in each design. One data to consider is that the SNR of the ADC used is around 86.04 dB which was calculated using the equation 28 [30], where N is the number of bits of ADC.

$$SNR_{ADC} = 6.02 * N + 1.78dB \quad \textbf{(28)}$$

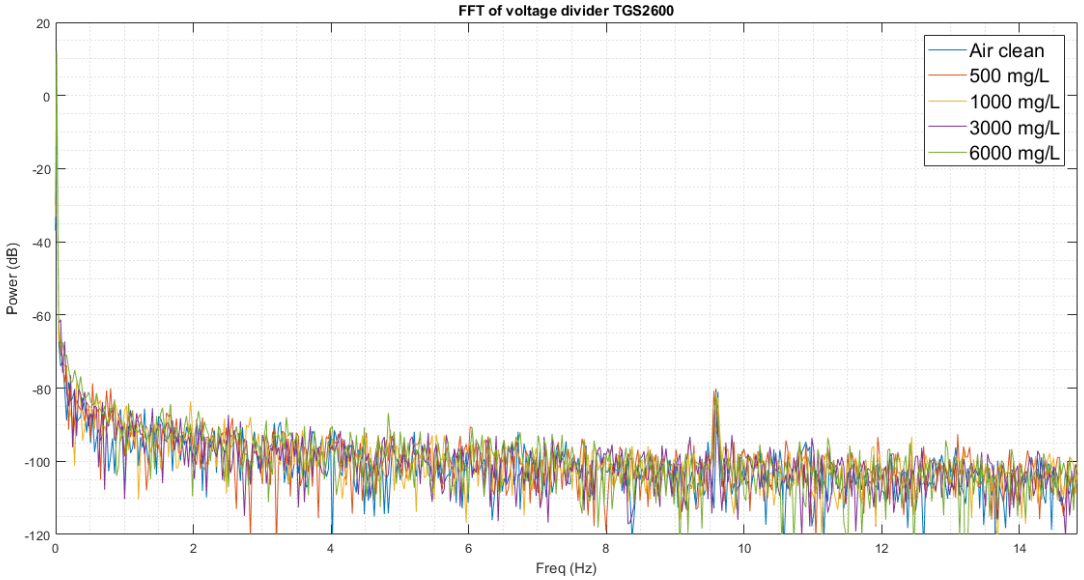

Figure 78: FFT of voltage output of voltage divider design with the sensor TGS2600

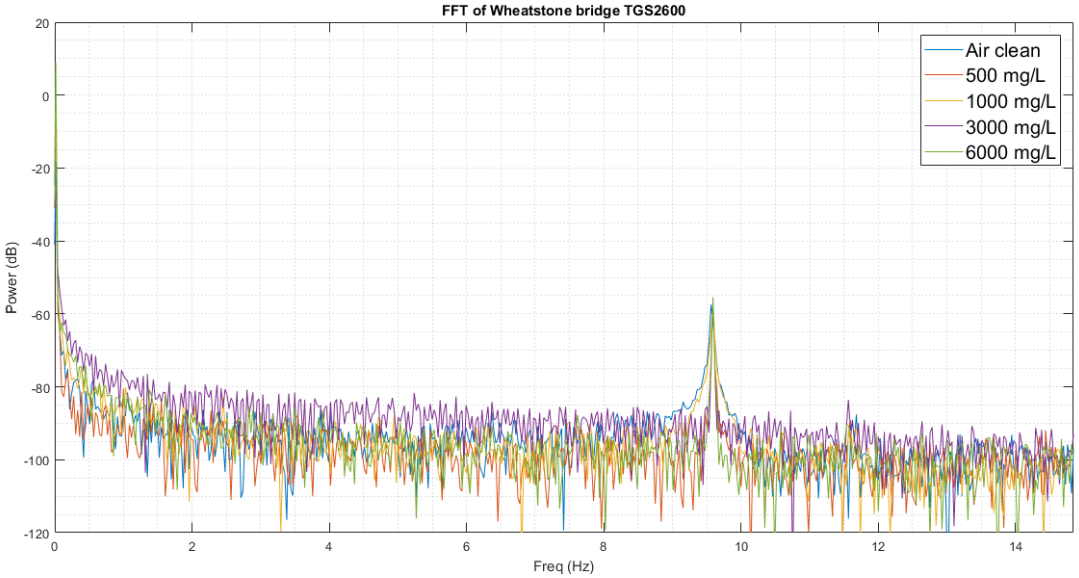

Figure 79: FFT of voltage output of Wheatstone bridge design with the sensor TGS2600

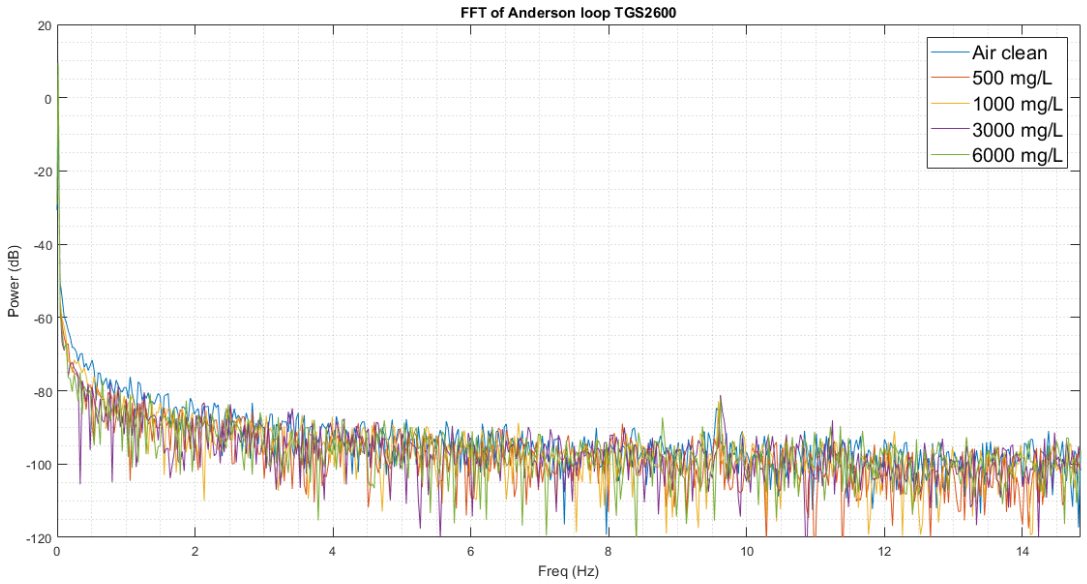

Figure 80: FFT of voltage output of Anderson loop design with the sensor TGS2600

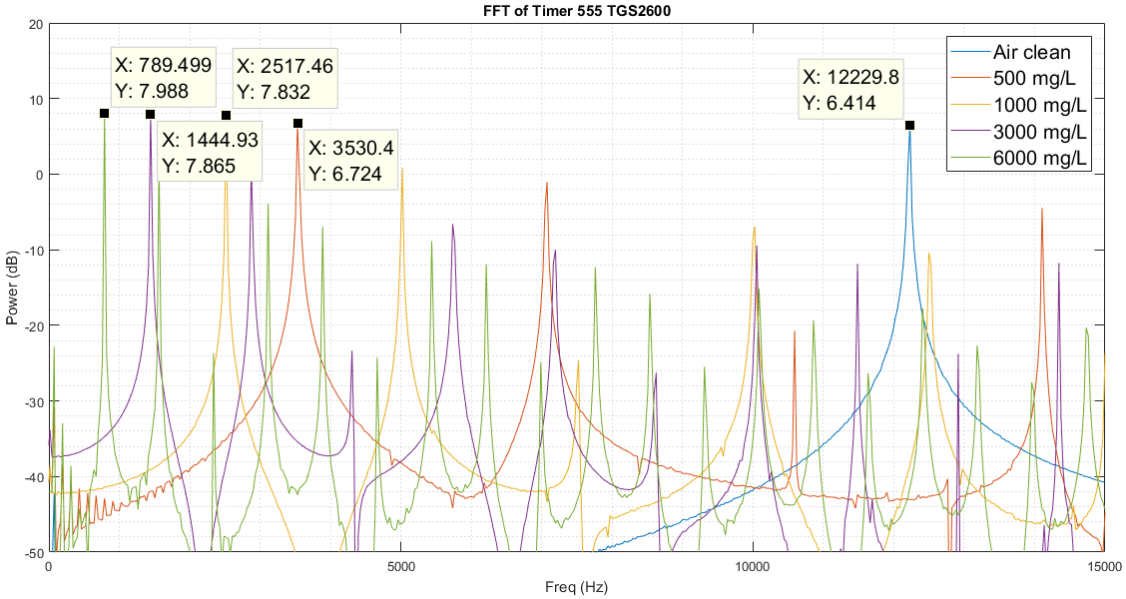

Figure 81: FFT of voltage output of timer 555 design with the sensor TGS2600

In the figures Figure 78, Figure 79 and Figure 80 the FFT are similar, they show the noise floor cause by the ADC, but in the Wheatstone bridge close of 9.5 Hz has a peak power around -55 dB. This peak power is in the FFT of the voltage divider and in the Anderson loop too but it has less power. In both cases it is around -80 dB. This peak power gets worse the measure taken, because in this case the signal which is measuring is considering that is a DC level. Even though this noise peak can be attenuated using a Low Pass Filter (LPF). In the case of the Figure 81, noise is bigger than in the others, but that is because the voltage output is a digital signal, in other words a square waveform. For this reason the odd-integer harmonics frequencies of the main frequency of the signal have significant power.

	Power consumed	
Design	**Air clean**	**Sensor saturated**
Voltage divisor & Wheatstone bridge	1.35mW	2.28mW
Anderson loop	114.77mW	114.91mW
Timer 555	41.85mW	21.56mW

Table 1: TGS2600 power consumed

In above table is shown power consumed by each design, where the heater resistance is not considered to calculate on this power. The Anderson loop is the circuit which most power consume. This is because the current selected is bigger than the current which flows through the Voltage divider. Moreover, in the Anderson loop design and in the timer 555 design, the conditioning stage is more complex than in the voltage divider and in the Wheatstone bridge, where only passive components were used.

4.2. TGS2610

As with the sensor TGS2600, all these measures were taken with a temperature between 23 to 24 °C, and the followings figure shows how the output voltage changes with respect to time following the measurement process described in the section 3.4.

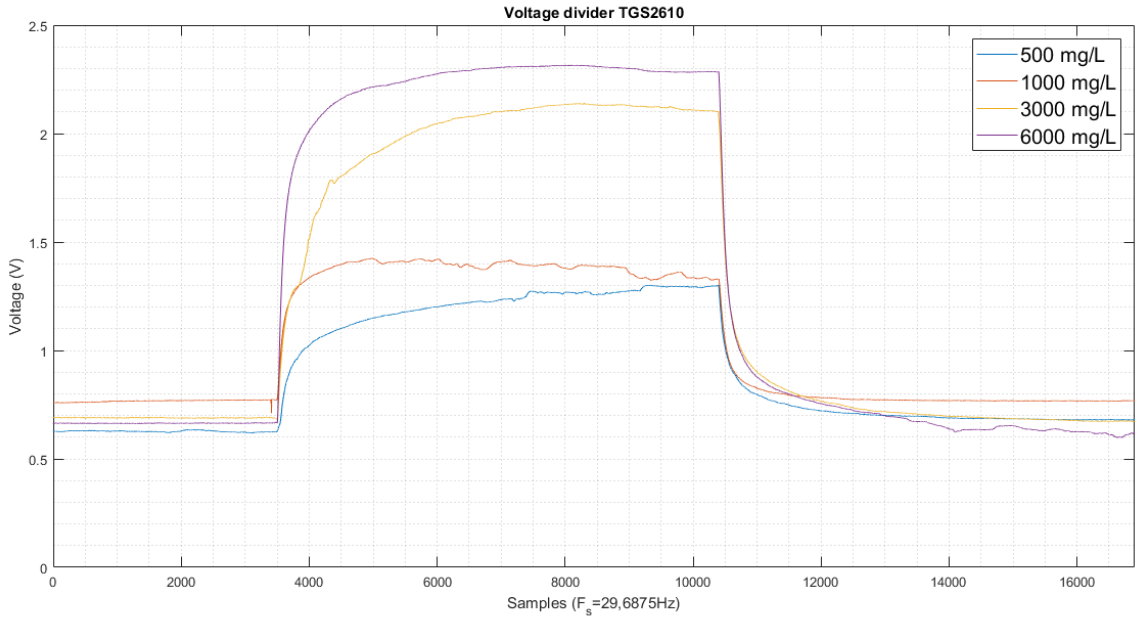

Figure 82: Voltage output of voltage divider design with the sensor TGS2610

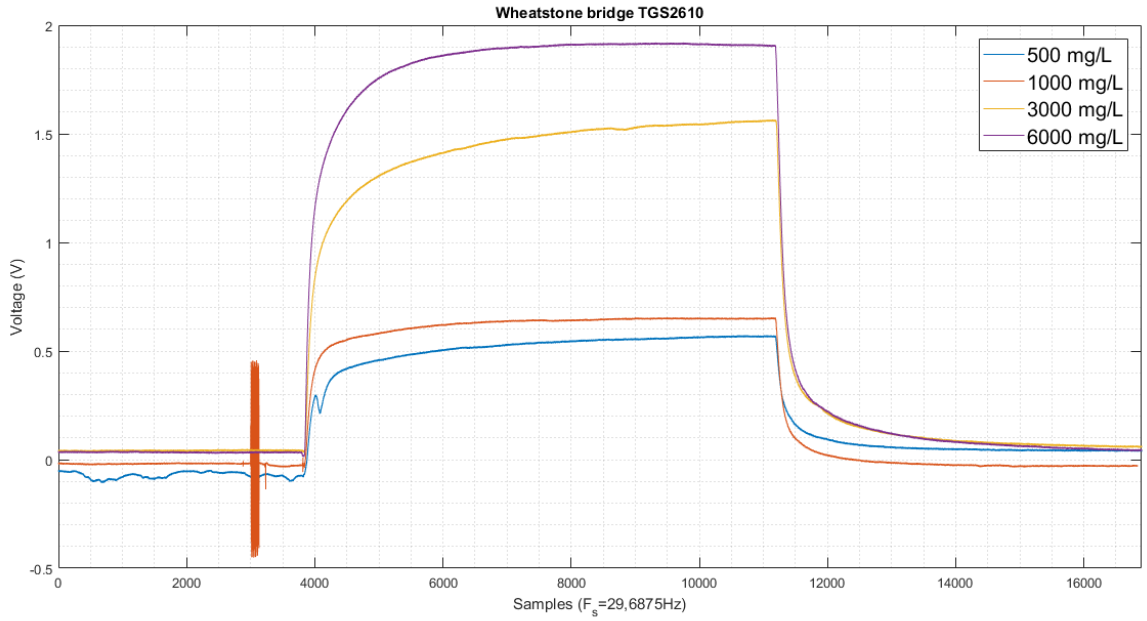

Figure 83: Voltage output of Wheatstone bridge design with the sensor TGS2610

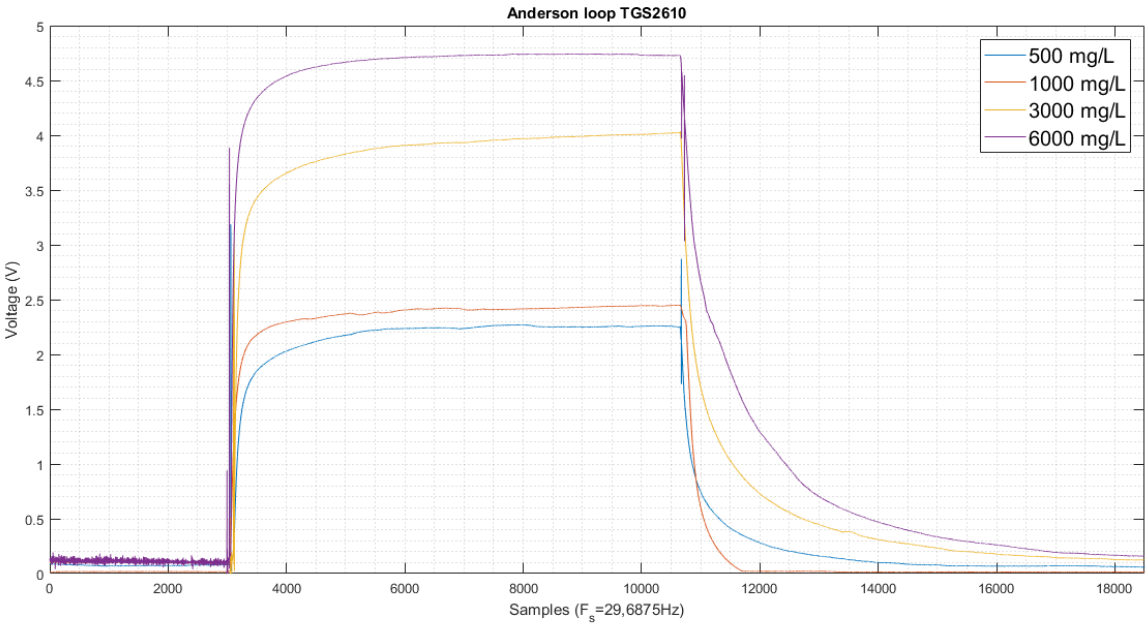

Figure 84: Voltage output of Anderson loop design with the sensor TGS2600

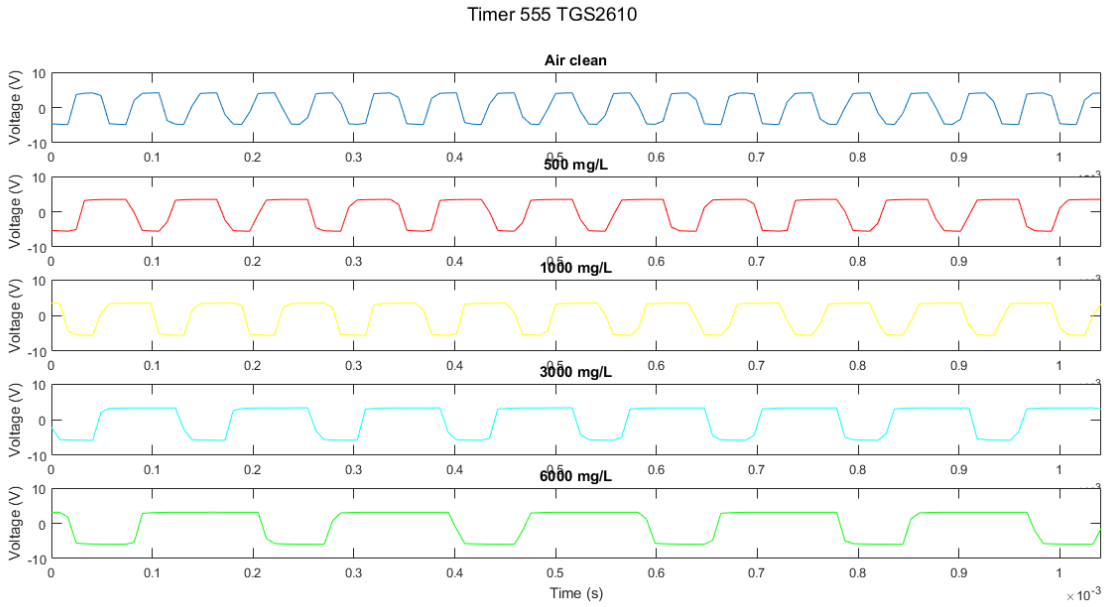

Figure 85: Voltage output of timer 555 design with the sensor TGS2610

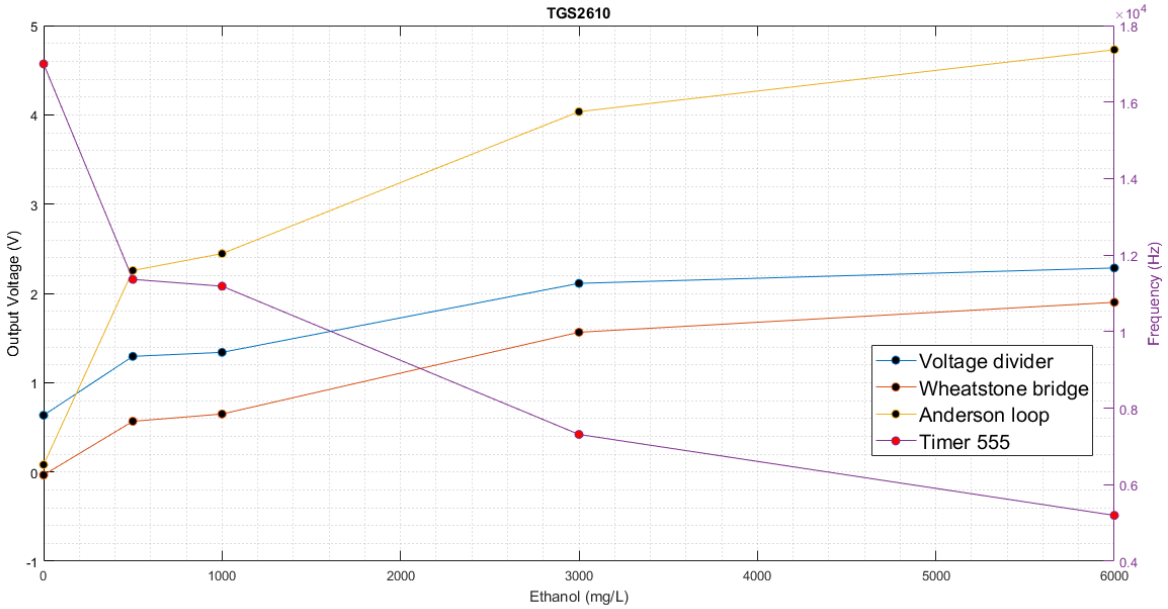

Figure 86: Magnitude of output voltage measured versus the concentration of ethanol in each sample using the TGS2610

The Figure 86 confirms that with the sensor TGS2610 all designs continues working properly. In this case can be confirmed that the design with the timer 555 has a linear change in a range of sensor resistance. This is because its shape of its results is similar to the shape of the result of the Anderson loop design changing the magnitude which is measured and making a vertical mirror in one of shapes.

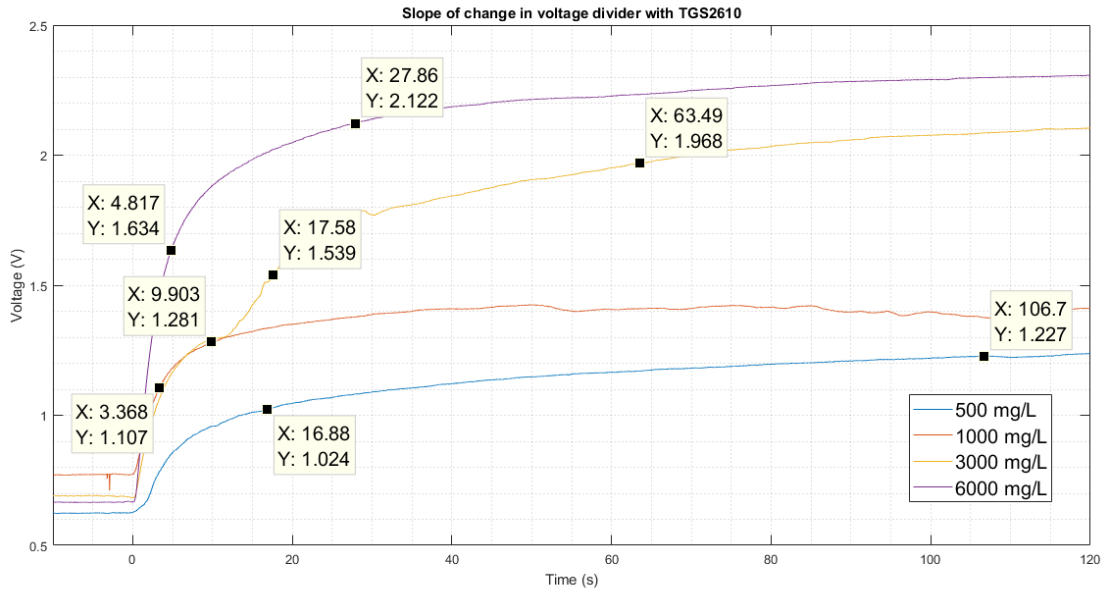

Figure 87: Slopes of voltage divider design with the sensor TGS2610 where are markers in the 60% and 90% of each slope

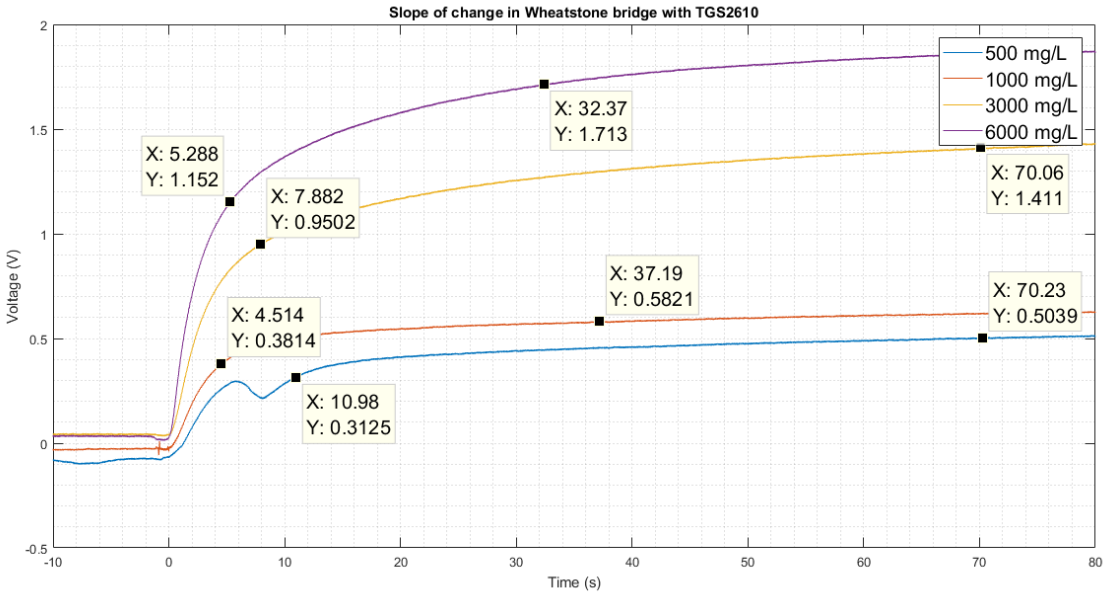

Figure 88: Slopes of Wheatstone bridge design with the sensor TGS2610 where are markers in the 60% and 90% of each slope

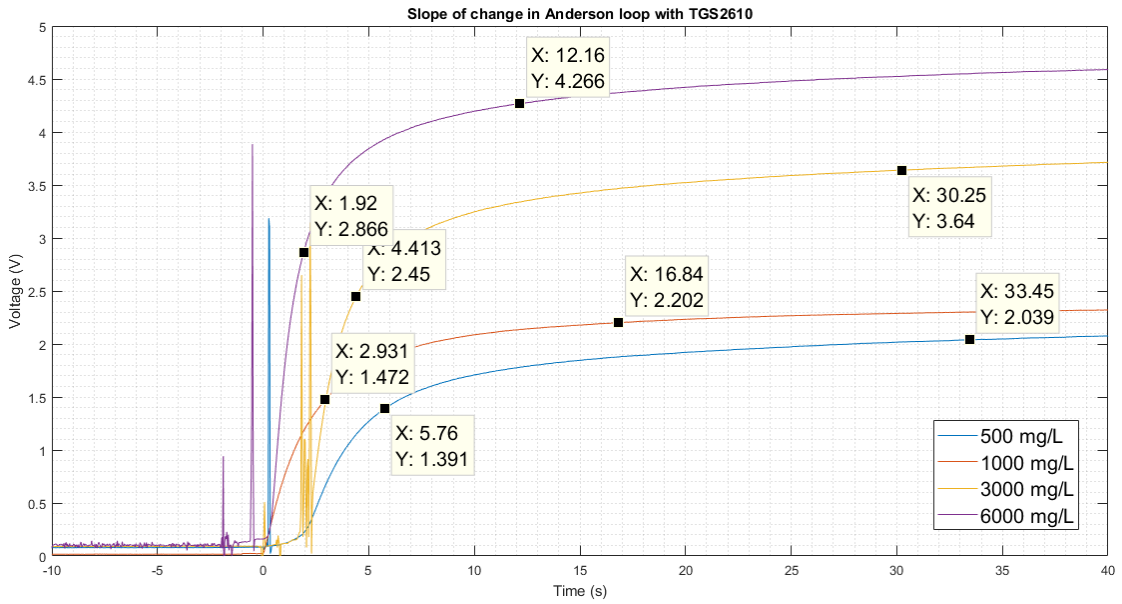

Figure 89: Slopes of Anderson loop design with the sensor TGS2610 where are markers in the 60% and 90% of each slope

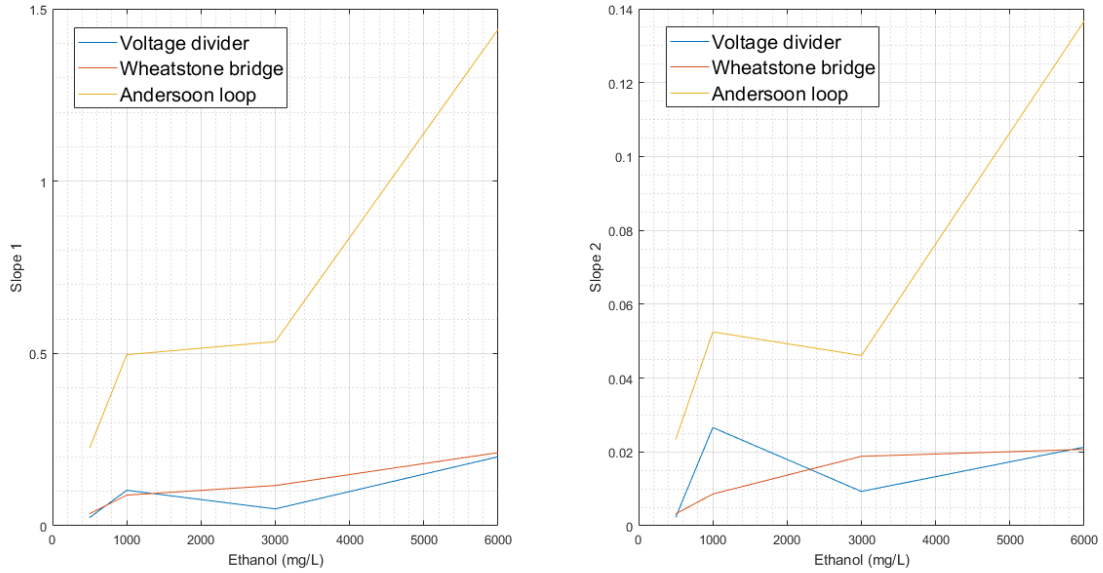

Figure 90: Slopes versus Ethanol of each design with the sensor TGS2610

Figure 90 shows how each design works if the magnitude measured are the slopes, but in these graphs are different problems. First problem is the same than using the sensor TGS2600, which is that the Anderson loop can not use the second slope to find the concentration of ethanol. Another problem is in the voltage divider there is some slopes with high noise, as Figure 87 shows. For this reason, the results obtained of this design are not correct. But taking into account that the voltage divisor should has the same behaviour than the Wheatstone bridge, because the behaviour of its output voltage is the same but in the Wheatstone bridge is deleted the offset voltage, could be confirmed that with the slope of the change in the output voltage can be measured the quantity of ethanol in a dissolution.

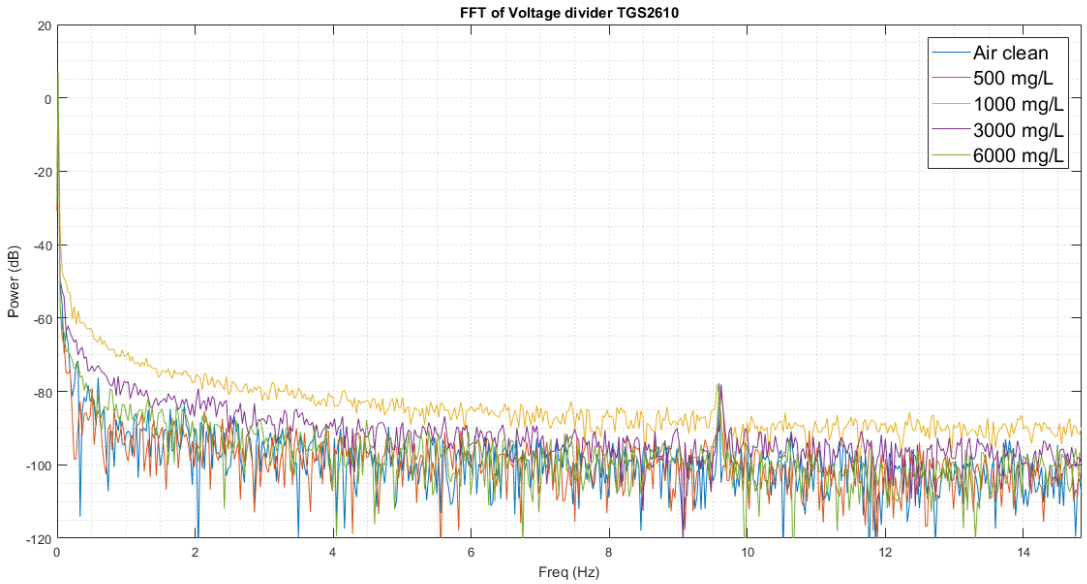

Figure 91: FFT of voltage output of voltage divider design with the sensor TGS2610

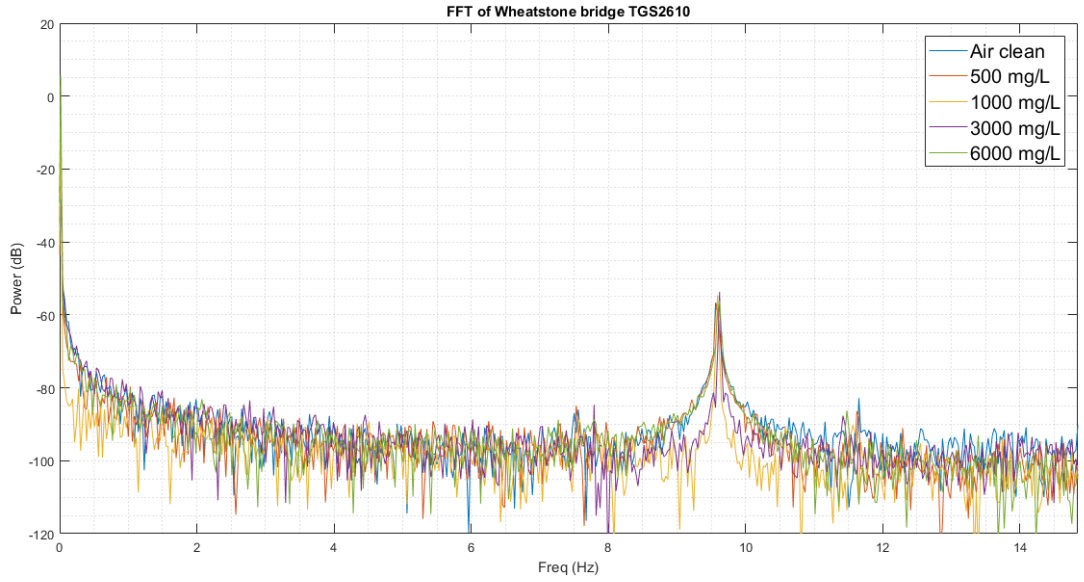

Figure 92: FFT of voltage output of Wheatstone bridge design with the sensor TGS2610

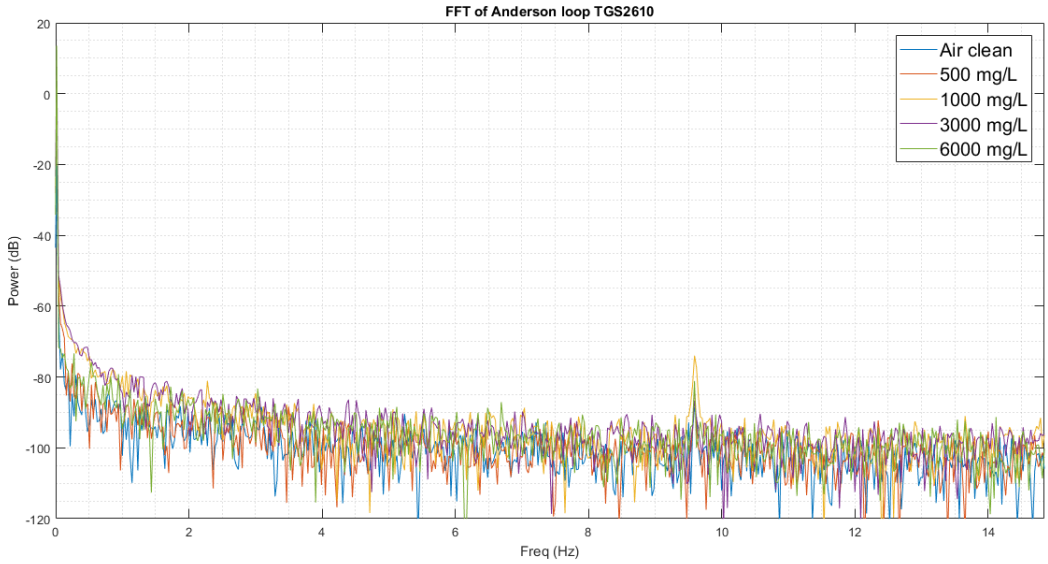

Figure 93: FFT of voltage output of Anderson loop design with the sensor TGS2610

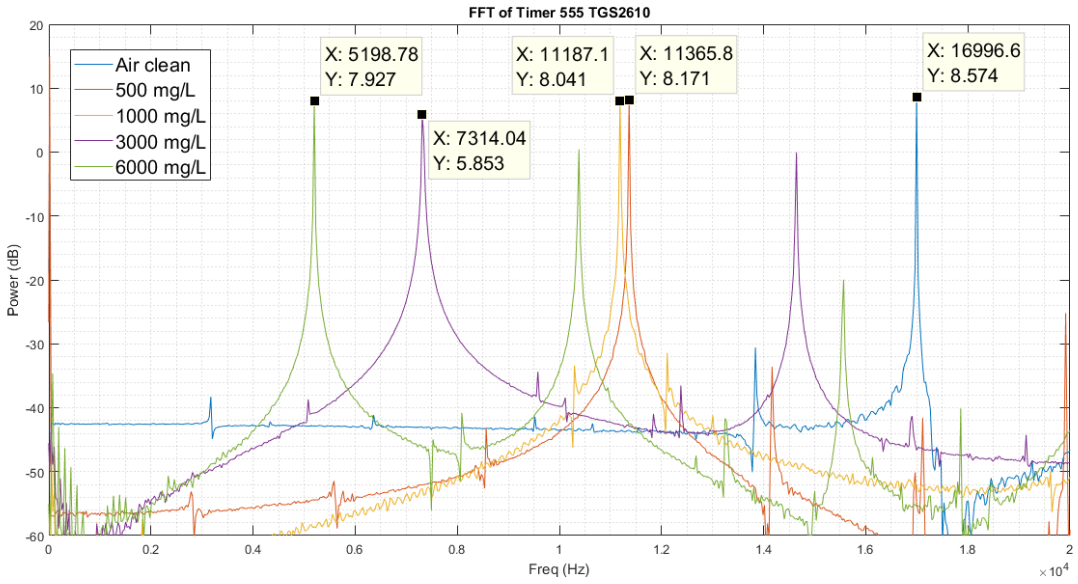

Figure 94: FFT of voltage output of timer 555 design with the sensor TGS2610

The above figures have similar information than the FFT of the measure with the sensor TGS2600. In Figure 91, Figure 92 and Figure 93 appear the floor noise created by the number of bits of the ADC used, but in Wheatstone bridge appears noise close of 9.6 Hz with a power of -54 dB. This peak of noise appears in the others two circuits but with lower power. In the voltage divider it appears with a power of -77 dB. In the Anderson loop appears only in one measure with a power of -75 dB. In contrast, in the FFT of the design with the timer 555 appears a higher noise but this is because the type of the output. The odd-fundamental harmonics have high importance in this FFT due to the voltage output is a square waveform, where the important data is the fundamental frequency of the output voltage.

	Power consumed	
Design	**Air clean**	**Sensor saturated**
Voltage divisor & Wheatstone bridge	1.275mW	2.015mW
Anderson loop	119mW	120.53mW
Timer 555	50.67mW	49.34mW

Table 2: TGS2610 power consumed

Last data obtained of each design was power consumed, without the heater sensor. With this sensor the results were similar to the results obtained with the sensor TGS2600, and that are for the same reason explained in the section 4.1.

5. Conclusions and future works

Considering all results obtained, in the gas sensor type MOS, the type of the power in the heater resistance only affects to the time of ready of the sensor, although in all cases this time is very high (at least 24 hours recommended). Due to this the power to the heater recommended by the author of this thesis is use or a continuous voltage or a square waveform, because these types of power are the easiest of find to put to any circuit.

In the part of the sensor resistance, each circuit has benefits and problems, in the case of the voltage divisor is the topology which less power consumption, and the noise is enough small to obtain good results, this made to this topology, the best to implement in a portable device. The Wheatstone bridge in this case is very difficult to implement using this type of sensor, due the big range which can be the value of the resistance of the sensor, for this reason, this topology is not recommended to use with this circuit. The Anderson loop have some benefits, as the output voltage is linear dependent of the changes of the resistance sensor, and in the case of the design made the resistance can have big range of values to the resistance sensor and can be redesigned to has more than one sensor easily. But it is the design which has the higher power consumption, and it needs at least two different voltage sources, for this reason is the topology recommended to use in designs which are connected to the power in long time and it uses an array of sensors. The last topology is which use the GIC with the timer 555, this is recommended to use it when the voltage output can not be measured with a good ADC, because the voltage output of this circuit is a digital output, and a controller can measure its frequency using a clock with higher frequency than the voltage output, and a counter which count the cycles of the faster clock which are in one cycle of the slower signal.

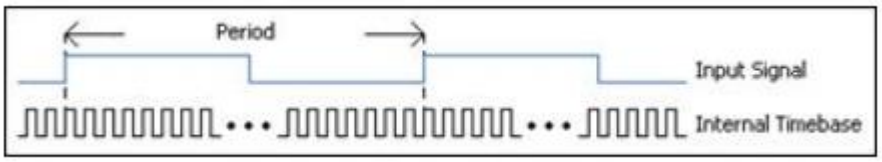

Figure 95: How measure a frequency of a signal with a fast clock [31]

A paper to the IEEE sensor journal is going to be written about the results obtained in this thesis, this article is going to have as title ‘Comparations of different topologies to MOS-type gas sensor’.

The future works of this thesis is study different techniques of power in each topology studied, such as the lock in technique [32], [33] among others, To try to improve the precision of the measures.

6. References

[1] J. Chilo, J. Pelegri Sebastia, M. Cupane, and T. Sogorb, "E-nose application to food industry production," *IEEE Instrum. Meas. Mag.*, vol. 19, pp. 27–33, 2016.

[2] M. Cupane, J. Pelegri Sebastia, E. Climent, V. Guarrasi, T. Sogorb, and M. A. Germana, "Application of MOOSY32 eNose to Assess the Effects of Some Post Harvest Treatments on the Quality of 'Salustiana' Orange Juice," *J. Biosens. Bioelectron.*, vol. 06, no. 04, pp. 4–7, Oct. 2015.

[3] O. Olarte, J. Chilo, J. Pelegri Sebastia, K. Barbé, and W. Moer, "Glucose detection in human sweat using an electronic nose," *Conf. Proc. IEEE Eng. Med. Biol. Soc.*, vol. 2013, pp. 1462–1465, 2013.

[4] T. C. Pearce, S. S. Schiffman, H. T. Nagle, and J. W. Gardner, *Handbook of Machine Olfaction*. Wiley-VCH Verlag GmbH & Co. KGaA, 2004.

[5] Figaro USA inc., "Operating principle -MOS-type gas sensor." [Online]. Available: http://www.figaro.com/en/technicalinfo/principle/mos-type.html. [Accessed: 19-Jun-2018].

[6] Figaro USA inc., "Technical Information for TGS2610," *Datasheet*.

[7] Figaro USA inc., "TGS 2610 - for the detection of LP Gas," *Datasheet*.

[8] Figaro USA inc., "TGS 2600 - for the detection of Air Contaminants," *Datasheet*.

[9] Alphasense Ltd., "p-type Metal Oxide Sensor Overview and Interface Circuit," Essex, 2017.

[10] A. del Cueto Belchi, N. Rothpfeffer, J. Pelegrí-Sebastia, J. Chilo, D. Garcia Rodriguez, and T. Sogorb, "Sensor characterization for multisensor odor-discrimination system," *Sensors Actuators A Phys.*, vol. 191, pp. 68–72, Mar. 2013.

[11] S. Franco, *Design with Operational Amplifiers and Analog Integrated Circuits*. McGraw-Hill, 2001.

[12] A. Durán Carrillo de Albornoz, D. Ramírez Muñoz, J. S. Moreno, S. C. Berga, and E. N. Antón, "A new gas sensor electronic interface with generalized impedance converter," *Sensors Actuators, B Chem.*, vol. 134, no. 2, pp. 591–596, 2008.

[13] Texas Instruments, "TLC555 LinCMOS ™ Timer," *Datasheet*.

[14] K. F. Anderson, "NASA's Anderson Loop," *IEEE Instrum. Meas. Mag.*, vol. 1, no. 1, pp. 5–15, 1998.

[15] K. F. Anderson, "The loop technique for strain gage rosette signal conditioning," *Exp. Tech.*, vol. 24, 2000.

[16] Integrated Device Technology Inc., "ZSSC5101 xMR Sensor Signal Conditioner," *Datasheet*.

[17] D. Ramírez Muñoz, J. Sánchez Moreno, C. Reig Escrivà, S. Casans Berga, and A. E. Navarro Antón, "Constant current drive for resistive sensors based on Generalized Impedance Converter," *IEEE Trans. Instrum. Meas.*, vol. 57, no. 10, pp. 2290–2296, 2008.

[18] D. Ramírez-Muñoz, J. Sánchez, S. Casans, C. Reig, and A. E. Navarro, “Series sensor current loop from a Generalized Impedance Converter circuit with reference current input,” *Conf. Rec. - IEEE Instrum. Meas. Technol. Conf.*, no. April, pp. 2265–2270, 2006.

[19] Texas Instruments, “OPA454 High-Voltage (100-V), High-Current (50-mA) Operational Amplifiers, G = 1 Stable,” *Datasheet*.

[20] Texas Instruments, “OPAx202 Precision , Low-Noise , Heavy Capacitive Drive , 36-V Operational Amplifier,” *Datasheet*.

[21] P. Sanchis Kilders, M. C. Part Escrivá, and J. Marín-Roig Ramón, *Curso práctico de análisis de circuitos*. Valencia: Editorial de la UPV, 2006.

[22] Texas Instruments, “INA188 Precision, Zero-Drift, Rail-to-Rail Out, High-Voltage Instrumentation Amplifier,” *Datasheet*.

[23] O. Casas and R. Pallás-Areny, “Basics of Analog Differential Filters,” *IEEE Instrum. Meas. Mag.*, vol. 45, no. 1, pp. 275–279, 1996.

[24] EFY Team, “IC 555 Timer Working: Pin Diagram, Specifications & Features,” *June 4*, 2017. [Online]. Available: https://electronicsforu.com/resources/learn-electronics/555-timer-working-specifications. [Accessed: 21-Aug-2018].

[25] “3.1.1. STEMlab 125-10 vs. STEMlab 125-14 (originally Red Pitaya v1.1) — Red Pitaya STEMlab 0.97 documentation.” [Online]. Available: https://redpitaya.readthedocs.io/en/latest/developerGuide/125-10/vs.html. [Accessed: 20-Jun-2018].

[26] “2.4.4.4.2. Signal acquisition on external trigger — Red Pitaya STEMlab 0.97 documentation.” [Online]. Available: https://redpitaya.readthedocs.io/en/latest/appsFeatures/examples/acqRF-exm2.html. [Accessed: 20-Jun-2018].

[27] “New feature: high speed continuous recording - Redpitaya Forum.” [Online]. Available: https://forum.redpitaya.com/viewtopic.php?f=7&t=317. [Accessed: 25-Jul-2018].

[28] J. A. Baglivo, *Mathematica Laboratories for Mathematical Statistics: Emphasizing Simulation and Computer Intensive Methods*, SIAM. Philadelphia, 2005.

[29] J. Hokanson, “TDMS Reader,” *2012*. [Online]. Available: https://se.mathworks.com/matlabcentral/fileexchange/30023-tdms-reader. [Accessed: 21-Aug-2018].

[30] W. Kester, “Taking the Mystery out of the Infamous Formula,"SNR = 6.02N + 1.76dB," and Why You Should Care,” pp. 1–7, 2009.

[31] “Cómo Realizar una Medición de Frecuencia - National Instruments,” 2013. [Online]. Available: http://www.ni.com/tutorial/7111/es/. [Accessed: 14-Sep-2018].

[32] J. Aguirre, D. García-Romeo, N. Medrano, B. Calvo, and S. Celma, “Square-signal-based algorithm for analog lock-in amplifiers,” *IEEE Trans. Ind. Electron.*, vol. 61, no. 10, pp. 5590–5598, 2014.

[33] D. García-Romeo *et al.*, “Sub-mA current measurement by means of GMR sensors and state of the art lock-in amplifiers,” *Proc. IEEE Int. Conf. Ind. Technol.*, vol. 2015–June, no. June, pp. 3377–3381, 2015.

Annex I: Block diagram of the program developed in LabVIEW to acquire signals for the heater resistance study of each sensor

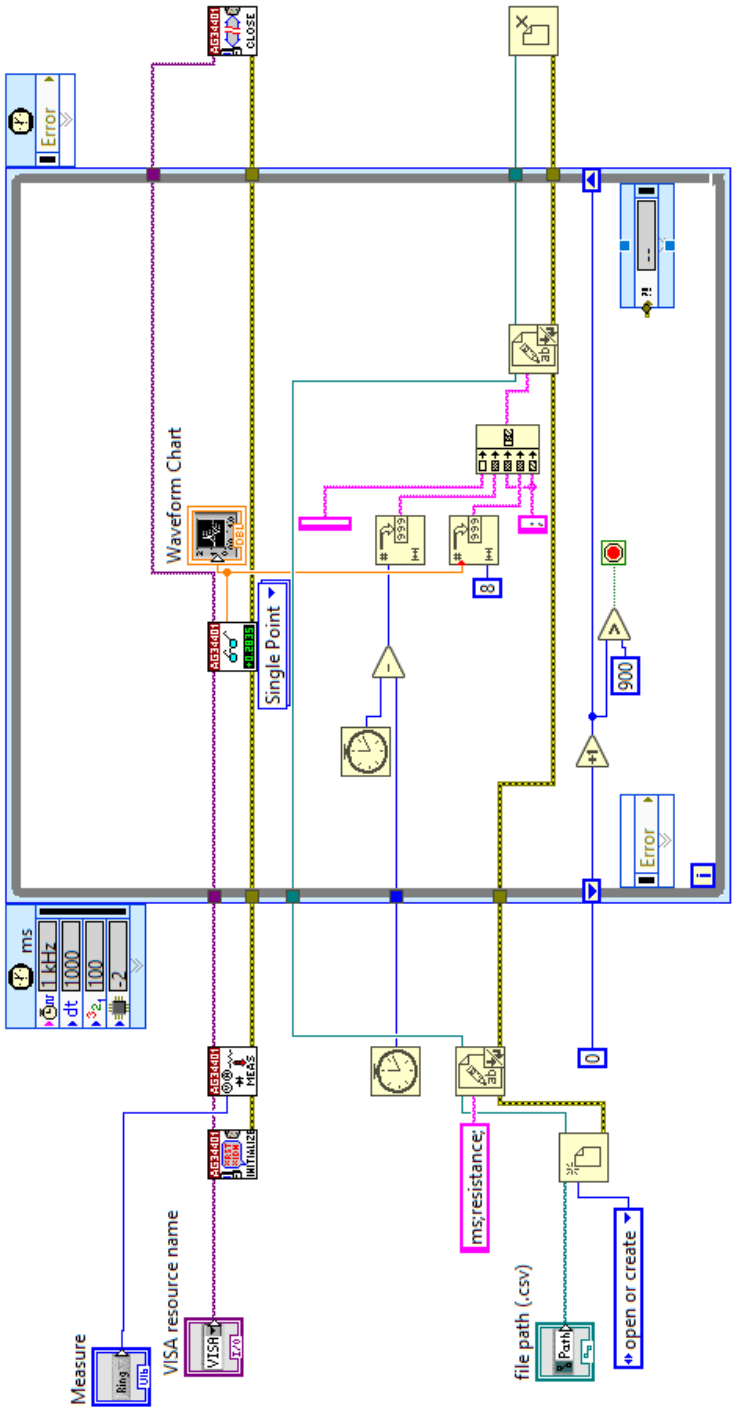

Annex II: Block diagram of the program developed in LabVIEW to acquire the signal of the voltage divider, Wheatstone bridge and Anderson loop

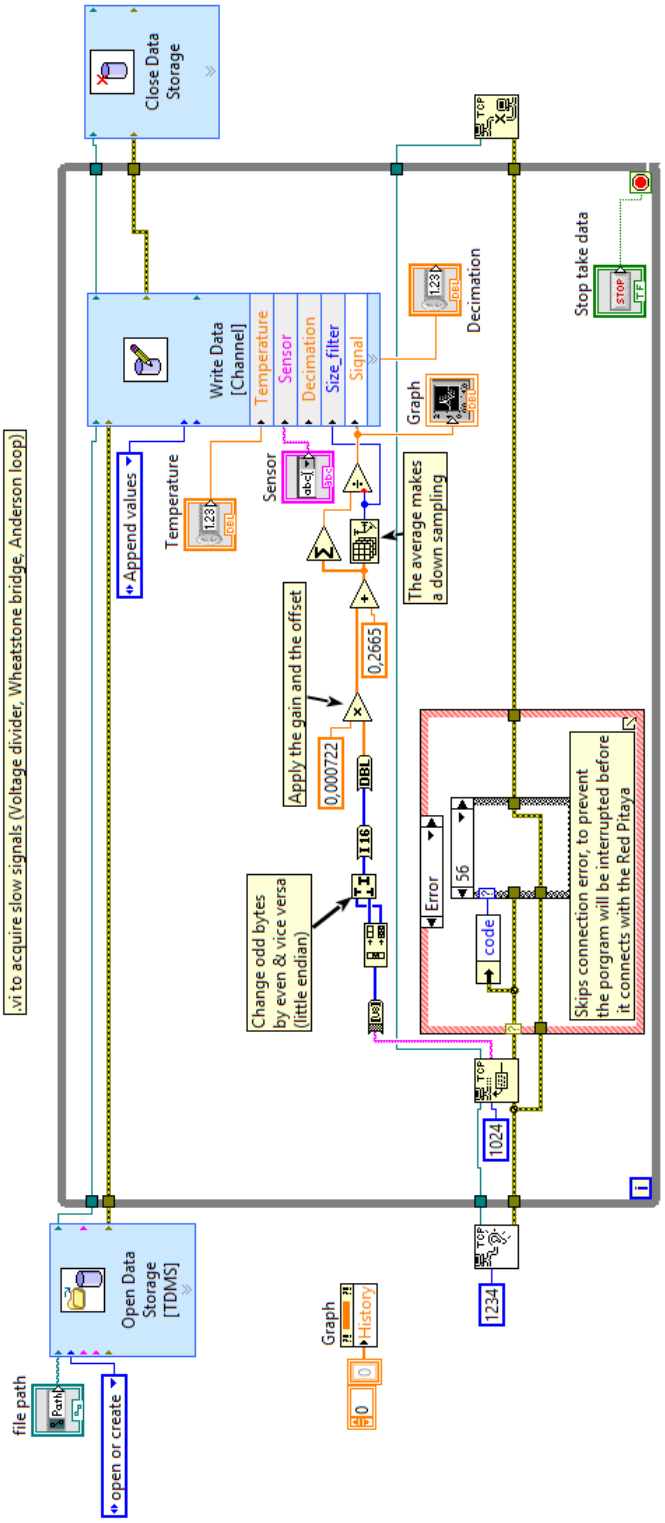

Annex III: Block diagram of the program developed in LabVIEW to acquire the signal of the design with the timer 555